Instrument Tracking in the Operating Room
Optimization of RFID tag performance

Mariëlle Haring

Technische Universiteit Delft

TUDelft
Delft
University of
Technology

Challenge the future

Instrument Tracking in the Operating Room

Optimization of RFID tag performance

by

Mariëlle Haring

in partial fulfillment of the requirements for the degree of

Master of Science

in Mechanical Engineering

at the Delft University of Technology,
to be defended publicly on Wednesday August 22, 2018 at 10:00 AM.

TUDelft Delft
University of
Technology

Acknowledgements

Abstract

In hospitals, the duration of surgical procedures vary even when the same procedure is performed. Surgical end-time of the procedure is currently predicted using historical data about similar procedures, the procedure time and sometimes an indication of the operating surgeon is also taken into account. After the start of the procedure, there is no documented communication between the operating room (OR) planner and the surgical team inside the OR. When the procedure is finished, a nurse has to call to inform that the next patient can be prepared for surgery. If an update of the progress of the procedure is needed, there has to be communication between the staff outside the OR and the surgical team inside the OR. To lower the workload and reduce the distractions for the surgical staff, the communication needs to be automated. This can be done by developing a support system that communicates the progress of the procedure in the OR automatically to the staff outside the OR without the need for human interaction.

In this study, automatically communicating the progress of the procedure is realized by introducing a radio frequency identification (RFID) system that tracks the instruments during the procedure. With this information, the different phases of the procedure can be recognized and this will aid in the communication and the prediction of the surgical end-time. To be able to detect the instruments with an RFID system, a minimal reading distance is required. In this study, different approaches are tested to increase the maximal reading distance of RFID 'on-metal' tags to ensure the range is far enough for the technique to be used during a totally extraperitoneal (TEP) procedure in the OR. The desired reading distance is 50 cm. The study started with a set of instruments with RFID tags attached to them. In a pilot study, the reading distances were measured and resulted in an average reading distance from the antenna which was too low. Using a larger antenna resulted in a slightly higher average reading distance, but still not high enough. Raising the power of the antenna could be increasing the reading distance. The tests are, however, already performed with the maximally allowed 2 W.
To determine the problem with the reading distance, the different properties of the attachment of the RFID tag to the instruments are investigated. The influences of the different properties are tested and the results are combined to make a final design that is supposed to have a higher maximal reading distance than the instruments in the pilot study. The final design is tested both in the clinical lab at the TU Delft and in an operating room at the Reinier de Graaf hospital in Voorburg. The reading distances of the tags on the final design were improved and sufficient for the use in a TEP procedure. Finally, the tags are attached to three instruments with a temporary connection to measure the reading distances with the influences of the instruments. The results of this test show that the desired reading distances can be accomplished with RFID technology.

Abbreviations

The following abbreviations are used throughout this report:

- CE-mark: Conformité Européenne
- CSSD: Central Sterilization Service Department
- CT: Computed Tomography
- DEMO: Dienst Elektronische en Mechanische Ontwikkeling (Electronic and Mechanical Support Division)
- DORA: Digital Operating Room Assistant
- EMI: ElectroMagnetic Interference
- FDA: Food and Drug Administration
- ICU: Intensive Care Unit
- MRI: Magnetic Resonance Imaging
- NaN: Not a Number
- OR: Operating Room
- RFID: Radio Frequency Identification
- TEP: Totally Extraperitoneal
- UHF: Ultra High Frequency
- WBP: Wet Bescherming Persoonsgegevens (Personal Information Protection Law)

Contents

1

Introduction

1.1. Tracking

Hospitals are complex institutions with many employees and even more patients. Most of the labour is performed manually, introducing the risk of human error. Hospitals have been trying to automate parts of the workload, and thereby minimizing the risk of these errors, for over 10 years [1]. One of the adaptations was to automatically track and trace assets around the hospital. For example: beds, wheelchairs, and stretchers have been traced, saving nurses time as they were spending on average 20 minutes per 8-hour shift on 'hunting down' equipment [2] [3].

Just like beds and wheelchairs, smaller pieces of equipment, like surgical equipment, can be traced [4]. Traceability of instruments allows for better localization, facilitates information about the use and sterilization thereby aiding in the purchase process [5]. With this information, it is known what instruments are in the inventory, at the Central Sterilization Service Department (CSSD) or at the operating room (OR). Furthermore, this information can be used for problem analysis or if problems arise like contamination after surgery is detected, the used instruments can be tracked down.

As mentioned, there are many applications for tracking instruments throughout the hospital. However, the focus in this study will be on tracking the instruments inside the OR. Knowing which instruments are used during the surgery, combined with an analysing algorithm creates the possibility of knowing in what phase the surgery is. This enables the personnel outside the OR to get updates of the progress inside the OR, without any active communication or distractions in the OR.

1.2. Communication

Currently, the end time of a surgery is predicted using historical data about similar procedures, procedure time, and sometimes an indication of the operating surgeon [6]. After the start of a procedure, there is no registered communication between the OR planner and the surgical team inside the OR. When a procedure is finished, a nurse has to call to inform that the next patient can be prepared for surgery. If an update of the progress is needed, there has to be communication between the staff outside the OR and the surgical team inside the OR. When communication between the staff outside the OR and the surgical team is needed, for example to give an update about the progress, the procedure is disturbed as communication has to be done by phone, by looking through a window, or by walking into the OR (Figure 1.1). This is undesirable as this can be distracting and calls for extra labour, it can even jeopardize the sterility of the room in the case of someone walking in.To prevent these problems from occurring, a support system has to be developed to automate the communication about the progress of the procedure in the OR. This system would eliminate the need for human interactions.

1.3. Problem Statement

A new technology is needed to automate the communication about the progress of a procedure in the OR. With this technology, a progress report of the procedure and a surgical end-time prediction can be made. This technology has to work autonomously, supporting the humans in their tasks, whilst

Figure 1.1: Left, OR staff looking into the OR. (From: https://www.gettyimages.ca/photos/) Top right, vision through the window of an OR. (From: https://www.gettyimages.nl/detail/foto/) Bottom right, OR planning board. (From: https://www.pthgroep.nl/hypermoderne-schipholborden-voor-oks-antonius-ziekenhuis)

ensuring no extra workload is added neither for the surgeons nor the nurses. The system also has to prevent distractions, this will lower the risk of human errors.

1.4. Required Information

For the study, intra-operative surgical data are needed about the use of instruments during a procedure. The required data should include which instrument is used when, for how long and how often during surgery. These data can be analysed by an algorithm, which can recognize different phases of the surgery and make a surgical end-time prediction [7].

1.5. Tracking Technology

There are different techniques to track objects like instruments. Camera recordings, barcodes, and Radio Frequency Identification (RFID) are some of the most commonly used techniques. These three approaches have some clear advantages and disadvantages (Table 1.1). The advantage of using a camera recording of the operation is that no extra actions and no changes in work flow are needed for the surgical team [8]. The recordings can be analysed with a pattern recognition algorithm. This technique only has to be developed once for many uses. A disadvantage of using a camera is the need for a line of sight, otherwise the instruments cannot be detected, making tracking 100% of the time impossible. Furthermore, the surgery will be recorded. This is a disadvantage because it jeopardizes the privacy of the surgical team, as errors can be related to individual people.

Barcodes are already used in hospitals and are an inexpensive way to track objects. However, a line of sight is needed from the scanner to the barcode. To be able to track instruments during a surgery, every instrument would have to be scanned before and after handing it to the surgeon. This requires a lot of extra actions during the surgery and is a clear disadvantage. Furthermore, only one item can be registered per scan, so every individual item has to pass the scanner, taking up a lot of time [1]. Another disadvantage is that dust, chemicals and physical damage can make barcodes illegible.
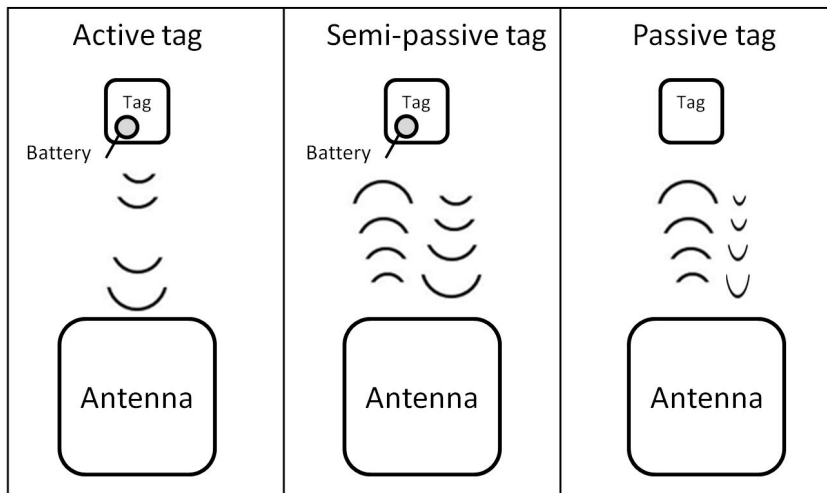
Figure 1.2: The working principle of active, semi-passive and passive tags. From left to right, first the active tag containing a battery, sending out periodical radio waves to the antenna. Second, the semi-passive tag, also containing a battery, but only sending radio waves responding to an antenna. Third, the passive tag, backscattering the radio waves received by an antenna.

The RFID system is a more expensive technology, but no line of sight is required and multiple items can be read simultaneously. The ability to scan multiple items simultaneously makes RFID time efficient. Furthermore, there are no extra actions from the surgical team needed [9]. A disadvantage of RFID is the possible privacy issue. RFID signals can be intercepted by unauthorized parties, which is a problem when RFID is used to communicate patient information. Using RFID in the operating room to track instruments introduces privacy issues as errors made by the surgical team might be identified when analysing the instrument use. Another disadvantage is the availability of multiple radio frequencies at which RFID can be used, making standardisation difficult. Overall RFID seems to be the best solution for tracking surgical instruments in the OR.

Table 1.1: Pros and cons of tracking technologies.

	Pro	Con
Camera	No extra actions Pattern recognition	Line of sight Voice recordings Privacy issues
Barcodes	Inexpensive	Line of sight Extra actions One item per scan Sensitive to dust, chemicals, and physical damage
RFID	No line of sight No extra actions Multiple items in one scan	Expensive Privacy issues Multiple different frequencies

1.6. Basic RFID Working Principle
RFID is short for Radio Frequency Identification. It is a technology used to transfer data to identify objects or people without needing a line of sight, using radio waves. An RFID system consists of a transponder (tag), an antenna, a reader, and a computer or database to process the data. The tags are attached to the object or person that needs to be identified. A reader or antenna can read multiple tags simultaneously.

RFID tags
RFID tags exist in many shapes and sizes, from large plates to very small chips. The tags can be active, semi-passive, or passive [10] (Figure 1.2). An active tag has a build-in battery and periodically sends a signal to communicate its ID. A semi-passive tag also has a build-in battery, but only sends

Table 1.2: RFID operating frequencies and associated characteristics, adapted from [11].

	LF Low frequency	HF High Frequency	UHF Ultra High Frequency	Microwave
Frequency	30 - 300 kHz	3 - 30 MHz	300 MHz - 3 GHz	2 - 30 GHz
Typical RFID Frequencies	125 - 134 kHz	13.56 MHz	433 MHz 865 - 956 MHz	2.45 GHz
Approximate read range	less than 0.5 m	up to 1.5 m	433 = up to 100 m 865 - 956 MHz = 0.5 to 5 m	up to 10 m
Transfer rate	< 1 kbit/s	25 kbit/s	30 kbit/s	up to 100 kbit/s

information when it receives signals from an antenna. The passive tag requires no battery but uses the radio energy transmitted by an antenna to create a signal to communicate back, also known as backscatter. Because the passive tags are dependent on the energy sent by the reader, the tags are used for a shorter range than the active tags. They are, however, smaller and cheaper than active tags. Furthermore, passive tags have a virtually unlimited lifetime [9].

The reading distance of an RFID system is determined by the combination of the reader and its power, the antenna and the antenna size, and the RFID tags and their orientation. Most important though is the frequency on which the RFID tag works (Table 1.2). For this study, ultra high frequency (UHF) is used between 865 - 956 MHz, as this frequency operates in the desired reading distance. Furthermore, using the same RFID tags on the instruments for other applications, such as tracking the instruments throughout the hospital, is possible because the reading distance is not limited to a maximum of 1.5 m like the high frequency (HF).

The antenna and orientation

The RFID technology is based on radio waves sent by an antenna to a tag. The tag responds with backscatter of the radio waves. The backscatter is intercepted by the antenna. Two type of antennas can be used: an omnidirectional antenna or a directional antenna. An omnidirectional antenna emits radio waves in all directions. A directional antenna emits waves only in a specific direction. In this study, the first tests are performed with a small antenna, while later on a larger antenna is tested. This is done because the size of the antenna influences the maximal reading distance. This influence can be explained by looking at the left image in Figure 1.4. With a larger antenna, the radiation pattern will be spread over a larger area and the surface to intercept the backscatter from the tags is also larger. An RFID tag has wires in a plane, see Figure 1.3. When radio waves interact with the RFID tag, an electromagnetic field is formed around the wires. For many RFID tags this is a form of a dipole [12]. Figure 1.4 on the right shows the field around one of the wires in a tag, on the left a radiation pattern transmitted by the antenna is shown. The wire located inside the tag is orientated along the y-axis. When the tag is oriented with the y-axis parallel to the plane of the antenna and the x-axis perpendicular to the plane of the antenna, the orientation is optimal (Figure 1.4). According to Ahson et al. (2008) [12] this orientation results in the greatest reading distance.

Influencing factors

Different environmental factors are known to influence the reading distance of the RFID system. The reading range can be affected by metal reflecting the radio waves and dielectrics, such as water, absorb radio waves, both changing the normal behaviour of the waves [13]. Another important factor is the interference from obstructions. For RFID, no line of sight is required. However, it is desired to have as little obstructions as possible between the antenna and the tags [14].

1.7. Selected Surgery and Surgical Setting

The surgery selected for this study is a totally extraperitoneal (TEP) procedure. A TEP procedure is a laparoscopic surgery to repair a weakness in the abdominal wall, specifically inguinal hernias. Inguinal hernia repair is the most commonly performed surgery in the United States [15] and therefore it is relatively easy to gather the sufficient amount of data.

Visiting several TEP procedures at the Reinier de Graaf hospital provided insights into the general positions of the staff during the surgery (Figure 1.5 and 1.6). During the surgery, an anesthesiolo-
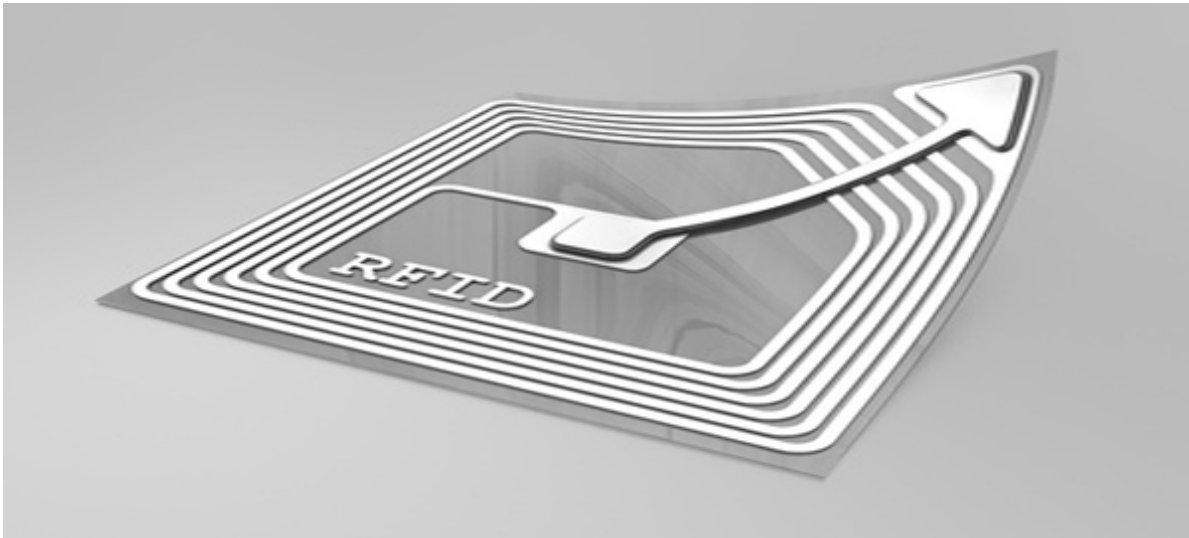
Figure 1.3: An example of the wires in an RFID tag. From http://www.asiarfid.com/rfid-basics/rfid-tag-best-practices-13-tips-for-in-the-field-tagging.html.
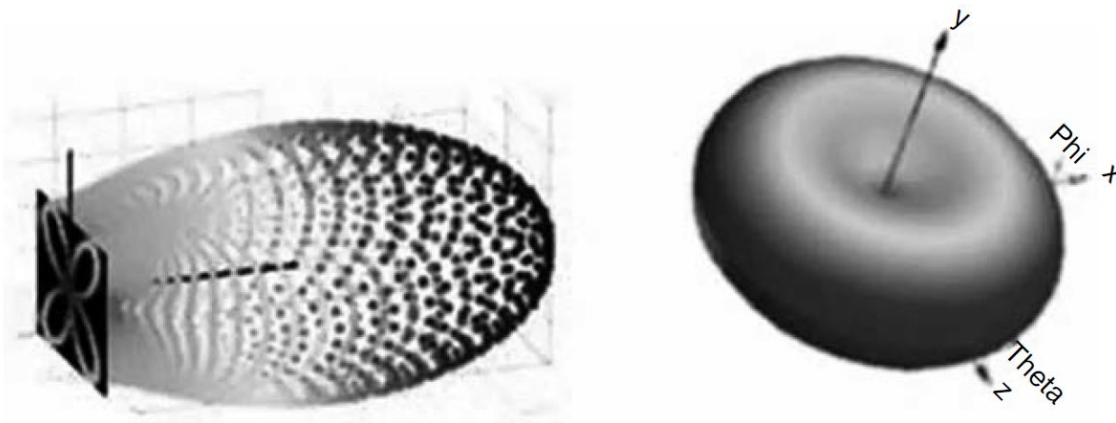
Figure 1.4: Left: a directional antenna with its interrogator radiation pattern. Right: an ideal dipole, which is formed around the wires of an RFID tag. From [12].

gist sits at the head of the bed to monitor the patient. Two surgeons are performing the surgery, each positioned on one side of the bed, and one nurse stands between the instrument table and the surgeons to hand them the necessary instruments. As the surgery is laparoscopic, the image of the camera is shown on the screen at the end of the bed. A top view of this setting is shown in Figure 1.5. The patient is covered with surgical drapes. The surgical drapes are held above the head of the patient, allowing the anesthesiologist to see the patient and the patient to breathe easily. Figure 1.6 shows a side view of the surgical setting. Here the raised drapes near the head of the patient are visible.

Direct measurements

Tracking the instruments can be done either by detecting the instruments on the instrument table or by detecting the instruments whilst they are being used in the surgical area. Tracking instruments on the instrument table has already been done [4], however, measurements obtained in this way are indirect because the instruments missing from the table are assumed to be 'in-use'. This causes false positives as instruments missing from the table are not necessarily 'in-use'. The instruments can be held by the nurse or not placed back on the table. Directly measuring the instruments in the surgical area has the advantage that misplaced instruments are not labeled as 'in-use'. Only the instruments present in the surgical area are registered.
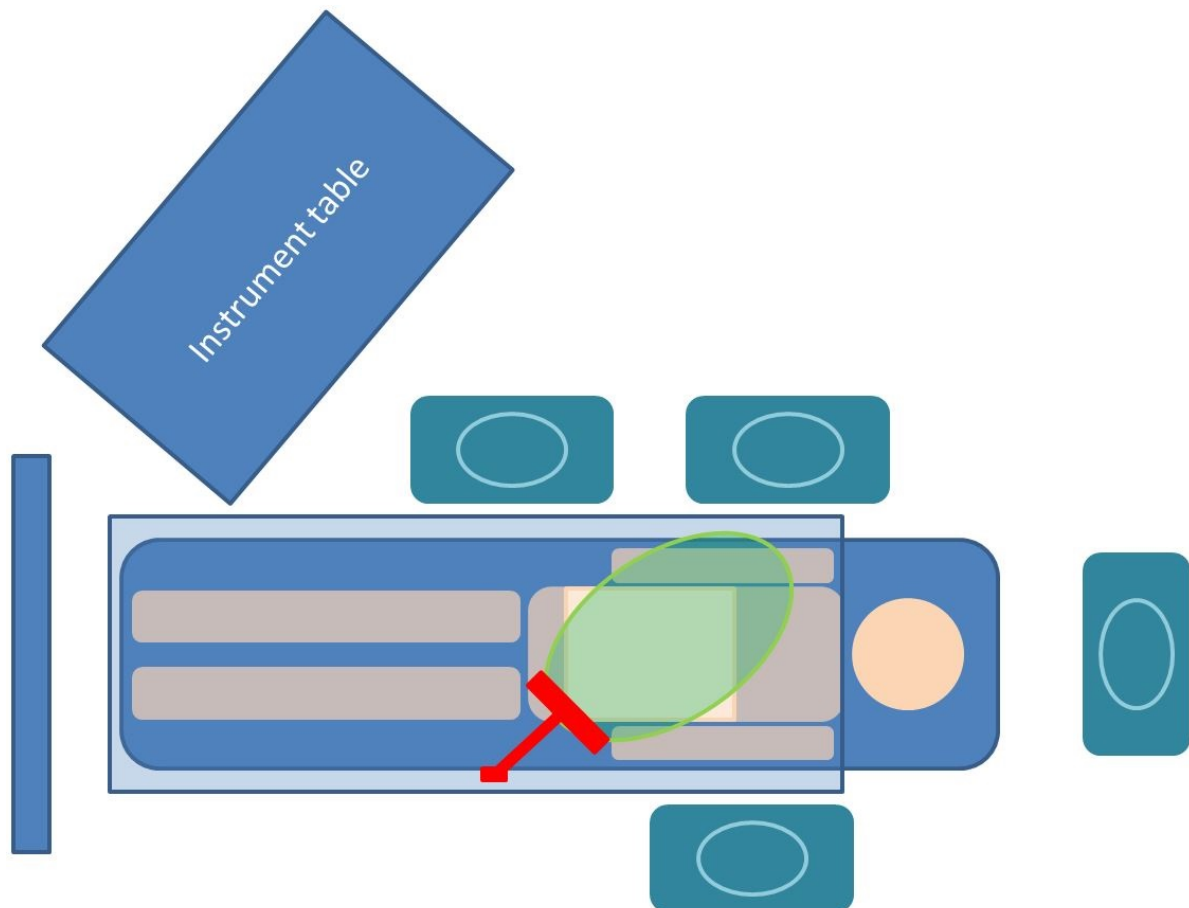
Figure 1.5: Top view of a schematic setting during a TEP procedure. Patient on the table, anesthesiologist at the head of the bed, one surgeon an each side of the bed, a nurse between the surgeon and the instrument table. A screen at the foot of the bed. The antenna connected to the bed is shown in red. The green area shows the desired detection range of the antenna.

Antenna with desired reading distance

In this study, the instruments are measured directly on the surgical area to minimize the detection errors. The antenna will be placed on the side of the bed next to the surgeon, opposite of the nurse, and will be facing the surgical area. Figure 1.5 and Figure 1.6 show the antenna in red placed on the side of the bed. The antenna will be attached to the surgical bed by an arm specially made for this application, explained in Appendix B. For this study, a directional antenna is chosen. This way, the measurements will not be performed in a radius around the antenna, but only in the area in front of the antenna.

To ensure all instruments used during the surgery are detected, a minimal reading distance of the instruments to the antenna is required. With the antenna placed on the side of the bed as shown in Figure 1.5 and 1.6, the required reading distance to cover the entire surgical area is 50 cm. With these 50 cm, not only the surgical area is covered, but also a small area around the surgical area. This is shown in Figure 1.5 by the green area.

1.8. Research Scope

The aim of this study is to track surgical instruments inside the OR during procedures. Tracking provides the information about which instruments are used during different phases of the surgery. With this information, an algorithm can be used to perform phase recognition. When different phases of a procedure can be distinguished, the progress of the procedure can be tracked. This information can then be used to make a prediction of the end time of the procedure. The current phase of the procedure can be communicated to the staff outside the OR, making it possible to optimize the workflow around the OR. It will also improve the communication, as more information is available without extra work
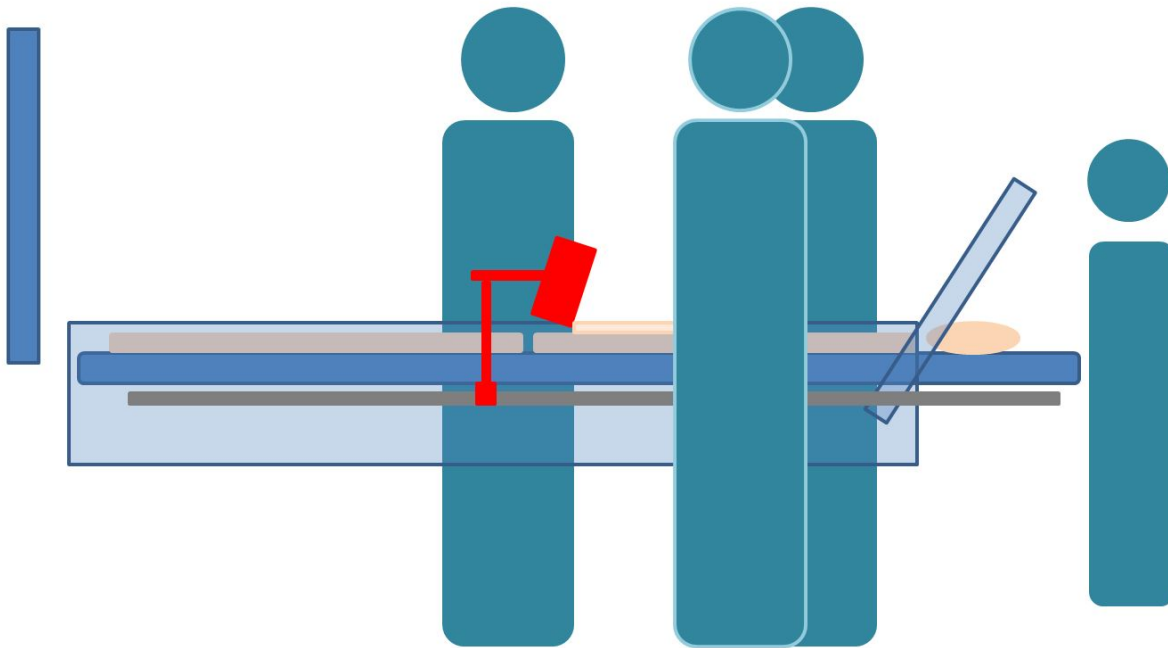
Figure 1.6: Side view of a schematic setting during a TEP procedure. Patient on the table, anesthesiologist at the head of the bed, one surgeon an each side of the bed, a nurse between the surgeon and the instrument table. A screen at the foot of the bed. The antenna connected to the bed is shown in red.

for the surgical staff. This reduces the workload, making the OR a safer place as the chances of errors due to distractions and an excessively high workload are reduced. Furthermore, less visits from staff outside the OR are needed. The measurements of the instruments will be done directly on the surgical area instead of indirectly on the instrument table.

1.9. Thesis Outline

In Chapter 2, a pilot study with Van Straten Medical instruments is done to evaluate the current state of the technology and to determine whether this technology can be directly used in in-vivo tests in the OR. Chapter 3 summarizes the pilot study and provides an outline of the continuation of the study. Chapter 4 outlines the approach to test the maximal reading distances of RFID tags on different metal plates. Furthermore, the methods used to test the final design are explained. Chapter 5 shows the maximal reading distances obtained in the experiments. The influences of the tested parameters are shown here. The results will be discussed and interpreted in Chapter 6. The chapter concludes with a composition of the final design. In Chapter 7, the final design is elaborated. Furthermore, the results of the experiments with the final design are given. In the Discussion in Chapter 8, the results will be interpreted. The outstanding results will be discussed and the limitations of the study will be explained. The report will be concluded with some recommendations for future work.

Appendix A, explains the current use of RFID in hospitals and looks into the question whether it is safe to use RFID in a hospital. In Appendix B, the requirements of the antenna arm used to position the RFID antenna in the OR are given. Furthermore, the final antenna arm is explained and shown. Appendix C shows the results of all experiments discussed in this report. In Appendix D, an extra experiment that is not included into the report is shown. Furthermore, the results of this experiment are also given. This experiment was performed in case all types of casings would turn out to be blocking the signal. The next appendix, Appendix E, shows the detailed drawing of the two versions of the final design. In the final appendix, Appendix F, the Matlab codes used during this study are presented.

2

Pilot Study

The pilot study was performed with a complete set of surgical instruments for a totally extraperitoneal (TEP) procedure, all equipped with RFID tags by Van Straten Medical BV, the Netherlands. Figure 2.1 shows four of the instruments with RFID tags. The tags are placed on a metal plate and a metal casing surrounds the tag. The casing is covered with a protective layer of epoxy to protect the RFID tag from the extreme temperatures during the sterilization process. To ensure the CE mark of the instruments is not affected the metal plate is attached without making permanent changes to the instruments. Currently, the connection of the attachments is welded to itself enclosing the instrument and not welded to the instrument so when the tags have to be removed the instruments are unaffected. The tagged instruments are ready for use in the OR; only the reading distances of the instruments are still uncertain.

For in-vivo testing the instruments must be detected at at least 50 cm from the antenna. This distance is determined by analysing TEP procedures. In the analysis, the surgical area, the possible placement of the antenna, and the area the instruments used are taken into account. With a range of 50 cm, the detection of the used instruments in the surgical field during the operation should be ensured.
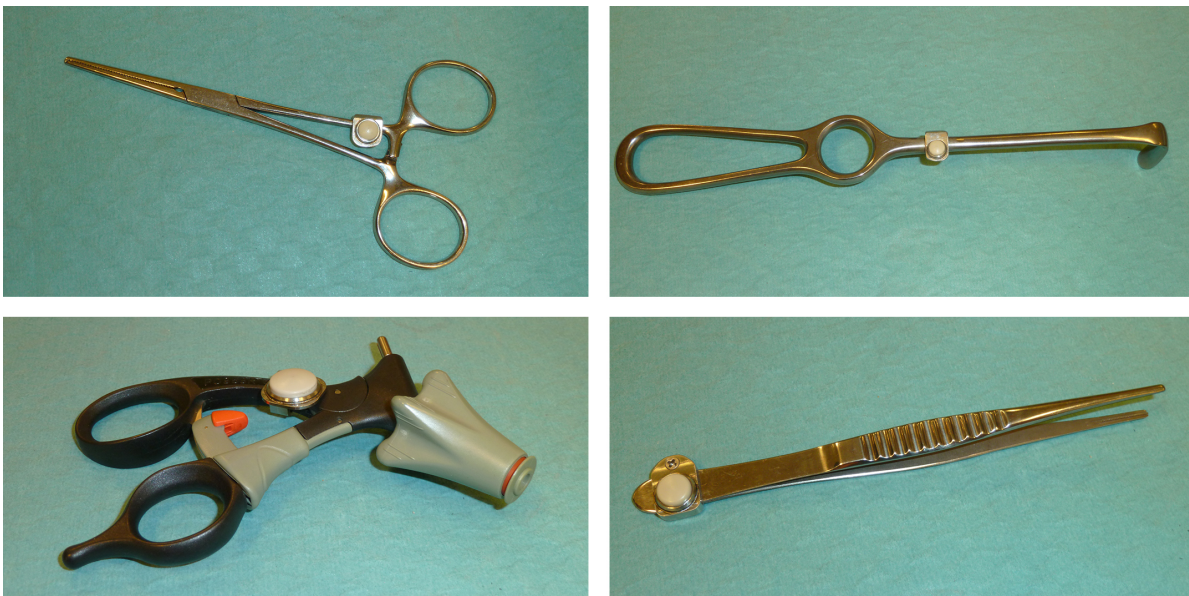
Figure 2.1: Four instruments tagged with RFID tags by Van Straten Medical BV. Within each white circle added to the instruments a RFID tags is located.

2.1. Method

The following section explains the method to test the maximal reading range of the RFID tags. First, the composition of the RFID system is explained. Next, the system specifications will be given. Third, the used test set-up will be shown and finally, the followed test procedure will be explained.

2.1.1. General RFID System

To be able to detect RFID tags, an RFID set is required. A set consists of RFID tags, an antenna, a reader, and a computer with software suitable for the RFID set, see Figure 2.2. With the computer, the reader can be turned on. The reader sends out electromagnetic waves via the antenna that forms a magnetic field when it couples with the antenna on the tag. The tag gets power from the reader and sends information back. This information is intercepted by the antenna and sent to the reader. The reader is connected to a computer, which can store and show the tags with software.
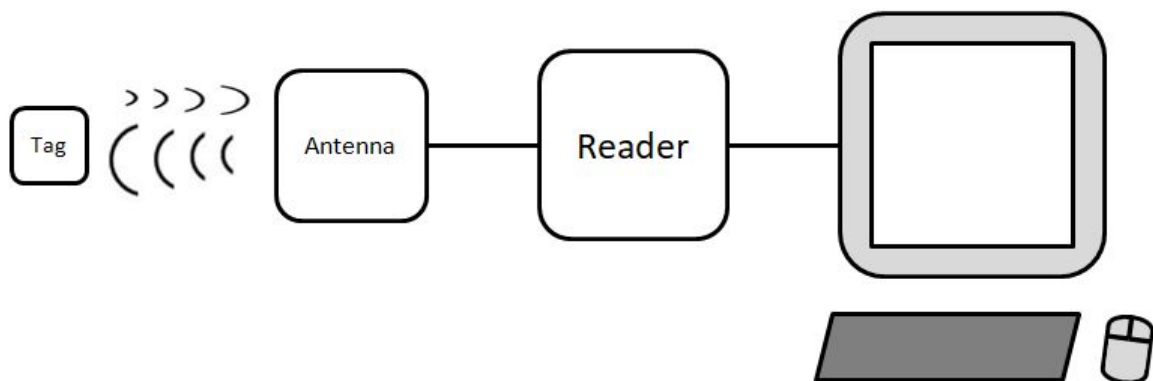
Figure 2.2: Schematic overview of an RFID system; tag, antenna, reader, and computer with software. On the right a computer is connected to the reader. The computer activates the reader, which sends a signal to the antenna. The antenna sends out radio waves. The radio waves are intercepted by the RFID tag and the backscatter of the tag is captured by the antenna and communicated back to the computer through the reader.

2.1.2. System Specifications

The system uses ultra high frequencies (UHF), which are frequencies from 866 to 868 MHz. The reading distances are tested with a reader, two antennas, and software from Harting BV, Germany. The used reader is RFID Reader RF-R500-c-EU, with an output power of $0.3W - 2W$, and a frequency range of $860 - 960$ MHz. The first antenna is Ha-VIS RF-ANT-MR20-EU, with a frequency range of $865 - 870$ MHz and a power of 0.5W ERP, see Table 2.1. The second antenna is Ha-VIS RF-ANT-WR30-EU, with a frequency range of $865 - 870$ MHz and a power of 2W ERP. The software is Ha-VIS RFID Config V2.05.02, which stores and displays information about the tags. The experiment is first conducted with Antenna 1 and then repeated with Antenna 2.

Van Straten Medical used two different types of Xerafy tags on the instruments. The first type is the Xerafy Dot-On XS and the second type is the Xerafy Dash-On XS, see Table 2.1. These tags work in a frequency range of 866-868 MHz and are detectable up to respectively 1.5 m and 2 m.

2.1.3. Test Set-Up

The set up shown in Figure 2.3 is used for this experiment. During the experiments either Antenna 1 or Antenna 2 was used. Antenna 1 is the plate on the left circled in red and Antenna 2 is the larger plate on the left with the blue circle. The second antenna is larger to increase the maximal reading distance, as size of the antenna is an influencing factor according to Ahson et al. (2005) [12], as explained in Section 1.6. The used antenna is connected to the reader. The reader is connected to an HP laptop, running software from Harting BV. The tags will be tested in the open space in front of the reader. The area of the table in front of the antenna is 96 cm x 60 cm, the area next to the table is empty, so if more space is needed, the tags can be moved away from the table. The table on which the experiments are performed is made of wood, as wood does not reflect or absorb radio waves like metal and water, to minimize the influence on the experiments.

Table 2.1: System specifications of the components used in the pilot study.

	Reader	Antenna 1	Antenna 2	Xerafy tags	Xerafy tags
Type	Ha-VIS RFID Reader RF-R500-c-EU	Ha-VIS RF-ANT-MR20-EU	Ha-VIS RF-ANT-WR30-EU	Dot On XS X4102-EU000-H3	Dash XS X4101-EU040-H3
Frequency	865-870 MHz	865-870 MHz	865-870 MHz	866-868 MHz	866-868 MHz
Power	2 W	0.5 W ERP	2 W ERP	-	-
Dimensions (LxWxH)	70x260x153 mm	156x126x25 mm	270x270x45 mm	$\varnothing$6x2.5 mm	12.3x3x2.2 mm
Reading range	Wide range Up to 16 m	Mid range Up to 2 m	Wide range	Mid range Up to 1.5 m	Mid range Up to 2 m

2.1.4. Test Procedure

To test the reading range of the tags, the following steps are taken.

Step 1: Start position

The measurement starts with the tag touching the antenna. The tag is held approximately 13 centimeters above the table, in the centre of the antenna.

Step 2: Signal detection

When the tag is detected by the antenna and software, the tag is moved further away from the antenna, still held in the middle, until the signal is no longer detected. The output of the antenna is set to 2W by the software and is sampling the tag once per second.

Step 3: Second signal detection

Upon loss of signal the tag will slowly be moved back towards the antenna, until the signal is detected again for 3 seconds. Then the tag is again slowly moved away from the antenna until the signal is lost again. Next, the tag is moved to the antenna to recover the signal for the third time, with an even slower movement to reduce the movement during the sampling time.

Step 4: Final detection range

As these movements get smaller and slower, the maximal reading range of the tag is determined by reading the distance on the tape measure, see Figure 2.3. If the steps are still >1 cm after the third time the tag is detected, the same steps can be repeated.

The maximal reading distance of each instruments is individually tested, first with Antenna 1 and subsequently with Antenna 2. The test is performed once per instrument, per set-up. According to Ahson et al. (2005) [12], the best results will be accomplished when the RFID tag is facing the antenna. This is the orientation the instruments are tested in.

2.1.5. Data Analysis

From the tests, the maximal reading distance of each instrument will be measured. The distances will be rounded up to a whole number. The individual results are shown in a graph made with Matlab displaying the maximal reading distance per instrument and the average reading distance per antenna. To compensate for outliers, the 3σ rule is applied [16]. This means that when a value is higher than $\mu + 3 * \sigma$ or lower than $\mu - 3 * \sigma$, the value is not taken into account .

2.2. Results

Figure 2.4 shows the results of the reading distances obtained with the Antenna 1 on the left and Antenna 2 on the right. The experiment with Antenna 1, shows reading distances ranging from 0.5 cm from the antenna to 65 cm. The green line in the figure is the desired reading range, which is at 50 cm. As can be seen in the figure, four instruments were detected at a reading distance of more than 50 cm. The red line shows the average reading distance of all instruments and is 21.08 cm.

The second experiment, displayed on the right, was conducted with Antenna 2. As in the figure on the left, the green line shows the desired reading distance of 50 cm. The reading distances vary from 6 cm to 85 cm. In this experiment, five instruments were detected above the desired 50 cm line. The red
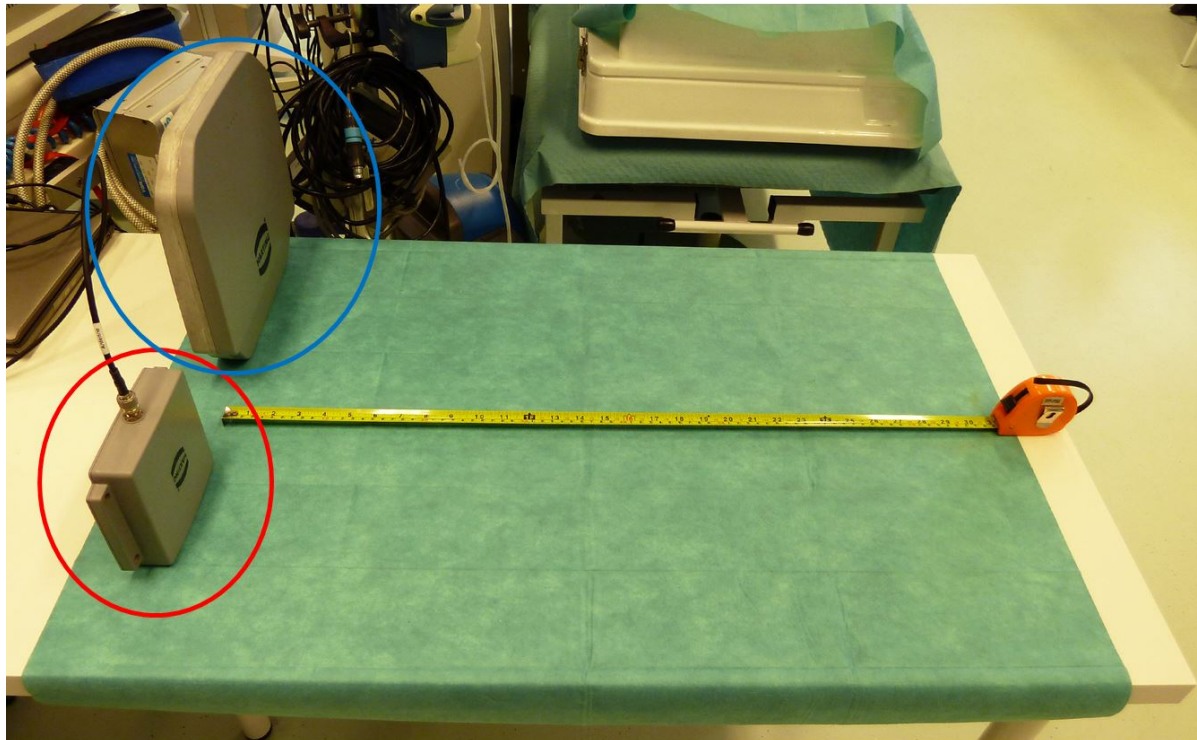
Figure 2.3: The test set-up in the clinical lab at the TU Delft. Antenna 1 is circled in red and Antenna 2 is circled in blue. The instruments are tested in above the table in the centre of the antenna.

line is the average reading distance and is 32.37 cm. As can be seen in the figure, the maximal reading distances obtained with Antenna 1 is significantly lower than the maximal reading distances obtained with Antenna 2 (p=0.0200). However, both averages are still below the desired reading distance.

2.3. Discussion

In the pilot study, the different maximal reading distances of the surgical instruments equipped with RFID tags by Van Straten Medical are determined. The reading distances are determined for two test set-ups, the first with Antenna 1 and the second with Antenna 2.

The desired reading distance for the instruments during a surgical procedure is at least 50 cm from the antenna. To be able to detect all instruments during surgery the used tags need to have a reading distance of at least 50 cm from the antenna. Figure 2.4 shows the reading distances obtained in the pilot study. The average reading distance for Antenna 1 is 21.08 cm and for Antenna 2 is 32.37 cm. These reading distances are too low as they are below the desired reading distance. In the experiment with the Antenna 1, only four of the 30 instruments were detected above the desired reading distance of 50 cm and with Antenna 2, only five of the 30 instruments were detected above the 50 cm. From these data, it can be concluded that the maximal reading distances obtained with the combination of either of the antennas and the instruments with tags fabricated in this manner are not far enough for this research. According to the specifications of the tags, the reading range of the used RFID tags on metal is for the first type up to 1.5 m and for the second type up to 2 m. The reading ranges obtained in this study are up to 85 cm, this is lower than can be expected from the manufacturer. The shorter reading ranges can be caused by metal plates behind the tags, the casing of the tags, the attachment to the instruments, or the protective layer of epoxy. To be able to use RFID tags to identify instruments and trace them during an operation, the problem needs to be identified and eliminated by creating a system that is detectable further away from the antenna.
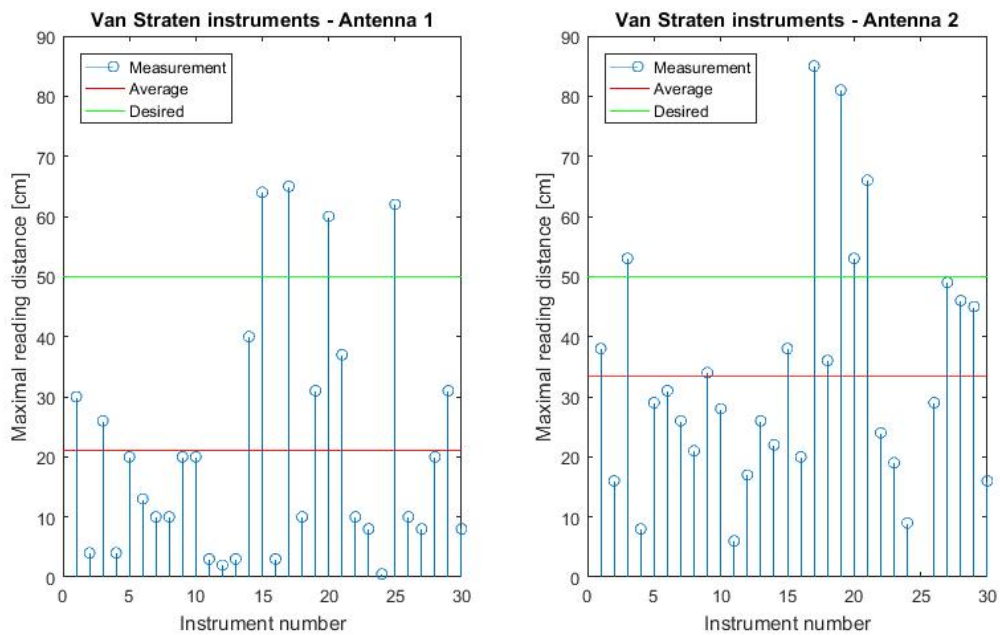
Figure 2.4: Reading distances of the instruments, the desired reading distance, and the average reading distance. Left the results with Antenna 1, right the results with Antenna 2. The red line is the average reading distance obtained with the instruments, the green line is the desired reading distance of 50 cm, and the blue dots are the obtained reading distances per instrument. Every instruments is tested once per antenna.

2.4. Conclusion

The pilot study concludes that it is possible to detect the surgical instruments for a TEP procedure with RFID technology in a lab setting. The maximal reading distances obtained with the current antennas from Harting BV and the attachment and casing, made by Van Straten Medical, are not far enough for in-vivo testing. The desired reading distance of 50 cm is needed for in-vivo testing, to ensure the instruments are detected during the operation. As only by five of the 30 tested instruments reached the desired reading distance, the range has to be increased. In this study, the problem will be identified and eliminated for the current RFID system.

<div align="right">

3

</div>

Research Outline

3.1. Research Motivation

As explained in Section 1.7, the desired reading distance of the instruments is 50 cm. According to the specifications of the tags, they should be detectable up to 1.5 and 2 m. In the pilot study with Antenna 1, only four of the 30 instruments were detected above the desired reading distance of 50 cm. Antenna 2 detected five of the 30 instruments above 50 cm. The averages for Antenna 1 and Antenna 2 are, respectively, 21 cm and 32 cm. These distances are not long enough for application in the OR and the maximal reading distance of the instruments needs to be increased. To increase the reading distance, the limiting factor in the set-up needs to be identified and eliminated.

3.2. Aim of the Study

The aim of this research is to identify and eliminate the problem of the set-up from the pilot study and thereby obtaining the desired reading distance of 50 cm. This will be done by answering the main question and the two subquestions. The main question in this study is:

- *Is it possible to increase the maximal reading distance of RFID 'on-metal' tags up to 50 cm with the current set-up?*

The subquestions are:

- *Can the detection distance be increased to an average of at least 50 cm by changing the set-up?*

- *What factors of the casing design influences the maximal reading distances of the RFID tags?*

Different aspects of the set-up can be causal the limited reading distance. The pilot study showed that a larger antenna increases the reading distance. The increase was, however, not big enough for the application. The detection distance could be increased by using an even larger antenna or by using a higher power through the antenna. However, 2 W is already the maximum allowed power in the EU. Using an even larger antenna could be a solution, this is, however, not desired for the operating room, as the system should not obstruct the surgery even further.
The current RFID system should already be able to detect the tags on the desired reading distance based on its specification, so it is preferred to try and solve the problem for the current set-up. Looking at the current set-up, excluding the antenna and its power, the hypothesis is that the casing around the RFID tag is limiting the maximal reading distance. The scope of this research is to study the casing of the tags, and the basic metal plate properties.

3.3. Approach

Finding the limiting factor in the current method will be approached by first looking at the basic properties of the metal plate behind the tags. As the tags are 'on-metal' tags, they need the metal plate behind the tag to better receive the signal from the antenna [17]. First, the basic properties are tested,

starting with the surface area of the metal plate, the thickness, and the bar length of the plate. Furthermore, the tags are tested on a plate with cut-outs, to see the influence of missing pieces of metal on a surface. Next, the tag is clamped between two plates to see if the signal can still be detected through metal plates on both sides. With the information obtained from the basic properties tests, the possible enclosures around the tags can be evaluated. The enclosure in the pilot study fully surrounds the tag by a metal wall, to ensure the placement of the tag. Therefore, the first casing test will also be a full enclosure of the tag and and later on partial enclosures will also be tested and compared to previous results. As the plates with the enclosures are made with a 3D printer, they have a rough surface between enclosures as these places are hard to reach with polishing tools. To test the effects of the rough surface of the metal plates, the tags are also placed on a rough surface, outside the enclosures, to see if the detection distance is better or worse than on the smooth surface. The tags are shielded by a layer of epoxy to protect them from extreme circumstances during sterilization. As the tags were completely coated during the pilot study, the interfering abilities of epoxy on the reading distance will be tested by placing pieces of epoxy in varying sizes and thicknesses in front of the tags.

3.4. Final Design

The final design is created based on the combined information acquired from the basic properties tests, the casing properties tests, the surface test, and the protection layer test. In this final design, the most promising properties are combined. After the design is created, it will be made with a 3D metal printer and tested first in the lab, to measure the detection distances. Afterwards, the design will be tested in an empty OR, to make sure that the results obtained in the lab are representative for an actual surgery. Finally, the final design will also be tested with the small antenna from the pilot study, to see if it is possible to use this antenna. Using the smaller antenna would be preferable to the large antenna, as chances of the small antenna getting in the way of the normal procedure are smaller than with the large antenna.

4

Method

4.1. System Specifications

As explained in Section 2.1.1 an RFID set consists of RFID tags, an antenna, a reader, and a computer with software suitable for the RFID set. For the experiments, the same reader, antennas and the Dot On XS tags are used as described in Section 2.1.2. Next to the Xerafy tags, HID Brick ceramic tags are also used for the experiments. The Xerafy tags can be detected up to a distance of 1.5 m and the HID Brick ceramic tags can be identified in a range of 2 m, see Table 4.1.

Table 4.1: System specifications of the components used in the experiments explained in this chapter.

	Reader	Antenna 1	Antenna 2	Xerafy tags	HID tags
Type	Ha-VIS RFID Reader RF-R500-c-EU	Ha-VIS RF-ANT-MR20-EU	Ha-VIS RF-ANT-WR30-EU	Dot On XS X4102-EU000-H3	Brick ceramic new MR6-chip
Frequency	865-870 MHz	865-870 MHz	865-870 MHz	866-868 MHz	866-868 MHz
Power	2 W	0.5 W ERP	2 W ERP	-	-
Dimensions (LxWxH)	70x260x153 mm	156x126x25 mm	270x270x45 mm	$\varnothing$6x2.5 mm	5x5x3 mm
Reading range	Wide range Up to 16 m	Mid range Up to 2 m	Wide range	Mid range Up to 1.5 m	Mid range Up to 2 m

4.2. Test Set-Up

Lab set-up

To measure the influence of the metal plate geometry on the maximal reading distance of the RFID tags, a similar set-up as in the pilot study was used (Section 2.1.3). The set-up is built in the clinical lab at the TU Delft. Two set-ups are made, the first with Antenna 1 and the second with Antenna 2. The antenna is placed on the wooden table and the tags are held in front of the antenna to measure the maximal reading distance of the RFID tags, see Figure 4.1 where Antenna 1 is circled in red and Antenna 2 is circled in blue. Table 4.2 shows the performed experiments and which set-up is used.

OR set-up

The experiment in the OR is performed at the Reinier de Graaf hospital in Voorburg. For the experiment, the antenna is placed on the side of the OR table and connected with an arm, see Figure 4.2. The antenna is connected to the side of the bed with an arm designed for this study, see Appendix B. The antenna is aimed towards the surgical area on the table and connected to the reader. The tags will be tested in the open space above the OR table and ultimately in the space next to the table, if the tags are still detectable beyond the table. During the experiments, the laminar airflow around the OR table

17

Table 4.2: Overview of used components during the performed tests.

	Antenna 1	Antenna 2	Xerafy tags	HID tags
Pilot study	x	x	x	
Basic properties		x		x
Surface area		x	x	x
Bar length		x		x
Thickness		x		x
Plate with cut-outs		x		x
Top and bottom plate		x		x
Casing properties		x		x
Full enclosure		x		x
Partial enclosure		x		x
Surface		x		x
Protection layer		x		x
Final design		x		x
In the lab	x	x		x
In the OR		x		x

will be turned on, as it is during surgeries. This test is not in-vivo as there will be no patient present. The test is performed to be able to compare the results of the lab with the results in a surgical setting in the OR.

4.3. Test Procedure

The test procedure to determine the maximal reading distance of the RFID tags consists of the steps explained in Section 2.1.4. This procedure is followed in the lab as well as in the OR. First, the start position is reached. Then, when the signal is detected, the tag is moved away from the antenna until the signal is lost. Third, the tag is moved back towards the antenna, until the signal is detected again and this time the tag moves slower. And fourth, the maximal reading distance is determined when the movement converges to less than one centimeter.

During the experiments, the RFID tags are placed in the centre of the plates and are attached to the plates by adhesive tape to make sure the tag is in contact with the metal plate, see Figure 4.3a. Even though tape is not always necessary when the tag is form-locked by the casing onto the metal plate, it is always used for consistency and to exclude the influence of the adhesive tape on the results. The experiments are performed in two orientations of the tag (Figure 4.3b). First, orientation A, where the RFID tag is facing the antenna. As earlier explained (Section 1.6), this configuration should result in the largest reading distance. The second orientation, orientation B, where the back of the metal plate is facing the antenna is tested as well. This position is supposedly the shortest reading distance according to the HID white paper [17], because of the metal blocking the signal.

4.4. Data Analysis

The dependent variable measured during the experiments is the maximal reading distance. The distances will be rounded up to a whole number. If the tag is not detected at all, even when placed against the antenna, the value zero is assigned to the test. This value was chosen instead of NaN to give an impression of the median value of the tests. When NaN would have been chosen, these measurements would not have been incorporated into the results, suggesting a better performance of the configuration during the tests.

The data of the maximal reading distances will be used to make boxplots in Matlab. To compensate for outliers, the 3σ rule is applied [16], meaning that when a value is higher than $\mu + 3 * \sigma$ or lower than $\mu - 3 * \sigma$, the value is not taken into account. A two-sample t-test is performed in Matlab to test whether the results had different means. The chosen significance level is $\alpha = 0.05$.
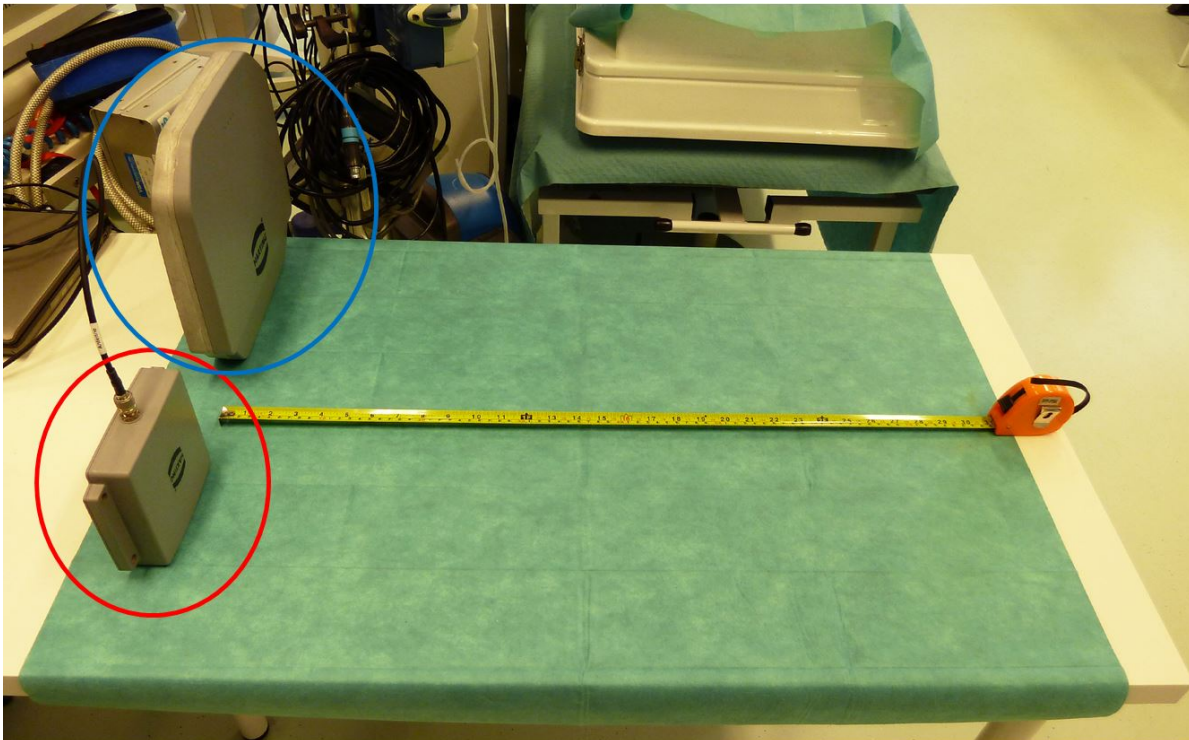
Figure 4.1: The test set-up in the clinical lab at the TU Delft. Antenna 1 is circled in red and Antenna 2 is circled in blue. The instruments are tested in above the table in the centre of the antenna.

4.5. Basic Properties

To explore the different properties of RFID 'on metal' tags, the first experiments are done to measure the influence of the basic properties of the metal plates on the maximal reading distance of the RFID tags. The plates are made of stainless steel by DEMO (Dienst Elektronische en Mechanische Ontwikkeling), Delft, the Netherlands. Stainless steel is chosen because this metal is allowed in operating rooms. Furthermore, Demo is able to print complex designs using a 3D metal printer, printing stainless steel. The dependent variable that will be measured is the maximal reading distance. The independent variables that will be tested are:

- Surface area

- Thickness

- Bar length

- Plate with cut-outs

- Top and bottom plate

For the experiments, three different HID tags and three different Xerafy tags are available, as mentioned in Table 4.1. Per test, the three tags are individually tested on each metal plate. The Xerafy tags are the same tags incorporated into the attachments in the pilot study. The Xerafy tags are unfortunately no longer available. To still be able to test influencing factors on the maximal reading distance, HID tags are used. The first experiment, the surface area test, is done with both the Xerafy and the HID tags, to be able to compare the results and to determine whether HID tags are a suitable replacement for the Xerafy tags. The other tests are only performed with the HID tags, see Table 4.2.

4.5.1. Surface Area

The first two experiments are performed to measure the influence of the volume of metal attached to the tag on the maximal reading distance. The volume of metal is the result of the surface area and
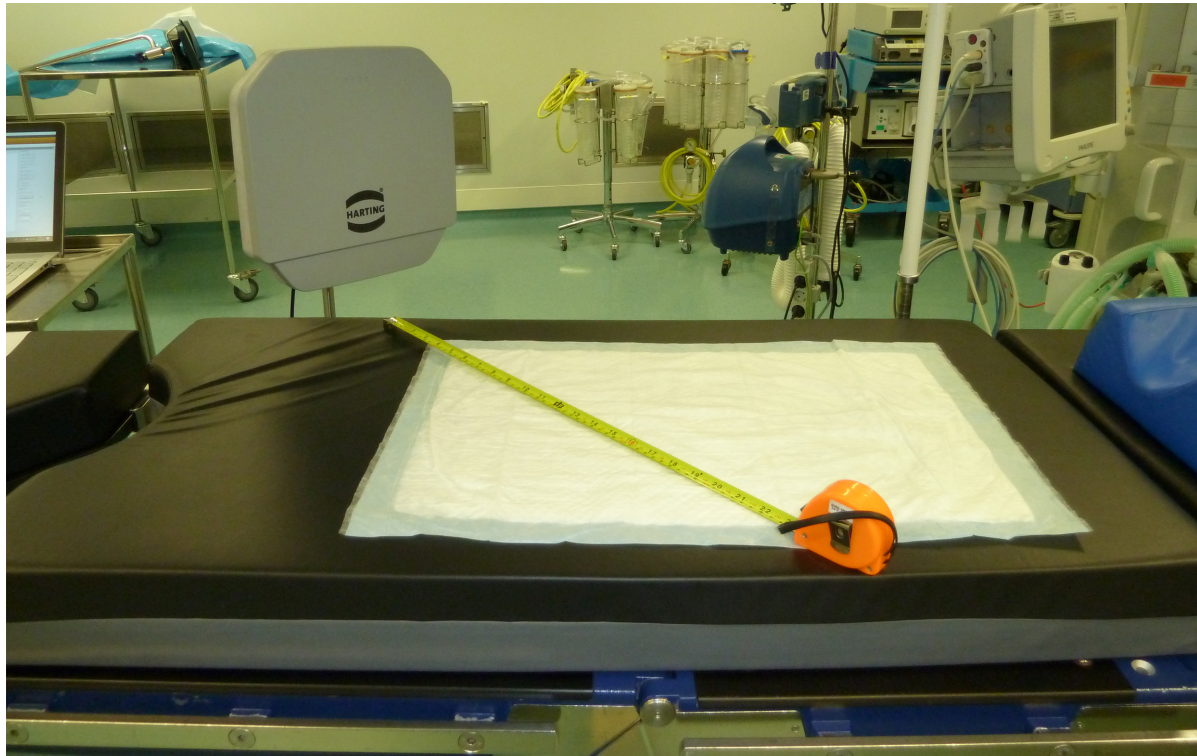
Figure 4.2: The test set-up in the OR at the Reinier de Graaf hospital in Voorburg. Antenna 2 is shown, the space in front of the antenna, above the surgical table is used to perform the experiments.

the thickness of the metal plate. The first experiment is performed to determine the influence of the surface area of the metal plate on the maximal reading distance.

The hypothesis is that a larger metal surface area behind the tag will result in a higher maximal reading distance. This because the tags are depending on the metal background [17]. The reading distance to the surface area is expected to follow a exponential function, first increasing rapidly and later stagnate to a maximal reading distance that does not increases anymore. The stagnation is expected because there is an expected maximal plate surface that is still useful. Even larger plates are expected to block the signal. The B orientation is, however, expected to decrease with an increase of surface area. This because the theory explains that metal objects between the tag and the antenna can block the signal [13]. Four stainless steel plates with increasing surface areas are tested, see Figure 4.4. The thickness of the four plates is 1 mm. The surface areas of the metal plates are 10x10 mm, 20x20 mm, 30x30 mm, and 40x40 mm. The smallest surface area of the metal plates is chosen as 10x10 mm because the tags have to be covered with a protection layer. To ensure there is enough space around the tag and that the tag itself will not be exposed during the sterilization, a margin of 2.5 mm is chosen around the tag. The 10x10 mm and 20x20 mm plates are both possible options for the tag attachment as the size of the plates is still relatively small. The 30x30 mm and 40x40 mm plates are tested to measure the influence of an increased surface area on the maximal reading distance. These sizes are, however, not realistic for the tag attached to the instruments as the plates are large relative to the instruments and they will impede the surgeon. The tags are placed in the centre of the plates and are kept in place with adhesive tape. This test is performed 24 times in total. The four plates are tested in the two orientations, resulting in eight unique configurations. Every configuration is tested three times, once for each tag. In this experiment, both the Xerafy and the HID tags are tested to learn whether the Xerafy tags, used in the pilot study, are comparable to the HID Brick ceramic tags.

4.5.2. Thickness
The metal plate thickness is the second factor contributing to the volume of the metal behind the tag. To determine the influence of the metal plate thickness on the maximal reading distance, four stainless steel plates of 20x20 mm are made with thicknesses of 0.5 mm, 1 mm, 2 mm, and 3 mm, see Figure
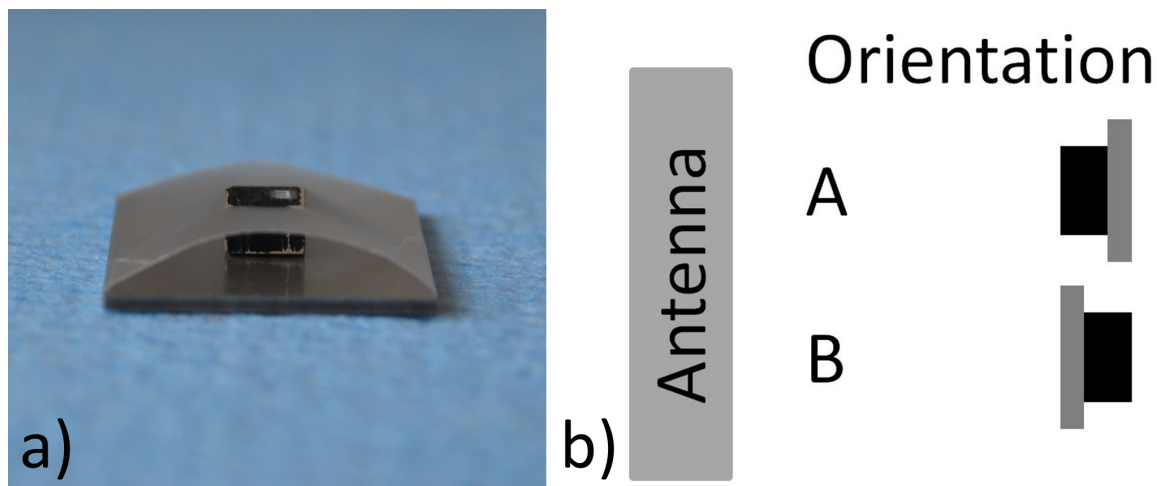
Figure 4.3: a) The RFID tag attached to the metal plate with adhesive tape, making sure the tag is in contact with the metal surface. b) Top view of the orientation of the RFID tags relative to the antenna.
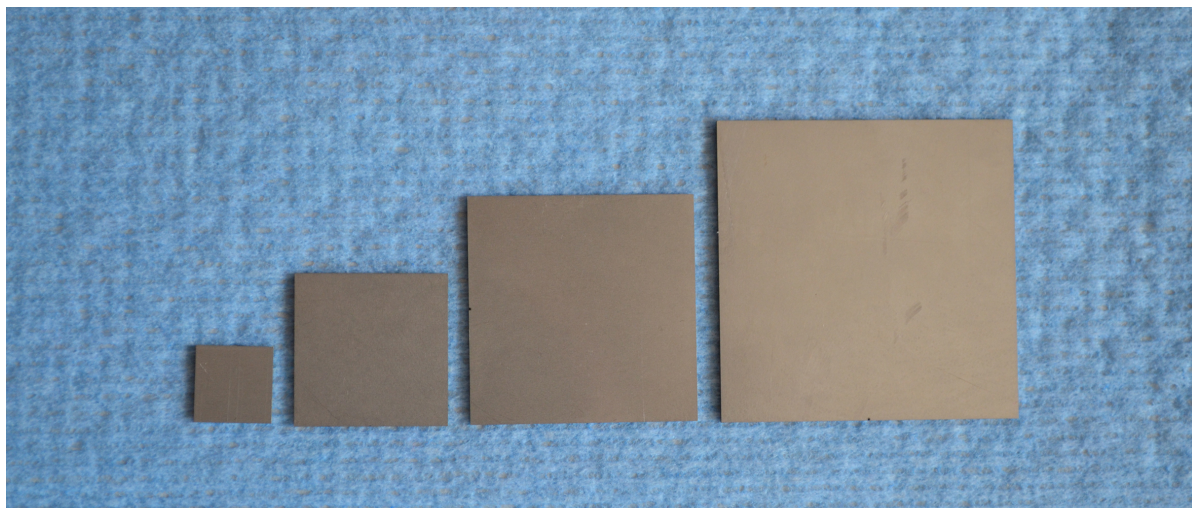
Figure 4.4: Different tested surface areas made of stainless steel; 10x10 mm, 20x20 mm, 30x30 mm, 40x40 mm, thickness 1 mm.

4.5. This range is interesting as the tags of the pilot study are 1 mm thick and this range covers both slightly thinner and thicker plates. The hypothesis is that thicker metal plates result in lower maximal reading distances. Metal is, according to Dobkin et al. (2005) [13], a disturbance and more metal is expected to disturb the RFID signal even more. This effect is mostly expected in the B orientation, when the metal is placed between the tag and the antenna. For this experiment, the HID tags are placed, with adhesive tape, in the centre of the plates. This test is performed 36 times in total. The four plates are tested in the two orientations, resulting in eight unique configurations. The configurations with the 0.5 mm and 1 mm thick plates are tested six times, twice for each tag. The configurations with the 2 mm and 3 mm thick plates are tested three times, once for each tag.

4.5.3. Bar Length
The influence of different bar lengths on the maximal reading distance is tested to determine whether it could be useful to create an attachment where the tag is placed further away from the instrument and the metal bar can function like an antenna. Furthermore, in a configuration where the bar is extended, the tag can be attached to a larger metal plate, whilst the plate does not have to grow in size in all directions equally. This is convenient for the surgeon as there is less obstruction of the workspace. The hypothesis is that larger bar lengths will result in higher maximal reading distances. Firstly, because
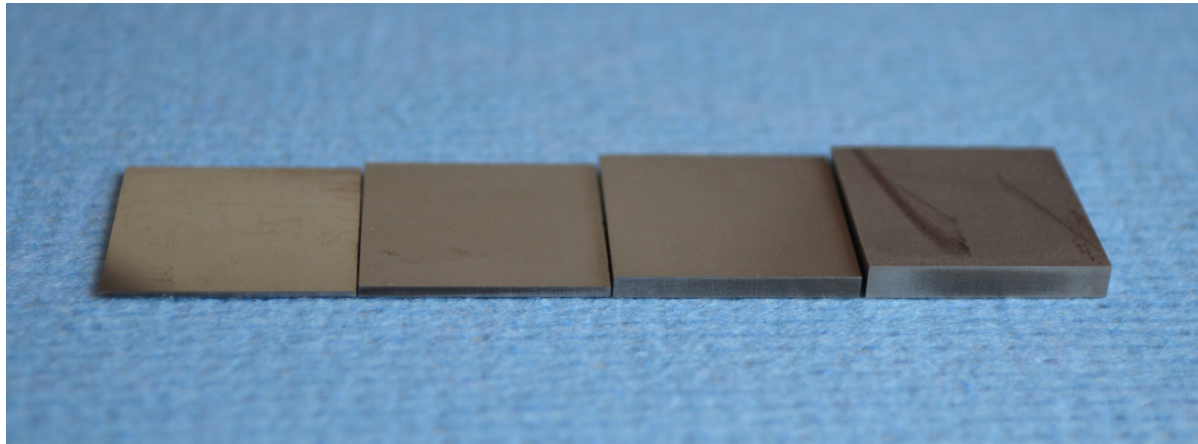
Figure 4.5: Four different plate thicknesses: 0.5 mm, 1 mm, 2 mm, and 3 mm, 20x20 mm surface.

the surface area of the metal plate increases with an increase of bar length and secondly, because the metal bar is expected to function like an antenna, picking up more signals when it is extended. For this experiment four stainless steel bars are made with a thickness of 1 mm and a surface area of 10x10 mm, 20x10 mm, 30x10 mm, and 40x10 mm, see Figure 4.6. The tags were placed with adhesive tape on both the corner of the stainless steel bars, see Figure 4.6a, and in the centre, see Figure 4.6b. This test is performed 48 times in total. The four bars are tested in the two orientations, once with the tag placed in the centre and once at the end of the bar, resulting in 16 unique configurations. Every configuration is tested three times, once for each tag.
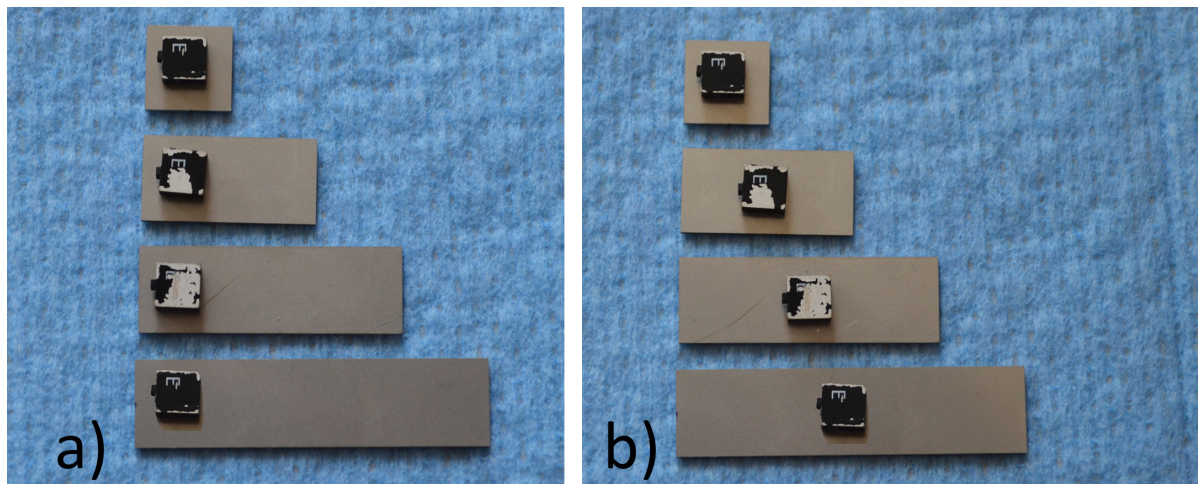
Figure 4.6: a) The four bars with the tag on the end of the bar. b) The four bars with the tag in the centre of the bar. Surface areas of 10x10 mm, 20x10 mm, 30x10 mm, and 40x10 mm and a thickness of 1 mm.

4.5.4. Standard Plate Size

To facilitate comparing different aspects, a standard plate size is chosen. The chosen surface area of the plate is 20x20 mm with a thickness of 1 mm. To be able to compare the variations to the standard plate size, an extra experiment is done where the tags are placed on the standard plates. During this experiment, the maximal reading distance of the standard plate is determined both with orientation A and B (Figure 4.3b). This experiment is repeated three times to gather more data and make the results more reliable. In total, this experiment is performed 18 times: the experiment has been repeated three times per tag in two different orientations.

4.5.5. Plate with Cut-Outs

To eventually attach the metal plate to the instruments, holes in the metal plate might be needed. The metal plate behind the RFID tags functions as an antenna to pick up RFID signal. Next to a solid metal plate, a plate with cut-outs could also function, like a grid antenna. To determine whether the cut-outs influence the maximal reading distance, a 20x20 mm plate with several cut-outs is made. The cut-outs are made in a shape similar to a hashtag, see Figure 4.7. The thickness of the plate is 1 mm, to be able to compare the results with the standard plate size. For the experiment, the tag is placed in the centre of the plate, see Figure 4.7a. The tag is placed on the metal plate with the cut-outs surrounding the tag, see Figure 4.7b. This is the same spot where the tag was placed with the 20x20 mm plate without the cut-outs. This test is performed 6 times in total. Once with each HID tag on the plate, in two different orientations. The hypothesis is that cut-outs in the metal plate do not affect the maximal reading distance. This is expected because a grid antenna also performs similar to a normal parabolic antenna [18].
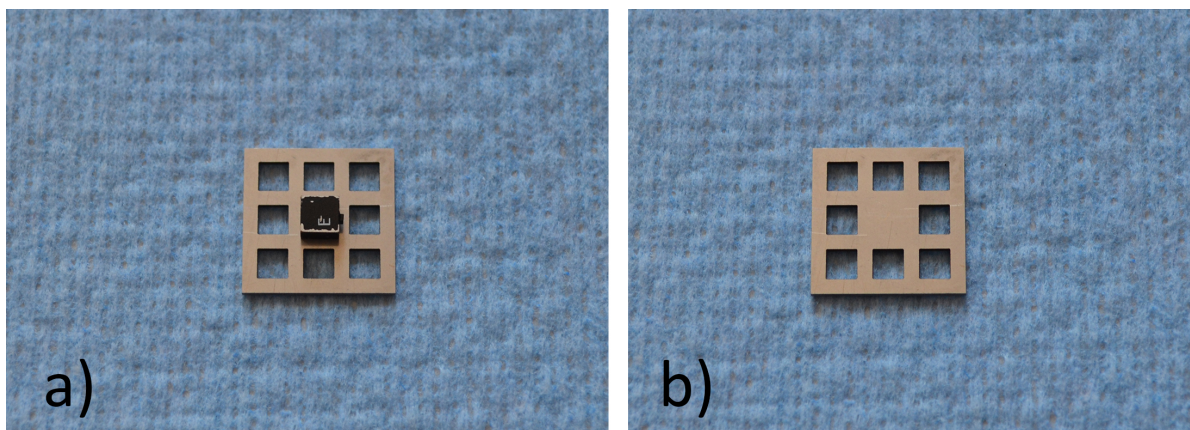
Figure 4.7: a) Tag placed in the centre of the plate with cut-outs of 20x20 mm, 1 mm thickness. b) Plate with cut-outs of 20x20 mm, 1 mm thickness.

4.5.6. Top and Bottom Plate

In theory, a metal obstruction between the tag and the antenna should decrease or even block the signal, resulting in a decrease of the maximal reading distance [14]. As the tags are also tested with orientation B, where the back of the plate is facing the antenna, it is also interesting to investigate if the tag is detectable when it is enclosed between two metal plates, see Figure 4.8. Enclosing the tag between two plates is one of the options to secure the position of the tag. For this experiment, two standard plates of 20x20 mm and 1 mm thick are used. The tag is placed in the centre of the first plate and the second plate is placed on top of the tag. For this experiment, only one of the plates is facing the antenna. As the plates are the same, the experiments is not performed in an other orientation. This test is performed 3 times in total: once with each HID tags between the plates.
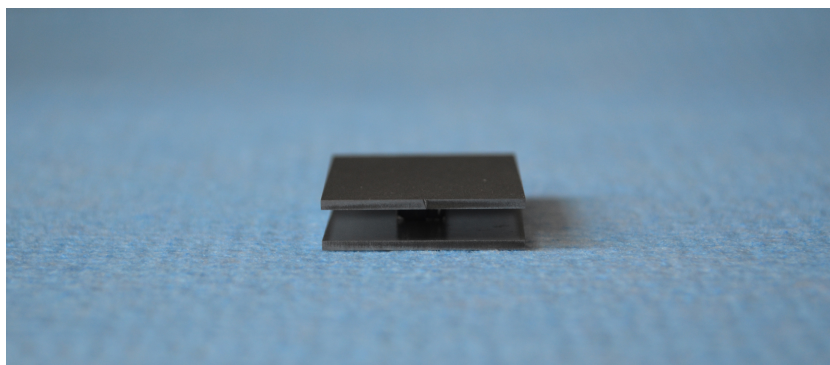
Figure 4.8: Tag between two 20x20 mm plates with a thickness of 1 mm.

4.6. Casing Properties

After the basic properties have been explored, more specific designs can be investigated. As seen in the pilot study, the instruments are placed in a casing to ensure the position of the tag on the bar. Placing the tag in the same position on every bar makes the end product more consistent and the results of the measurements more reliable. To measure the influence of different casings on the maximal reading distance, different casings are designed on the metal bars. The metal bars with the casings are made by DEMO with a 3D metal printer, printing stainless steel. The dependent variable that will be measured is the maximal reading distance. The independent variables that will be tested are:

- Full enclosure

- Partial enclosure

Furthermore, the 3D printed surface is rough, instead of the earlier tested smooth surfaces. A test is performed on the 3D printed bars to see the influence of the metal surface. The dependent variable that will be measured is the maximal reading distance. In this test the independent variable is:

- 3D printed surface of the bar

These tests are all performed with the three HID tags, see Table 4.1. Per test, the three tags are individually tested on each metal bar.

4.6.1. Full Enclosure

In the first design the tag is fully enclosed by the metal layer and secured on the bar, like in the pilot study. The position of the tag will be secured by the full enclosure on the bar. The hypothesis is that the full enclosure surrounding the tag decreases the maximal reading distance. The metal layer is expected to block the signal, because the dipoles around the wires of the tag [12] are disturbed by the enclosure. It is expected that the surrounding is a limiting factor in the pilot study. As Figure 4.9a shows, three different heights of enclosures are tested. From top to bottom, 3 mm, 2 mm, and 1 mm height are shown. The metal bar is 30x10 mm and the thickness is 1 mm. This test is performed 18 times. The three bars are tested in the two orientations, resulting in six unique configurations. Every configuration is tested three times, once for each tag.
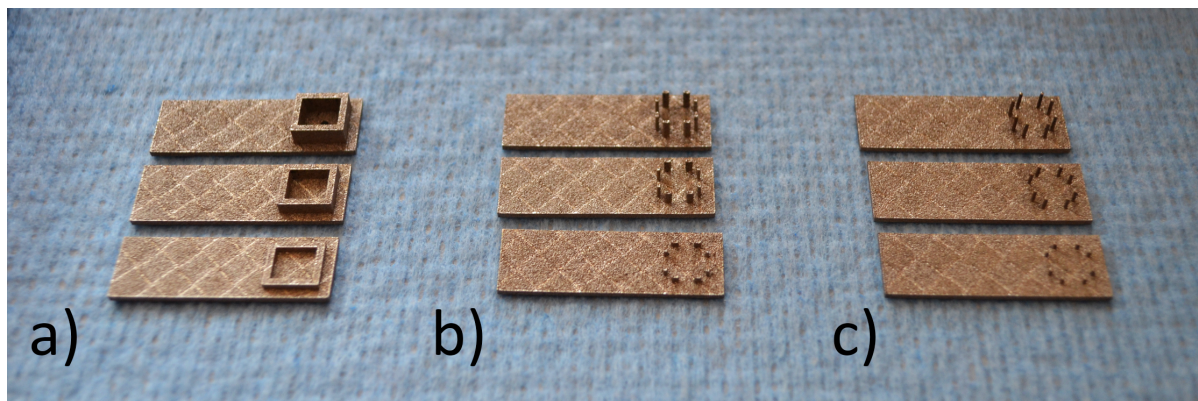
Figure 4.9: a) Metal bars with full enclosure around the tag. b) A partial enclosure made of metal bars with flat pins. c) A partial enclosure made of metal bars with round pins, from top to bottom height: 3 mm, 2 mm, and 1 mm.

4.6.2. Partial Enclosure

A full enclosure is not the only way to fix the positioning of the tags. Another option is to partially enclose the tags. To measure the influence of partial enclosures of the tag on the maximal reading distance, three types of partial enclosures are designed: the flat pins, the round pins, and the different corners. The designs are added to a metal bar of 30x10 mm and with a thickness of 1 mm. The hypothesis is that the reading distances of the partial enclosures are higher than the reading distances of the full enclosures. When the tag is only partially enclosed, the dipoles around the wires of the tags [12] are expected to be less disturbed. In total, this experiment is performed 48 times: once with all

three tags on each bar, in two different orientations. The three bars with the flat pins are tested in the two orientations, resulting in six unique configurations. Every configuration is tested three times, once for each tag. The same goes for the three bars with the round pins. And for the two bars with the two and four corners the two orientations are also tested, resulting in four unique configurations. Every configuration is tested three times, once for each tag.

Flat pins

For the first partial enclosure, parts of a full enclosure are removed leaving flat pins surrounding the tag and ensuring the position. This configuration is similar to the full enclosure, but there are gaps in the enclosure. Figure 4.9b shows the flat pins surrounding the tag. The tags are placed between the pins and three different heights are tested: 3 mm, 2 mm, and 1 mm.

Round pins

To minimize the contact area of the sides of the tag, possibly influencing the reading distance, a design with round pins is made. The pins are at the same positions as the flat pins in the previous design, the only difference is the shape of the pins. Here three different heights of the round pins are tested. The pins are from the top to the bottom, see Figure 4.9c, 3 mm, 2 mm, and 1 mm in height.

Different corners

When removing even more metal, the third design is made with only corners ensuring the position of the tag. The corners of the tags fall into corner parts on the metal bars, as can be seen in Figure 4.10a. The first bar, the upper bar in the figure, has only two corner parts on the diagonally opposing sides. The second bar, the lower bar in the figure, has four corner parts, one for each corner of the tag.
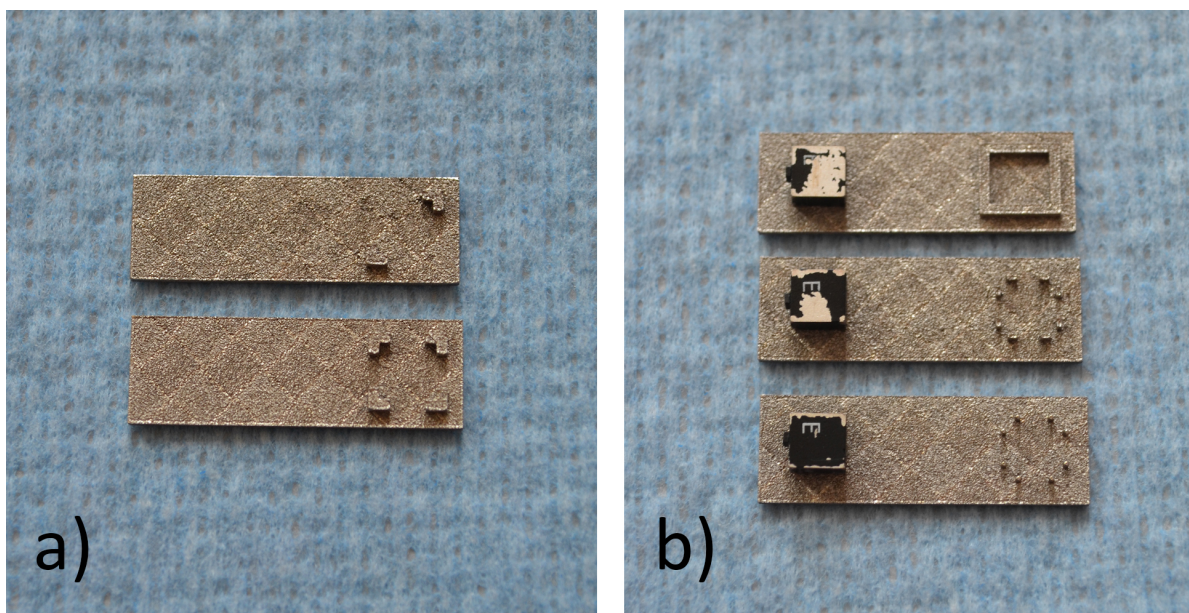
Figure 4.10: a) Metal bars with two corner parts (upper) and four corner parts (lower). b) Metal bars with the tag placed at the end of the bar, outside of the enclosures.

4.6.3. Surface

Due to production limitations the 3D metal printer can only create unpolished surface between enclosures, causing a rough surface instead of the smooth surface of the standard set up. To determine the influence of the rough surface on the maximal reading distance, the tags are also tested on the rough bars, this time not placed inside the enclosure but on the other end of the bar, as can be seen in Figure 4.10b. To make sure the enclosure at the end of the bar is not an influence in this test, three different enclosures are tested. First, the surrounding with a height of 1 mm; second, the two corners also with the height of 1 mm; and third, the round bars of 1 mm. These bars are the same as the ones previously used (Figure 4.9). The hypothesis is that rough surface is not of influence on the maximal

reading distance. The wires in the tag are not touching the metal plate directly, as they are surrounded by the casing of the tag, so the possibility of some air between the tag and the metal should form a problem. This test is performed 18 times. The three bars are tested in the two orientations, resulting in six unique configurations. Every configuration is tested three times, once for each tag.

4.7. Protection Layer

When the final design of the casing is made, the tags still need to be protected from the heat and extreme circumstance in the autoclave. This protection will be provided by covering the tags with a layer of epoxy. The epoxy used in the experiment is Araldite metal adhesive, an epoxy with hardener with a ratio of 100:25. To see if the epoxy is of influence on the reading distance, three different layers of epoxy are made and tested in front of the tags. Figure 4.11 shows the three different layers, the first layer (on the left) is a thin layer of about 1 mm. The second layer is thicker, about 2 mm and the third is in the shape of a bowl, so the outside of the layer is thick, about 6 mm and in the middle, a thinner layer about 2 mm is used, to enclose the RFID tag. The thickness of the side 6 mm high surrounding of epoxy is 5 mm. The tests are performed with the tags placed on the bar with the two corners, but at the end of the bar without the corners, as can be seen in Figure 4.10b. This test is performed 18 times. Once with all three tags covered by each layer of epoxy, in two different orientations. The three layers of epoxy are held in front of the tags and are tested in the two orientations, resulting in six unique configurations. Every configuration is tested three times, once for each tag. The hypothesis is that the epoxy does not influence the maximal reading distance. Epoxy is not a metal or dielectric, which are known to interfere with the signals [13]. Furthermore, it is recommended by Xerafy to use a layer of epoxy to protect the RFID tags [19].
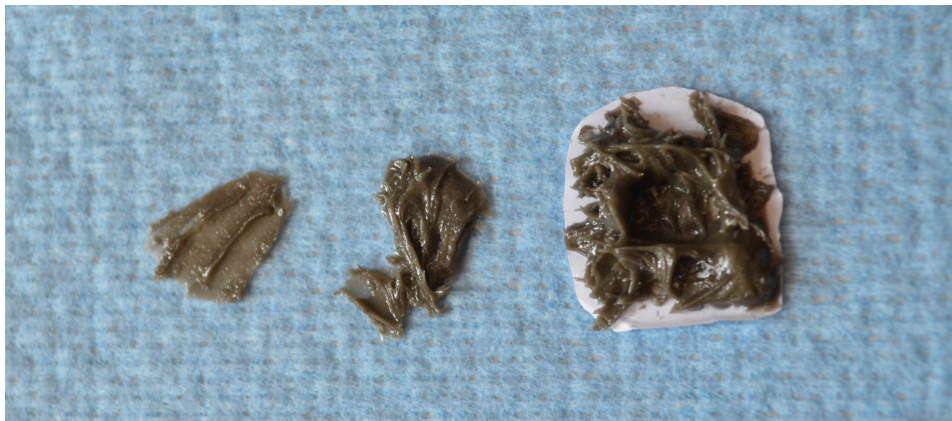
Figure 4.11: Three layers of epoxy, left to right: thin layer (1 mm), thick layer (2 mm), bowl (thick on the outside, thin in the middle).

4.8. Final Design

By combining the results from the previous tests, a final design is created.

In order to test the final design, an initial set of tests is done in the lab to see what the maximal reading distances are with Antenna 1 and Antenna 2. After determining the maximal reading distances in the lab, the final design will also be tested in the OR with Antenna 2. The tests in the OR are performed to see if the results in the OR are different from the results in the lab. As there are many devices present and active in an OR, it is possible that some interference or disruptions may occur. Finally the final design will be temporarily attached to surgical instruments to test the maximal reading distance on instruments. The experiments with the final design will be further explained in Section 7.2.

5

Results

In this chapter, the results of the experiments described in the methods chapter will be shown. For every test, the results of all three HID tags on each metal plate are used, both in orientation A and B (the tag facing the antenna and the back of the tag facing the antenna).

5.1. Basic Properties

5.1.1. Surface Area

The results of the experiments for the maximal reading distance of different surface areas are depicted in two boxplots, see Figure 5.1. The measurements used for these boxplots are the measurements of the surface area, explained in the Section 4.5.1. For the 20x20 mm plates with the HID tags, the measurements from the thickness where the plate is 1 mm thick (Section 4.5.2) and the standard plate size (Section 4.5.4) measurements are also included as these tests are performed on the same plate.
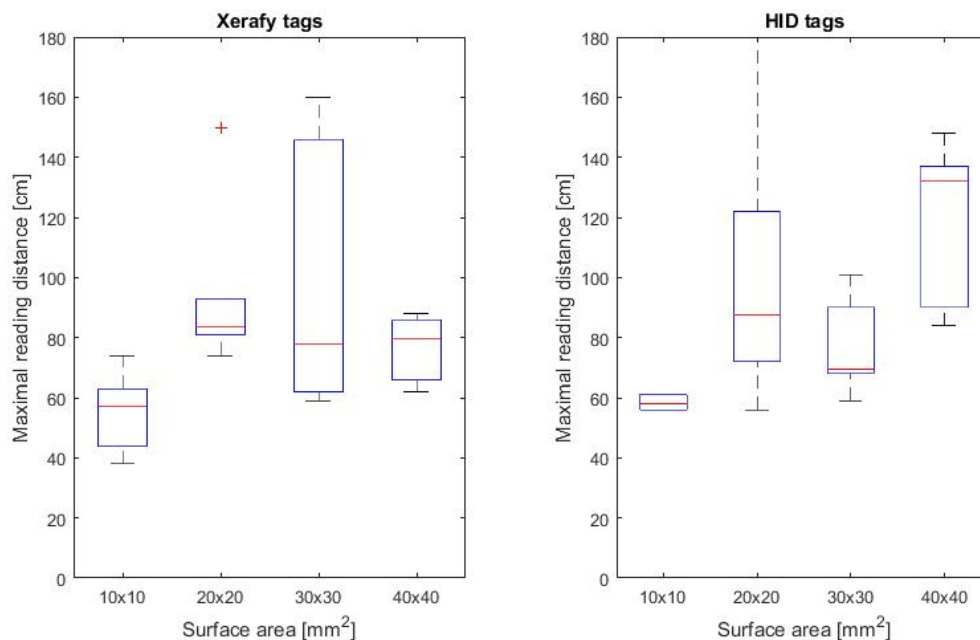
Figure 5.1: Boxplot of the maximal reading distances at different surface areas. Left, the experiments with the Xerafy tags per group n=6, right, the experiments with the HID tags the 20x20 mm group n=30, the other three groups n=6.

Figure 5.1 shows the two boxplots with the maximal reading distance of the four surface areas. On the left, the results with the Xerafy tags are shown and on the right, the results with the HID tags. The medians of the maximal reading distances vary for the Xerafy tags from 57 cm to 83.5 cm and

for the HID tags from 58 cm to 132 cm, see Table 5.1. As visible in the table, the medians of the 10x10 mm plates are for the Xerafy tags and the HID tags, respectively, 57 cm and 58 cm. However, the difference between the measurements is not significant. The differences between the tags on the 20x20 mm and the 30x30 mm plates are also not significant. However, the results of the 40x40 mm plates show a significantly higher maximal reading distance of the HID tag compared to the Xerafy tag ($p = 0.0003$).

Table 5.1: The medians of the Xerafy and HID tag measurements and the significance between the Xerafy and HID tests.

	Xerafy	HID	Significance
10x10 mm	57 cm	58 cm	No
20x20 mm	83.5 cm	87.5 cm	No
30x30 mm	78 cm	69.5 cm	No
40x40 mm	79.5 cm	132 cm	Yes ($p = 0.0003$)

To determine which surface area of the metal plate is optimal, a second order curve is fitted through the data of the maximal reading distances of the different surface areas of the HID tags (Figure 5.2 on the left). The curve starts at a surface area of 100 mm^2, is interpolated between 100 and 1600 mm^2, and extrapolates beyond the 1600 mm^2. When looking at this curve, it is expected that the maximal reading distance of the RFID tags improves with an increased surface area of metal behind the tag, as the figure shows an increasing curve.
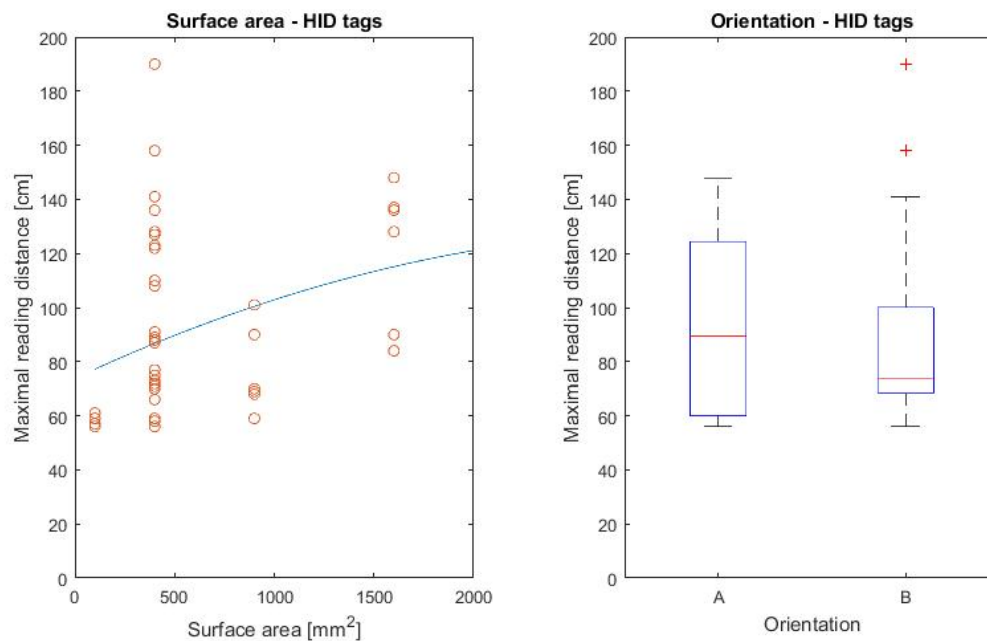
Figure 5.2: Left: A second order curve fitted through the data of the HID tags. Right: The results of the A and B orientation with the HID tags on the different surface areas per group n=24.

The boxplot 5.2 on the right shows the maximal reading distances in the A and B orientation. The medians of the maximal reading distance are 89.5 cm and 74 cm, respectively. The standard deviations are, respectively, 30.90 cm and 34.93 cm. The difference between the two groups is not significant.

5.1.2. Thickness
Figure 5.3 on the left demonstrates the influence of the thickness of a plate on the maximal reading distance of the HID tags. The data from the two orientations are combined in the boxplot. The figure shows that the medians for the 0.5 mm, 1 mm, 2 mm, and 3 mm thick plates are, respectively, 85.5

cm, 86.5 cm, 78.5 cm, and 84 cm. The standard deviations are 9.26 cm, 12.73 cm, 15.51 cm, and 4.56 cm. The difference in maximal reading distance between the groups is not significant.
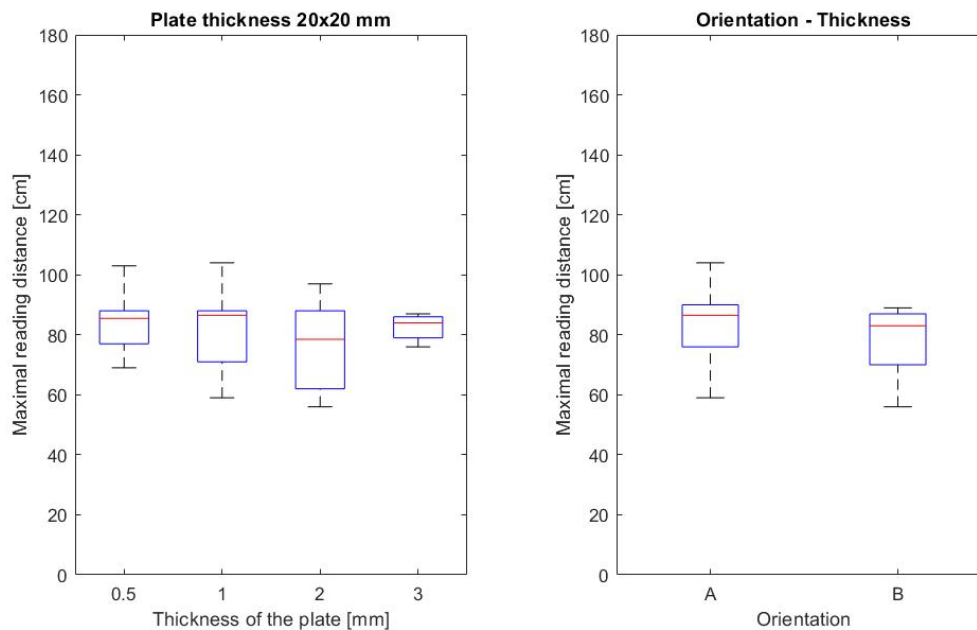
Figure 5.3: Left: Boxplot of the maximal reading distances of four 20x20 mm plates with a thickness of 0.5 mm, 1 mm, 2 mm, and 3 mm with HID tags, for the first two groups n=12, for the last two groups n=6. Right: The results of the A and B orientation on the 20x20 mm plates with the different thicknesses, per group n=18.

The boxplot on the right in Figure 5.3 shows the maximal reading distances in the A and B orientation of the plates with the different thicknesses. The medians of the maximal reading distance are 86.5 cm and 83 cm, respectively. The standard deviations are, respectively, 11.26 cm and 10.25 cm. The difference between the two orientations is not significant.

5.1.3. Bar Length
The maximal reading distance for the HID tags on the four bar lengths with a thickness of 1 mm is depicted in the boxplot in Figure 5.4. In this boxplot, the measurements of the bars with the tags on the corner and in the centre are combined. The medians are for the 10 mm, 20 mm, 30 mm, and 40 mm bars are, respectively, 58 cm, 58 cm, 56.5 cm, and 60 cm. The standard deviations of the measurements are, respectively, 2.22 cm, 1.90 cm, 3.13 cm, and 9.11 cm. The differences between the 10 mm, 20 mm, and 30 mm bars are not significant. The 40 mm bar has a significantly higher maximal reading distance compared with the 10 mm bar ($p = 0.0373$), the 20 mm bar ($p = 0.0242$), and the 30 mm bar ($p = 0.0328$).
The effect of the placement of the tag, either on the end or in the centre, on the maximal reading distance is shown in Figure 5.4. For this graph, data from bars with various lengths are combined. The figure shows that the medians are 58 cm and 58.5 cm. The standard deviations are 1.82 cm and 7.39 cm. The placement of the tag in the centre resulted in a significantly higher maximal reading distance than the placement of the tag at the end of the bar ($p = 0.0329$).

5.1.4. Different Shapes
The boxplot in Figure 5.5 compares effect of either a plate with cut-outs or a tag sandwiched between to plates on the reading distance with the reading distance of the reference plates (20x20x1 mm).

Standard plate size
To create the reference group in Figure 5.5, a combination of different measurements is taken. The used measurements of the maximal reading distance are from the standard plate size, the 20x20x1 mm plate of the surface area test, and the 20x20x1 mm plates from the thickness measurement. The
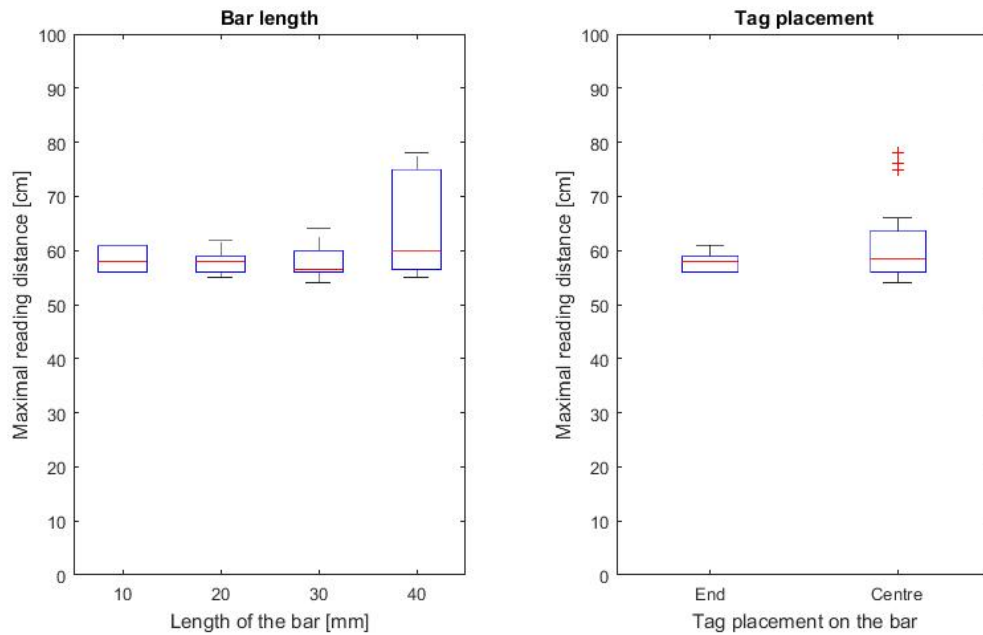
Figure 5.4: Left: Boxplot of the maximal reading distances of the HID tags on four 1 mm thick plates with a width of 10 mm and different lengths per group n=12. Right: Boxplot of the tag placed at the end of the bar or in the centre per group n=24.

reference group has a median of 87.5 cm and a standard deviation of 33.22 cm.

Plate with cut-outs

The different maximal reading distances of the three HID tags on the hashtag shaped plate with a thickness of 1 mm are taken to form the cut-out group in Figure 5.5. The results of the two orientations of the tag are combined. As can be seen in the figure, the median of the cut-out group is 85.5 cm. The standard deviation is 25.40 cm.

Top and bottom plate

The data for the top and bottom are the measurements from the test described in Section 4.5.6. This test is only performed with one of the plates facing the antenna as the other plate facing the antenna results in exactly the same situation. The median of these measurements is 41 cm with a standard deviation of 4.51 cm.

The difference in maximal reading distances between the reference group and the cut-out group is not significant. The top and bottom group, however, shows a significantly lower maximal reading distance than the reference group ($p = 0.0106$) and the cut-out group ($p = 0.0123$).
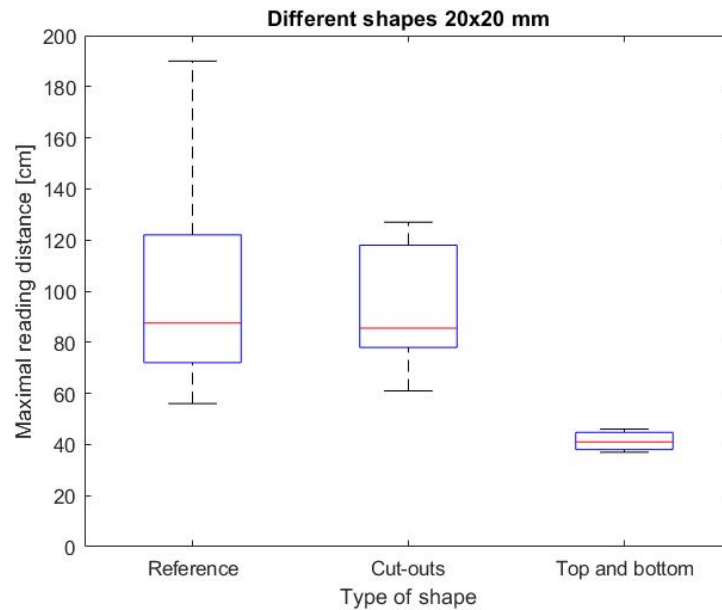
Figure 5.5: Boxplot of the maximal reading distances of different shapes of 20x20 mm plates of 1 mm thickness. For the reference group n=30, the cut-out group n=6, the top and bottom group n=3.

5.2. Casing Properties

Here the results of the tests described in Section 4.6 will be shown. The bars in these tests have an area of 30x10 mm and a thickness of 1 mm. The additional parts forming the enclosures are described in the text.

5.2.1. Full and Partial Enclosure

Full and partial enclosure

The maximal reading distance of the bars with the full and partial enclosures surrounding the tags are shown in Figure 5.6. These data are a combination of the two orientations. The partial enclosure contains three different enclosures: the flat pins, the round pins, and the different corners. An important note is that when the value zero is used within this figure this means that the tag was not detected at all, not even when the tag was held against the antenna. The median of the maximal reading distance of the tag with the full enclosure is zero (Figure 5.6). This means that more than 50% of the tags tested were not detected by the antenna. The median of the maximal reading distance of the tag with the partial enclosure is 51.5 cm. The standard deviation of the full enclosure is 17.51 cm and of the partial enclosure it is 15.22 cm. The difference in maximal reading distance between the full and partial enclosures is significant. So the partial enclosure has a higher maximal reading distance.

Different 1 mm high enclosures

Figure 5.6 shows a boxplot of the three tested enclosures: the flat pins, the round pins, and the different corners. For this figure, data of both orientations are taken. From the flat and round pins only the data with the 1 mm high enclosures are taken to exclude the influence of the height of the enclosure. The corners group is a combination of both the two and the four corners also with a height of 1 mm. The medians of the flat pins, the round pins, and the corners are, respectively, 54 cm, 52 cm, and 53.5 cm. The standard deviations are 9.56 cm, 21.94 cm, and 21.98 cm. The differences between the maximal reading distances of the three groups are not significant. This indicates that the type of partial enclosure is not of influence.

Casing height

To be able to determine whether the height of the enclosure is of influence to the maximal reading distance, the three different heights are compared in Figure 5.7. The boxplot of the casings of 1 mm, 2 mm, and 3 mm high is a combination of the full enclosure and the partial enclosures. Note that the
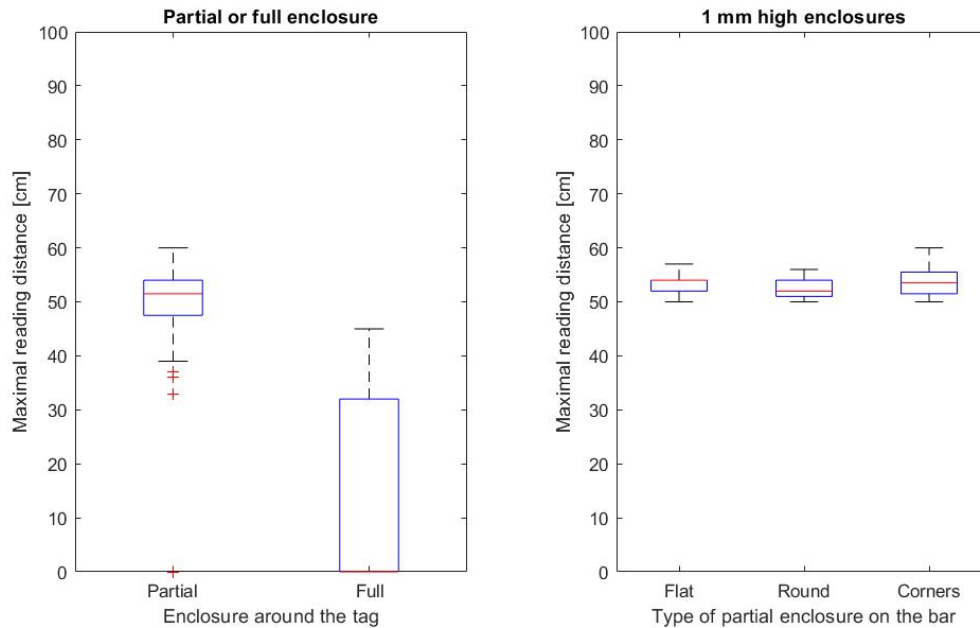
Figure 5.6: Left: Boxplot of the maximal reading distances of the HID tags on bars with a full or partial enclosure, for the partial group n=48 for the full group n=18. Right: Boxplot of the maximal reading distances of the HID tags on bars with the three different partial enclosures of 1 mm high. For the flat and round group n=6, for the corners group n=12.

value zero is chosen, when the tags were not detectable at all. The medians of the maximal reading distances of the 1 mm, 2 mm, and 3 mm high enclosures are, respectively, 51.5 cm, 48.5 cm, and 0 cm. As is clearly visible in the figure, over 50% of the measurements with the enclosure of 3 mm high were not detected at all. The tags placed in an enclosure of 2 mm were detected most of the time. The detection ranged from 0 cm to 57 cm. The 1 mm enclosure was always detected and the detection range was between 29 cm and 57 cm. The measurements of the maximal reading distance of the 1 mm high enclosure was not significantly higher than the 2 mm high enclosure. The measurements of the 3 mm high enclosures were, however, significantly lower than the measurements of the 1 mm and 2 mm high enclosures. The 1 mm high enclosure is in this case the best option as this is always detected even though it does not lead to a significantly better maximum reading distance.

5.2.2. Surface

The boxplot in Figure 5.7 is made with the data from the tests described in Section 4.6.3 and the 30x10 mm bars with the tag placed on the end of the bar from Section 4.5.3. The medians of the smooth surface and the 3D printed surface are, respectively, 57.5 cm and 57.5 cm. The standard deviations are 1.94 cm and 2.42 cm. The difference between the maximal reading distances is not significant. This indicates that the surface of the metal plate is not of influence on the maximal reading distance.

5.2.3. Side of the Tag Facing the Antenna

All mentioned experiments are performed in two orientations. The first with the tag facing the antenna and the second one with the bar facing the antenna (Figure 4.3b). The measurements of all tests with orientation A are combined to form the 'Front' group in the left boxplot in Figure 5.8. The same is done with the measurements of orientation B to create the 'Back' group. The median of the Front group is 59 cm and the standard deviation is 28.08 cm. The median of the Back group is 56 cm with a standard deviation of 29.91 cm. The difference in maximal reading distance is not significant, so the orientation of the tag in the A and B position do not differ.
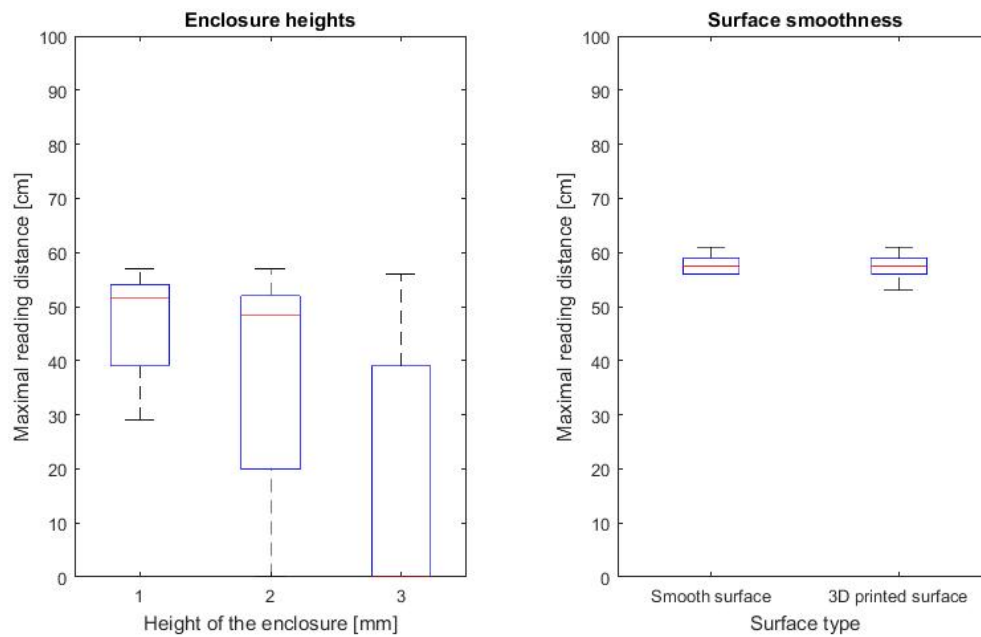
Figure 5.7: Left: Boxplot of the maximal reading distances of the HID tags on bars with casings of 1 mm, 2 mm, and 3 mm per group n=18. Right: Boxplot of the maximal reading distances of the HID tags on a smooth or 3D printed surface. For the smooth group n=6, for the 3D printed surface n=18.

5.3. Protection Layer

Figure 5.8 shows a boxplot of the different types of epoxy layers explained in Section 4.7 held in front of the tag. The first category in the figure is the measurement of the tag on the end of a 3D printed bar without a layer of epoxy. The medians of the maximal reading distance of the categories, no layer, thin layer, thick layer, and bowl, are 57.5 cm, 57 cm, 58 cm, and 59 cm respectively. The standard deviations are, respectively, 2.42 cm, 2.42 cm, 3.39 cm, and 3.39 cm. There are no significant differences between any of the categories. Indicating that the layer of epoxy does not influence the maximal reading distance.
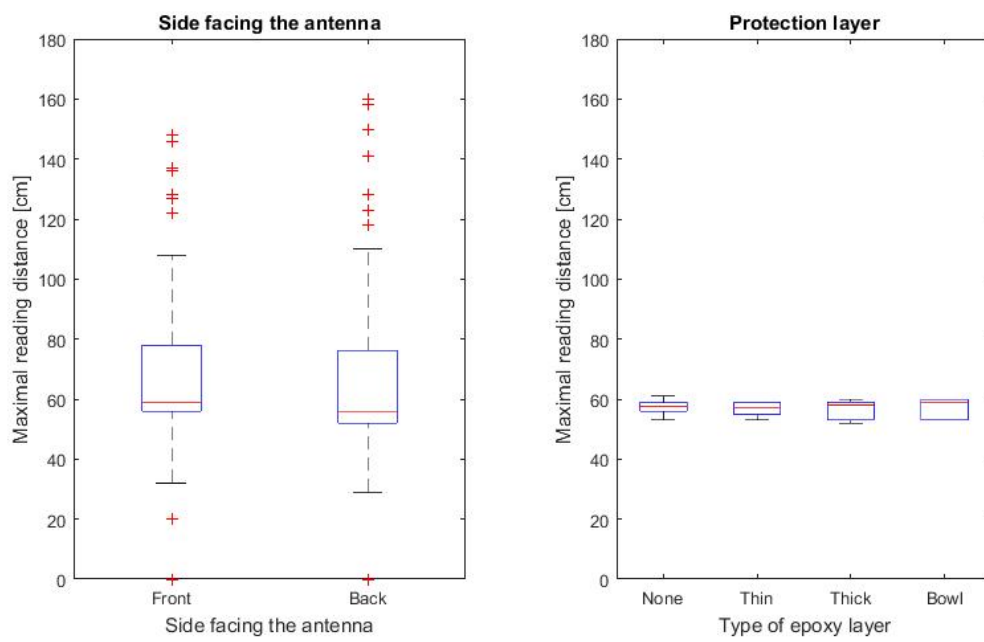
Figure 5.8: Left: Boxplot of the maximal reading distance of the two sides of the tag facing the antenna per group n=129. Right: Boxplot of the maximal reading distances with the three types of epoxy layers in front of the tags. For the no layer group n=18, for the other three groups n=6.

<div style="text-align: right; font-size: 4em; font-weight: bold;">6</div>

Preliminary Discussion

In the experiments up to now, the influences of the basic properties of the metal plate and casing properties on the maximal reading distance were tested. First, the basic properties of the metal plate, surface area, thickness, bar length and different shapes of the bar were studied. Next, the tested casing properties were a full and partial enclosure, different height of the enclosure, and different partial enclosures. Finally, the surface smoothness was tested and the different orientations were compared.

6.1. Key Findings of the Experiments

In the surface area tests, the Xerafy tags from the pilot study are compared to the HID tags. The medians of the maximal reading distance of tags on the 10x10 mm plates differ by 1 cm. The differences between the surface areas of the Xerafy and HID tags are not significant except for the 40x40 mm group. Fitting a line through the data of the HID tags shows an increasing maximal reading distance with an increase of surface area. However, the median of the maximal reading distance from the HID tags on the 40x40 mm plate is 120 cm: this is a factor 2 improvement over the 10x10 mm plate with a median of the maximal reading distance of 58 cm, while the surface area is increased by a factor 16.

When comparing the different plate thicknesses, the maximal reading distances show no significant differences.

When comparing the different bar lengths, the medians of the maximal reading distance are between 56.5 cm and 60 cm. The results of the 10 mm, 20 mm, and 30 mm bars showed no significant difference in the maximal reading distance. The 40 mm bar showed a significantly higher maximal reading distance, with a 3.4% higher median compared to the 10 mm bar. The medians of the maximal reading distance of the tags placed on the end or in the centre of the bar are, respectively, 58 cm and 58.5 cm. The difference in maximal reading distance of the tag placed in the centre of the bar is significantly higher than that of the tag placed at the end of the bar.

Comparing the different shapes shows that the plate with the cut-outs is comparable to the reference group. The top and bottom configuration, however, has a significantly lower maximal reading distance than both the reference group and the plates with the cut-outs. The median of the top and bottom group is 41 cm and the medians of the reference and cut-out groups are, respectively, 87.5 cm and 85.5 cm.

The results of the casing properties show a clear difference in maximal reading distance of the partial enclosures compared to the full enclosures. The median of the maximal reading distance of the partial enclosures is 51.5 cm, where the median of the full enclosures is 0 cm, meaning more than half of the tags were not detected. When comparing the three partial enclosures of 1 mm high with each other, the medians of the maximal reading distance were similar and no significant differences were observed. When comparing the different heights of the enclosures, the medians of the maximal reading distance are 51.5 cm, 48.5 cm, and 0 cm for, respectively, 1 mm, 2 mm, and 3 mm height. There is a clear trend visible showing a decrease in reading distance with an increase of the enclosure height although the difference between 1 mm and 2 mm height is not significant. When comparing the smooth and rough surface of the metal plate, the median of the maximal reading distance of a rough surface was 57.5

cm as well as the median of the smooth surface. No trend or significant differences were found. When comparing the two orientations (either the front or back of the tag facing the antenna) the medians of the maximal reading distances are, respectively, 59 cm and 56 cm. This difference is not significant. The final test, measuring the influence of the protection layer on the maximal reading distance shows no significant differences between the group without the epoxy layer and the groups with the different epoxy layer thicknesses. The medians of the maximal reading distances are 57.5 cm, 57 cm, 58 cm, and 59 cm. No trend or significant differences were observed

6.2. Interpretation of the Experiments
6.2.1. Basic Properties of the Metal Plate
The experiment with the different surface areas showed for the smaller surface areas, the 10x10 mm, 20x20 mm, and 30x30 mm plates, comparable behaviour for the Xerafy and HID tags. The results of the 40x40 mm plates are, for the HID tags, significantly different from the results for the Xerafy tags. For the application in this study, attaching the tags to surgical instruments, the smaller surface areas will be used. In these cases, the tags are considered to be similar and from this test on, the HID tags can be used and compared with the results of the Xerafy tags. The surface area tests with the HID tags showed slightly further reading distances for the larger surface areas. A relation between the surface area and the maximal reading distance is found. A larger surface area results in a higher maximal reading distance. This relations within this range is, however, not clearly exponential as thought in the hypothesis. The hypothesis that the B orientation would have lower reading distances than the A orientation is not correct, a small difference is detected, but this difference is not significant.

The results of the maximal reading distance for the different plate thicknesses show no significant differences. This is in contrast with the hypothesis that the maximal reading distance would decrease with an increase of the thickness. The hypothesis that the maximal reading distance would be lower for the B orientation is also not correct. The median of the A orientation is slightly higher, but the difference is not significant. From these results it seems that the thickness of the metal plate is not of influence on the maximal reading distance.

Although the difference between the 40 mm bar and the other bar lengths was significant, the difference in the median of the maximal reading distance was maximally 3.5 cm and with the 10 mm long bar 2 cm. A 10 mm, 20 mm, or 30 mm bar is preferred over the 40 mm bar, as the median of the maximal reading distance compared to the 10 mm plate was 3.5% improved at the cost of an increase in bar length of 300%. Within this range of bar length, the hypothesis that a longer bar results in higher maximal reading distances does seem to be correct. The difference, however, is small. As the length differences between the 10 mm, 20 mm and 30 mm bars were not influencing the maximal reading distance, the 10x10 mm plate should suffice. For the other experiments, the 10x30 mm bars are used. This is done, because the bar can be held at the end of the bar, minimizing the risk of accidentally changing the orientation of the bar relative to the antenna. Placing the tag at the end of the bar is more practical than in the centre. This because the addition to the instruments should be as small as possible in order not to interfere with the surgeon. The difference measured between the tag in the centre of the bar and at the end of the bar is significant. However, the medians differ by 0.5 cm. This is an improvement of 0.86%, so the outcome will still be similar.

The comparison of the cut-outs compared to the reference group shows no improvement of the maximal reading distance. This confirms the hypothesis that cut-outs in the metal plate do not affect the maximal reading distance of the tag. From these results it can be concluded that it is possible to make cut-out in the final design without influencing the maximal reading distance. The top and bottom plate has a significantly lower maximal reading distance than the reference group. Apparently, the signal is blocked by metal if not one of the sides of the RFID tag is free of metal, as expected. Even though this experiment is only performed three times, all results show a shorter maximal reading distance than the reference group. It is expected that more tests will result in similar measurements. As this configuration reduces the maximal reading distance, it will not be used for the final design.

6.2.2. Casing Properties
Comparing the partial to the full enclosures, a significant difference was found. The signal appears to be blocked when the casing is closed around the tag. As 10 out of 18 tags with a full enclosure were not detected at all, it is recommended to use a partial enclosure over a full enclosure. This is in line

with the hypothesis that the full enclosure would have a lower maximal reading distance. The results of the different partial enclosures with a height of 1 mm showed no significant difference. Looking at the different heights of the enclosures, the 1 mm height is clearly the best option of the three as all tags were detected. Furthermore, choosing the 1 mm high enclosure is not a disadvantage over picking the 2 mm or 3 mm high enclosure as it is high enough to position the tag. From this result it can be concluded that an enclosure around the tag is possible. However, the enclosure should not be higher than 1 mm or fully enclosed, because these properties can block the signal.

As there is no significant difference between the smooth and the rough surface, it does not matter which surface is used for the maximal reading distance. This is in line with the hypothesis that the rough surface would have a similar maximal reading distance as the smooth surface. Apparently, the wires in the tag can use the metal plate as an antenna on rough and smooth surfaces. When comparing orientation A and B, it is shown that similar reading distances can be accomplished in both orientations as no significant differences were found in the maximal reading distances over all experiments. This is in contrast with the theory explained in Section 1.6, where it is explained that a metal plate between the tag and the antenna should result in a decrease in reading distance. It is however possible that the metal plates used in this study are smaller than previously tested and the effect blocking the signal when the back of the plate is facing the antenna does not occur. Finally, the protection layer of epoxy showed no significant difference compared to the test without the protection layer. From this, it can be concluded that the protection layer of epoxy does not influence the maximal reading distance. This is in line with the hypothesis. This shows that the problem with the maximal reading distance in the pilot study was not caused by the layer of epoxy but by the design of the metal surrounding the RFID tag.

6.3. Limitations of the Experiments

The test set-up in the clinical lab at the TU Delft is used to perform the experiments (Figure 4.1). With the medical devices present at the clinical lab, the setting came close to the real setting at the operating room. However, testing the influences of different factors would have been preferably performed in an anechoic chamber. An anechoic chamber is a room designed to completely absorb reflections of either sound or electromagnetic waves [20], minimizing the influences of the surroundings.

For the tests, only three HID tags were available as these tags are still in production and not commercially available yet. Performing the experiments with a larger set of tags would probably result in more reliable results and yield more significant differences in the test results. For the different surface areas and the different heights of the enclosures a trend seemed to exist, more tests could determine if the differences are indeed significant or not.

6.4. Combining the Results into the Final Design

To determine the surface area of the plate of the final design, the results are taken into account. Although there was an improvement of the maximal reading distance, the improvement was not enough to justify the increase in surface area. A Harris Profile is made to include the size of the metal plate (Figure 6.1). Keeping in mind that the plate will be attached to small instruments, the 10x10 mm plate is chosen as the maximal reading distances are above the desired 50 cm.

	10x10 mm				20x20 mm				30x30 mm				40x40 mm			
	++	+	-	--	++	+	-	--	++	+	-	--	++	+	-	--
Maximal reading distance		█				█				█			█			
Size	█	█				█					█				█	█

Figure 6.1: Harris Profile to determine the surface area of the final design.

To pick a thickness for the final design, a Harris Profile is used, taking not only the maximal reading distance, but also other factors into account (Figure 6.2). The chosen factors are the material costs, strength, size, and weight. For the material costs not only the prize of the metal is considered, but

also the time it takes to print the material. The influence on the production time will change when an other technique than 3D printing is used. So this factor is only considered for the prototype stage. The strength of the attachment is an important factor during the sterilization process. Here the instruments are close to each other and the attachment can get hit by other instruments. It is important that the tag remains undamaged. As the attachments shouldn't impede during the procedure, the preferred size is as small as possible. The last factor is the weight of the attachment. In this case, a lighter attachment is better because it minimizes the change to the instrument.

	0.5 mm ++	+	-	--	1 mm ++	+	-	--	2 mm ++	+	-	--	3 mm ++	+	-	--
Maximal reading distance	G	G			G	G			G	G			G	G		
Material costs	G	G			G	G					R				R	
Strength			R			G			G	G			G	G		
Size	G	G				G					R				R	
Weight	G	G				G					R				R	

Figure 6.2: Harris Profile to determine the thickness of the final design.

Overall, the best solution is a thickness of 1 mm. The maximal reading distance is good, the plate is relatively thin, which makes the 3D print time shorter and it requires less material, making it lighter. Furthermore, the plate has a high enough bending resistance and the plate is relatively small.

As the length differences between the 10 mm, 20 mm and 30 mm bars were not influencing the maximal reading distance, the 10x10 mm plate should suffice. For the final design a 15 mm and a 20 mm long bar are used. The two versions are created to ease the temporary attachment to the instruments. As the cut-outs are not of influence on the maximal reading distance, two cut-outs are made in the end of the final design to be able to attach the bar to the instruments with ty-raps.

The choice of which partial enclosure is best for the final design is not solely dependent on their influence on the maximal reading distance. To determine which of the partial enclosures will be used for the final design, a Harris Profile is made taking other factors like the robustness and production possibilities into account (Figure 6.3). The robustness is chosen as a factor as the pins tended to bend or break during the experiments. Both the two and four corners did not visibly deform at all. The production possibilities show the ease of the production. The two corners scores better than the four corners, because this production process is less time consuming. Overall, the two corners are chosen for the final design.

	Flat pins ++	+	-	--	Round pins ++	+	-	--	Two corners ++	+	-	--	Four corners ++	+	-	--
Maximal reading distance	G	G			G	G			G	G			G	G		
Robustness			R				R	R	G	G			G	G		
Production possibilities			R					R	G	G				G		

Figure 6.3: Harris Profile to determine the type of enclosure for the final design.

The surface of the final design is chosen as smooth, except for the surface within the enclosure. Polishing the surface within the enclosure is difficult and time-consuming when the plates are made

with a 3D printer. The 3D printed rough surface has micropores that are more difficult to sterilize, but it might ease the adhesion of the epoxy to the surface. Outside of the epoxy layer, the surface is polished and smooth to ease the sterilization process. Later on, when the attachments are mass produced with a different technique to 3D printing, the surface inside the enclosure can also be smooth.
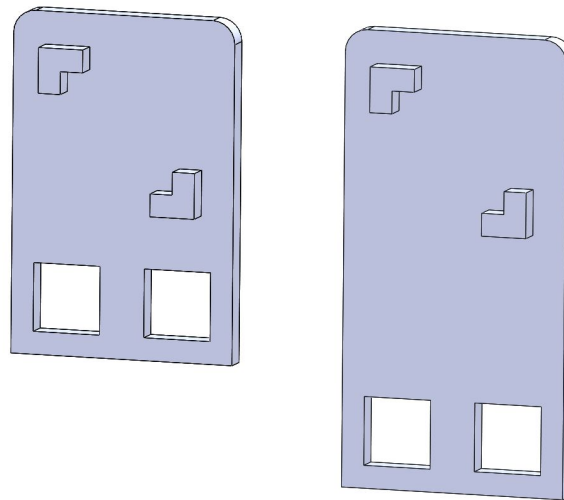
Figure 6.4: Final design created in SolidWorks, left the short version (15 mm long), right the long version (20 mm long). Both versions are provided with two corners on the opposite side of the tag. The holes at the end of the bars are for temporary attachment to instruments.

6.5. Conclusion of the Experiments

The test with the basic properties of the metal plates in combination with other factors mentioned in Section 6.2 resulted in the base of the final design. A 1 mm thick bar is chosen with a width of 10 mm. For the final design, two lengths are created, see Figure 6.4. The first length is 15 mm, and the second length is 20 mm. Two holes are made into the design at the end of the bar to fixate the final design with ty-raps to an instrument. In case the ty-raps construction did not succeed, the second version is longer than the first: 20 mm instead of 15 mm, as a back-up to create the possibility for an alternative, temporary connection to the instruments. As the length of the bar and the introduction of cut-outs were not of influence to the maximal reading distance, these different designs should result in the same maximal reading distances.

Based on the previous experiment, the partial enclosure is preferred and when choosing between the three tested examples, the choice goes to the plate with the two corners. This configuration is more robust than the flat or round pins because the pins tended to bend or break and the corners did not visibly deform at all. The two corners are chosen over the four corners as the design is easier and the results were similar. The chosen height of the enclosure is 1 mm because this height gave the best results. The surface underneath the tag can either be smooth or rough. To facilitate the manufacturing of the plate when made with a 3D printer, the surface within the enclosure is rough and the surface around the enclosure is smoothened. The smooth surface outside the epoxy capsule is chosen as this is easier to clean. Finally, the final design will be covered with a layer of epoxy to protect the tag from the extreme circumstances in the autoclave.

7

Final Design

7.1. Design Choices

From the results of the previous tests, the best properties are chosen and combined into a final design (Figure 7.1a). For the final design, two different lengths are realized. The tag is placed at the end of the bar in the centre of a 10x10 mm part of the bar. In the first version of the final design the bar is 10x15 mm and in the second version, the bar is 10x20 mm. The two versions are made to facilitate the possibility of connecting the final design to an instrument. In the 10x15 mm version, the 5 mm next to the tag part is equipped with two holes. These holes are made for ty-raps. In the 10x20 mm version, the ty-rap holes are also made at the end of the bar, but there is 5 mm extra space to make a connection to the instruments when the ty-raps do not function as desired. There should be no significant difference between the two versions of the final design as the previous tests did not show differences in this range due to the length of the bar or cut-outs. The thickness of the plate is 1 mm. The enclosure around the tag is done with two corners on the opposite corners of the tag. The corners are 1 mm in height. The surface of the bar where the tag is placed is rough and the rest of the surface around the enclosure is smooth. There is no difference in maximal reading distance found with the different surfaces. A smooth surface is easier to clean and a rough surface easier to manufacture with a 3D printer. The surface of the enclosure and underneath the tag, which will eventually be covered with a layer of epoxy, is rough and the surface that will not be covered with epoxy is smooth.

7.2. Test Method

The tests performed with the final design are explained in Section 4.2. The tests are performed in the clinical lab with both Antenna 1 and Antenna 2. Further testing is done in the OR with Antenna 2.

7.2.1. Test in the Clinical Lab

In the previous experiments only Antenna 2 was used because the pilot study showed that this antenna had a longer reading distance than Antenna 1. The final design, however, is tested in the clinical lab at the TU Delft with both Antenna 1 and Antenna 2 to see how the results obtained with Antenna 1 and Antenna 2 compare to the results in the pilot study. The hypothesis is that the reading distances obtained with the final design and Antenna 2 are similar to the results obtained with the test with the two corners. Meaning the measurements of the maximal reading distance will be between 50 cm and 60 cm. This because the length of the bar did not influence the reading distance in this range and the cut-outs didn't either. The results of the test with Antenna 1 are expected between 30 cm and 40 cm. This because the reading distances in the pilot study were also about 60 percent of the reading distances obtained with Antenna 2.

Next to the standard orientations will the final design also be tested in four other orientations: orientation C, D, E, and F, see Figure 7.1b. According to the theory, the best results should be accomplished with orientation A and the fewest results with orientation B [12]. The other orientations are tested to test at what reading distance the tags will still be detected when they are held in other orientations. This gives a more realistic representation of the circumstances, as the tags will not always be
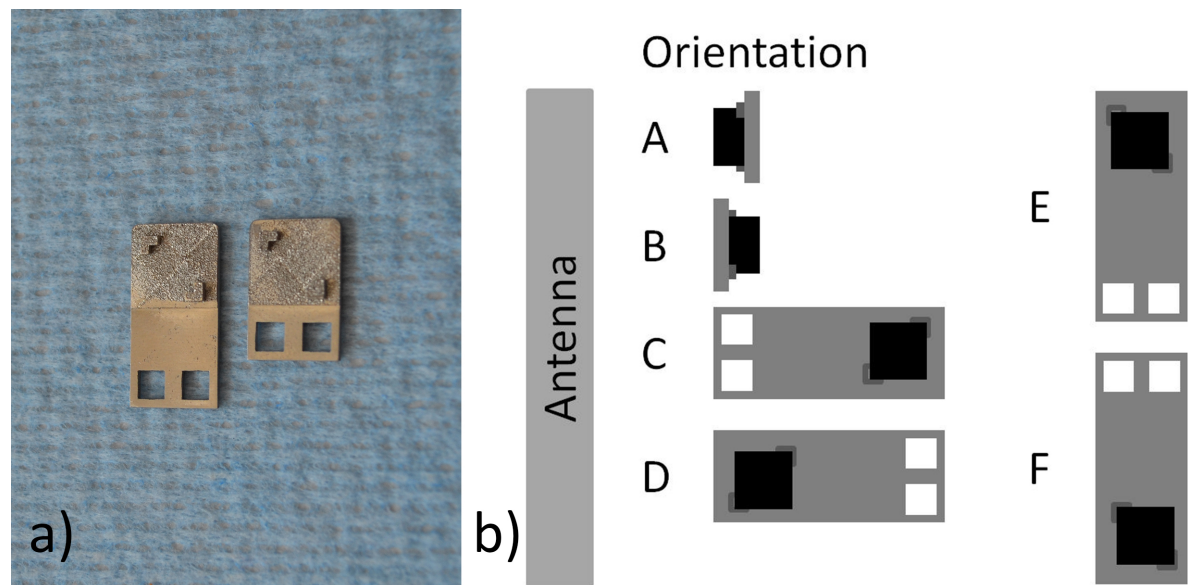
Figure 7.1: a) Final design: the long version is left, while the short is right. Both versions are provided with two corners on the opposite side of the tag. The holes at the end of the bars are for temporary attachment to instruments. The surface around the corners is rough from the 3D printer and the surface around the hole is smooth. b) Top view of the different tested orientations of the tag relative to the antenna.

perpendicular to the antenna, during the surgery. Furthermore it needs to be confirmed that the tags on the instruments are still detectable during the surgery if the orientation is not perpendicular to the antenna. The hypothesis is that these orientations perform less according to the theory in Section 1.6. In total, the tests with the final design in the lab are performed 120 times. For the first test, the two versions of the final design are tested in the two orientations, resulting in four unique configurations. Every configuration is tested nine times, three times for each tag. For the second test, the two versions of the final design are tested in the other four orientations, resulting in eight unique configurations. Every configuration is tested three time, once for each tag. These two tests are performed with both Antenna 1 and Antenna 2.

7.2.2. Test in the OR

After determining the maximal reading distances in the lab, the final design is tested in the OR at the Reinier de Graaf hospital in Voorburg. For the OR tests, Antenna 2 will be used as this antenna is expected to have a longer reading distance than Antenna 1. The tests in the OR are performed to see whether the same results can be obtained in the OR as in the clinical lab. The setting in the OR is closer to the real circumstances when the instruments are tracked during surgery. As there are many devices present and active in an OR, it is possible that some interference or disruptions occur. As in the clinical lab, the final design will also be tested in the OR in the four other orientations (Figure 7.1b).

Finally, the test in the OR will also be performed with the final design attached to three instruments with ty-raps. This is a temporary attachment to the instruments to measure the maximal reading distance of the final design when they are attached to the instrument. The three instruments used are shown in Figure 7.2. Two metal instruments and one laparoscopic instrument made from plastic. This is done to make sure the influences on the measurements are not only from the added metal. The final design is attached to the instruments with ty-raps around the instrument and through the holes in the final design. As can be seen in the figure, Instrument A and Instrument B are regular instruments without RFID tags, Instrument C is one of the instruments from the pilot study. The RFID tag from the pilot study is positioned next to the final design. This is not expected to be a problem, as the tag from the pilot study was only detected at a short distance from the antenna. The maximal reading distance of the final design attached to the instruments is tested in orientation A and B.

The tests with the final design in the OR are performed 60 times, like in the lab. For the first test, the two versions of the final design are tested in the two orientations, resulting in four unique configurations. Every configuration is tested nine times, three times for each tag. For the second test, the two versions

of the final design are tested in the other four orientations, resulting in eight unique configurations. Every configuration is tested three time, once for each tag. Furthermore, the final design in the OR is also tested on medical instruments. This test is performed 18 times in total. Once with all three tags on each instruments, only with the short version of the final design, in two orientations. The short version of the final design is attached to three different instruments and tested in two orientations, resulting in six unique configurations. Every configuration is tested three times, once for each tag.
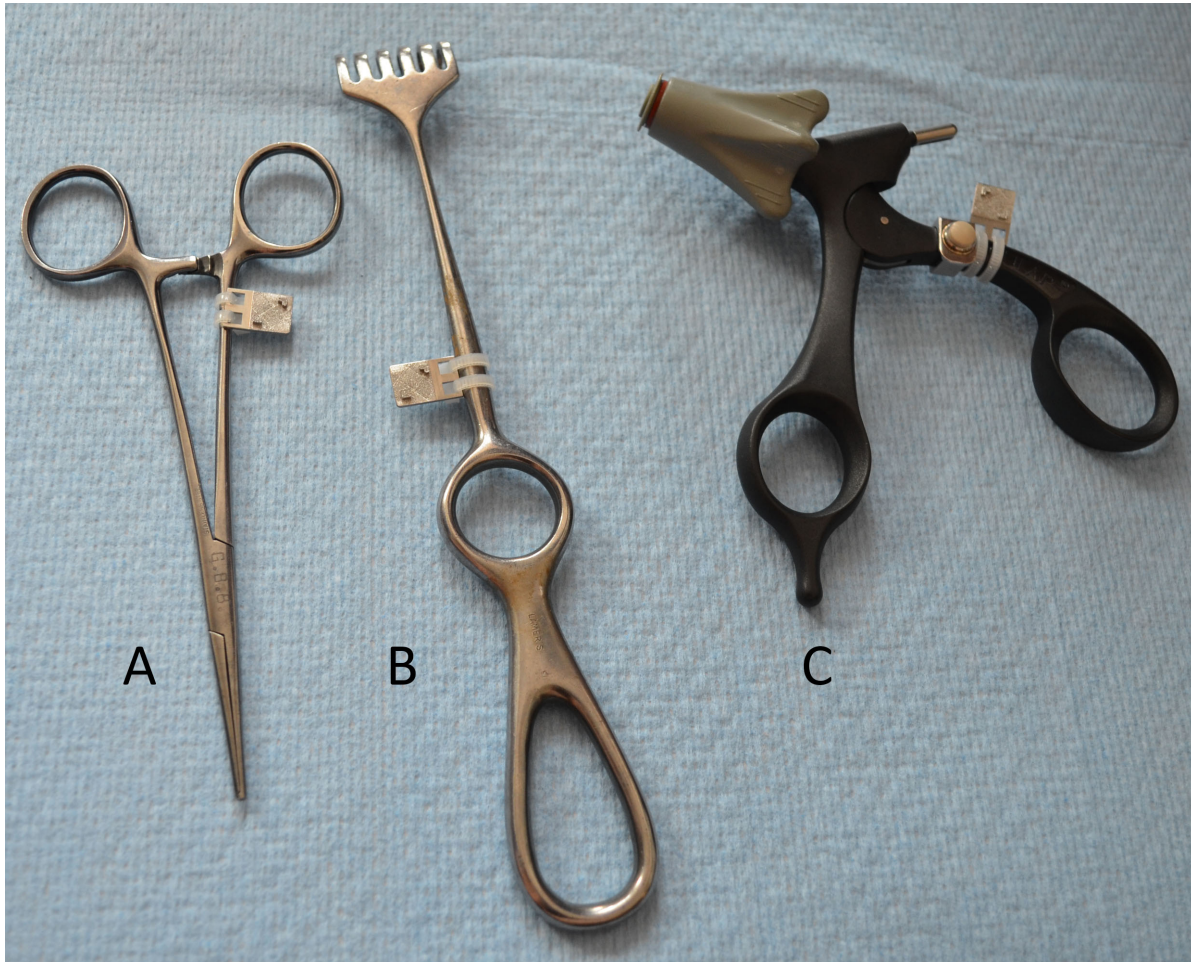
Figure 7.2: The three instruments tested with the final design. The final design is attached to the instruments with ty-raps.

7.3. Results

In this section, first, the results of the tests in the clinical lab where Antenna 1 and Antenna 2 are compared will be shown. Second, the results of the test performed with Antenna 2 in the OR are given. And finally, the test of the final design attached to the instruments in the OR with Antenna 2 will be discussed.

7.3.1. Test in the Clinical Lab
Long vs short design with Antenna 1 and 2
Figure 7.3 shows two boxplots of the maximal reading distance of the final design in the clinical lab. The figure on the left shows the results obtained with Antenna 1 and the figure on the right shows the results obtained with Antenna 2. For these results, the results of the A and B orientations of both the long and short version of the final design are combined. The medians of the maximal reading distances of the experiments obtained with Antenna 1 are for the long and short version of the final design, respectively, 27 cm and 29 cm. The standard deviations are 5.60 cm and 2.37 cm. The difference between the maximal reading distances is significant (p = 0.0021). For Antenna 2, the median of the

maximal reading distance of the long bar is 53.5 cm and of the short bar 53 cm. The standard deviation for the long design is 1.62 cm and for the short design 1.86 cm. The difference between the maximal reading distance is not significant.

Comparing the results from the long and short version of the final design with Antenna 1 and 2 shows that the maximal reading distances obtained with Antenna 1 are significantly smaller than the maximal reading distances obtained with Antenna 2, as can be seen in Figure 7.3.
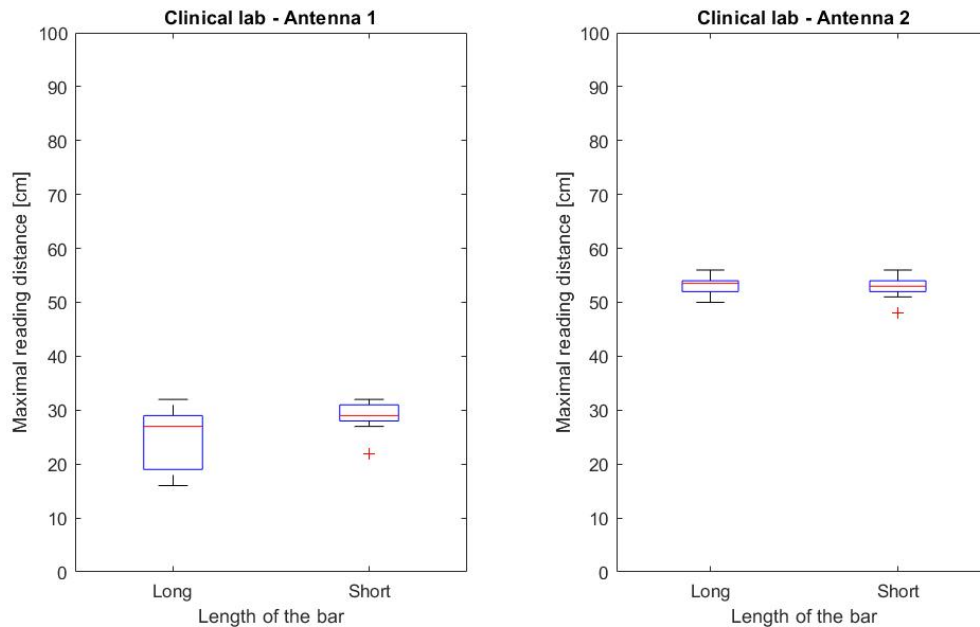
Figure 7.3: Boxplot of the maximal reading distances of the final design at the clinical lab, the long version compared with the short version. Left, are the results of the tests performed with Antenna 1. On the right are the results of the tests performed with Antenna 2.

Orientations with Antenna 1 and 2

To test whether the maximal reading distance of the tags would increase or decrease when the design was held in different orientations relative to the antenna, the orientations C, D, E, and F (Figure 7.1b) are tested.

When comparing the A, B, C, D, E, and F orientations tested with Antenna 1, the medians of the maximal reading distances are, respectively, 29 cm, 27 cm, 80 cm, 79.5 cm, 38 cm, and 28.5 cm. The standard deviations are 3.18 cm, 5.28 cm, 8.50 cm, 6.22 cm, 14.21 cm, and 14.87 cm. Comparing these results with each other shows a significantly higher maximal reading distance measured for the C and D groups than for the A, B, E, and F groups. The medians of the maximal reading distances of the orientations A, B, C, D, E, and F obtained with Antenna 2 are, respectively, 53.5 cm, 53 cm, 93 cm, 90 cm, 78 cm, 82 cm. The standard deviations of the orientations are 1.26 cm, 2.00 cm, 5.50 cm, 4.14 cm, 7.41 cm, and 21.06 cm. The results of the A and B orientation are significantly lower than the results of the C, D, E, and F orientation. The orientation E are significantly lower than the results of the C and D orientations. The differences between the C, D, and F groups are not significant. The results of the maximal reading distances of the different orientations of the tests performed with Antenna 1 are significantly lower than the maximal reading distances from the test with Antenna 2, see Figure 7.4.

7.3.2. Test in the OR

The first tests in the OR with Antenna 2 are the test with the long and short version of the final design. The results are shown in Figure 7.5 on the left. The tests resulted in a median of the maximal reading distance for the long design of 55 cm and for the short design of 50.5 cm. The standard deviations are, respectively, 10.59 and 9.28 cm. The difference in maximal reading distance is not significant.
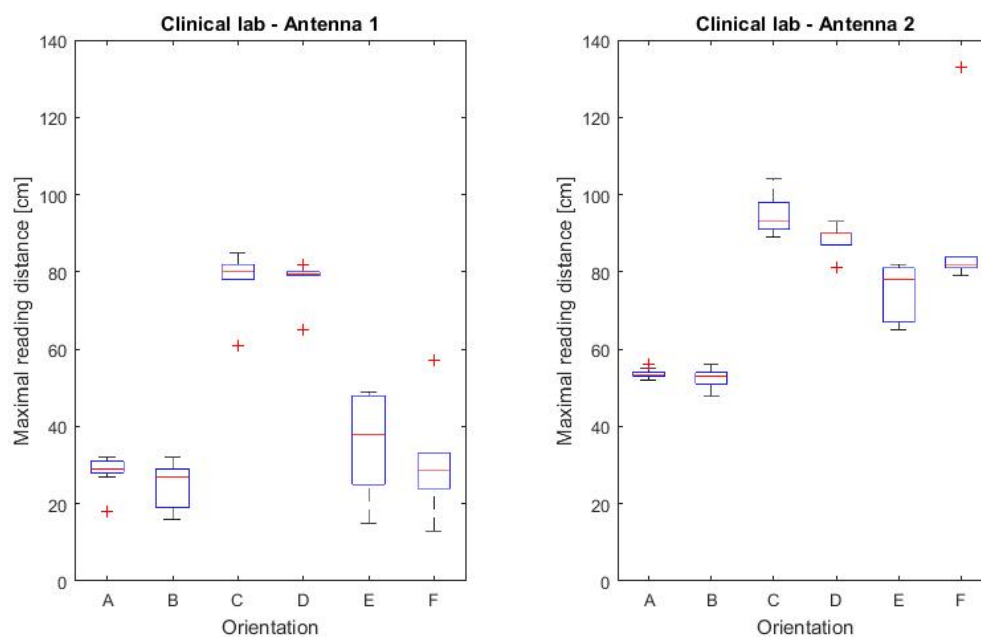
Figure 7.4: Boxplot of the maximal reading distances of the final design in the clinical lab, comparing the different orientations. Left, are the results of the tests performed with Antenna 1, right are the results of the tests performed with Antenna 2.

The different orientations, C, D, E, and F, are also tested in the OR. The results of the maximal reading distances are shown in the boxplot on the right in Figure 7.5. The tests resulted in the medians of the maximal reading distances of the orientations A, B, C, D, E, and F of, respectively, 55 cm, 49 cm, 112.5 cm, 117 cm, 122 cm, and 121 cm. The standard deviations are 10.02 cm, 9.49 cm, 12.39 cm, 20.96 cm, 16.33 cm, and 22.33 cm. The tests in the OR showed no significant differences between the measurements of the C, D, E, and F orientations. The A and B orientations are significantly lower than the C, D, E, and F orientations.

When comparing the results from the OR with the results of the same tests performed in the clinical lab with Antenna 2, no significant differences were found between the measurements of the maximal reading distances in the lab compared to the measurements in the OR. The measurements of the different orientations in the OR are significantly higher than the measurements in the lab, except for the F orientation.

7.3.3. Final Design Applied to Surgical Instruments

The results of the maximal reading distances of the final design attached to three different instruments are shown in Figure 7.6. The tests are performed in the OR with Antenna 2. Instrument C also had a tag from the pilot study attached: this tag was detected up to 5 cm facing the antenna and 4 with the back to the antenna. The results for Instrument C in the figure are from the HID tag in the final design. The medians of the maximal reading distances of Instrument A, B, and C are, respectively, 53 cm, 65 cm, and 52.5 cm. The standard deviations are 9.56 cm, 9.48 cm, and 8.96 cm. The maximal reading distances of the three instruments do not differ significantly.
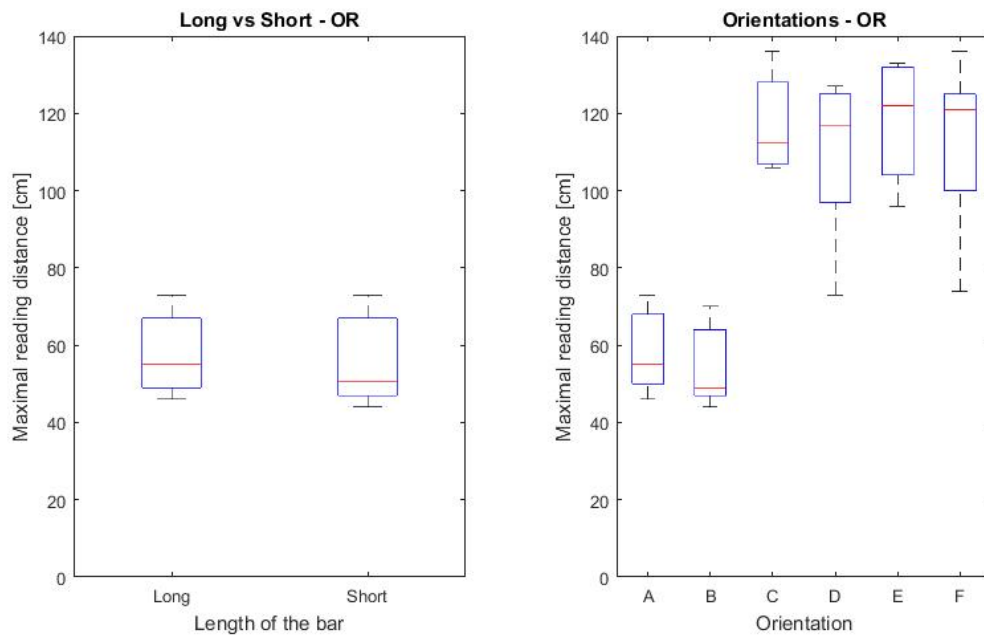
Figure 7.5: Boxplot of the maximal reading distances of the final design performed in the OR at the Reinier de Graaf hospital. Left, are the results of the tests performed with the long and short version. Right are the results comparing the different orientations.
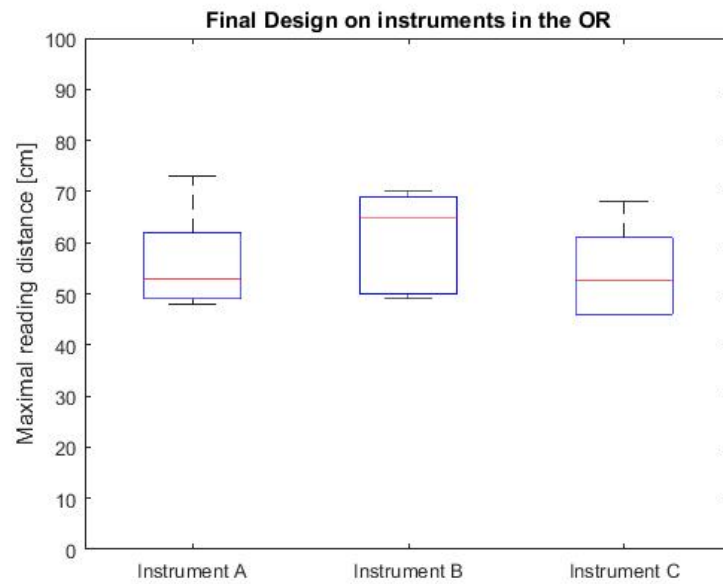
Figure 7.6: Boxplot of the maximal reading distances of the final design on three different instruments.

8

Discussion

This study started with a complete instrument set for a TEP procedure equipped with RFID tags. After looking into the maximal reading distances of the individual instruments, it became clear that the reading distances were not as far as desired and, therefore, the system had to be improved.

8.1. Key Findings

In the first part of this study, different properties of metal plates attached to the tags and different enclosure designs are tested to see what factors could influence the maximal reading distance of RFID tags. The key findings of this part are discussed in Chapter 6. One of the influencing factors was the type of enclosure around the tag. A full enclosure decreased the maximal reading distance significantly, compared to a partial enclosure. The reading distance often decreased to zero with the tag fully enclosed. The surface smoothness of the metal plate behind the tag was not a significant factor. Among others, these findings are combined to form a final design, in which the tags is supposed to be able to be detected at the desired reading distance of 50 cm.

For the final design a 1 mm thick plate with a surface of 10x15 mm and 10x20 mm was chosen. A partial enclosure was chosen for the casing on the metal plate ensuring the positioning of the tag. From the different partial enclosures, the two corner design was chosen because of the robustness and sufficient enclosing properties. The height of the enclosure was 1 mm, as higher enclosures lead to a diminished reading distance. The surface between the enclosure was rough which facilitates the manufacturing of the plates with a 3D metal printer. The surface around the enclosure and on the back of the bar was smooth, reducing the risk of dirt sticking to the plate. Once the final design was made by DEMO, the design was first tested in the lab set-up and secondly tested in an OR set-up at the Reinier de Graaf hospital.

The results of the test comparing the long and short version of the final design with Antenna 2 in the clinical lab shows no significant difference in maximal reading distance. The short version shows with Antenna 1 a small but significantly higher maximal reading distance than the long version. Furthermore, when looking at the measurements obtained with Antenna 2 a significantly higher maximal reading distance is detected between the orientations C, D, E, and F, than in orientations A and B. When comparing the results obtained with Antenna 1 and Antenna 2 in the clinical lab, the maximal reading distances of the measurements with Antenna 2 are significantly higher than the measurements with Antenna 1. Comparing the long version with the short version in the OR showed no significant difference. The orientations C, D, E, and F show no significant difference among each other, but a significantly higher reading distance than the A and B orientations in the OR. When looking at the final design attached to the three instruments, no significant difference in maximal reading distance is found. The medians of the maximal reading distances are between 52.5 cm and 65 cm.

8.2. Interpretation of the Results

As the pilot study stated the follow up study also showed that the maximal reading distances obtained with Antenna 1 are smaller than the distances measured with Antenna 2. This also aligns with the

theory that a larger antenna has a higher reading distance [12]. Neither the long nor short version of the final design showed significant differences, either in the clinical lab or in the OR. This result is as expected, as the length of the bar between 10 mm and 30 mm was also not significantly changing the maximal reading distance. The maximal reading distance of the C, D, E, and F orientations are significantly higher than in the A and B orientations. This result is in contrast with the theory, as orientation A is in theory the best orientation [12]. It is, however, recommended with the on-metal tags to experiment on site to determine the best orientation for a specific tag/reader combination [14]. The difference in performance in the orientations could be caused by the metal plate reflecting the radio waves. Due to the metal plate the dipole is not formed around the wire but only at the 'free' part, therefore, the dipole is partially formed. The reflection of the metal forms a different pattern around the plate. This is a possible explanation of why the other orientations are detectable at a longer reading distance.

The experiments in the OR with the different orientations did show significantly higher maximal reading distances than in the clinical lab. However, the standard deviations of the measurements in the OR are larger than the standard deviations in the lab. This could be caused by the laminar airflow system above the operating table, which reduces the amount of water in the air and thereby reduces the noise to the signal. It could also be influenced by other factors, like objects or devices in the room, or the metal in the hospital bed. As the measurements with the A and B orientations do not show significant differences when comparing the results from the lab with the results from the OR, more measurements are needed to determine if the maximal reading distance is different in the OR than in the lab. The test with the final design attached to the instruments shows that the maximal reading distances have a median between 52.5 cm and 65 cm. From this result, it can be concluded that the instruments do not influence the maximal reading distance and the desired reading distance of 50 cm is achieved with the final design created in this study.

8.3. Compared with Other Literature

Previous studies investigated the reading range of RFID tags. For example, Dobkin et al. (2005) [13] investigated the effect of the reading range of RFID tags close to water and metal plates. Dobkin's study was performed with normal RFID tags, where this study is performed with 'on-metal' tags. In both studies, the effects of metal plates have been investigated, but on different types of tags. In line with this study, Dobkin also found metal to be an influencing factor on the reading range. In this research, the influences of the metal could specifically be found in the tests with the top and bottom plate and the higher casings, as it appeared to be blocking the RFID signals.

Different studies have already been performed to design new RFID tags that can be mounted on metal surfaces [21] [22]. This study is focuses not on the design of the tags but on the possibilities and reading distances of the tags.

In Germany, similar research is used to track laparoscopic instruments, as RFID tags are attached to the instruments to measure their presence at the instrument table [4]. In contrast with this research, their measurement is indirect as they measured what instruments were not in use during the surgery and our measurements are direct. The advantage of direct measurements is that instruments held by a nurse or not placed back on the table will not be seen as 'in-use', causing fewer false positives.

8.4. Vision

This study shows a new approach to track surgical instruments during a surgery. Tracking of the surgical instruments is done directly by measuring on the surgical site. This approach is preferred over the already tested approach where indirect measurements were done to measure when the instruments were 'not in-use'. Errors made due to the fact that instruments are not directly placed back on the instrument table will be prevented with this approach. The new design made in this study is promising as the maximal reading distances are improved over the old design. As the desired reading distances are achieved, the casings are ready to be attached to the instruments and the technology is expected to be sufficient in the OR during laparoscopic surgeries. When this technology is installed and used, a considerable difference will be made to the communication and it will open up possibilities for automated communication. The OR planning will improve with more information and updates on the progress in the OR, ensuring the OR is used efficiently and thereby saving time and money.

8.5. Limitations of the Study

A limiting factor was the number of tags. As the HID tags are still being developed, only three tags were available for the study. To get more reliable results, the tests could have been performed with a larger set of tags. This could also yield more significant test results. Furthermore, the protection layer of epoxy was only held in front of the tags and not applied to the tags. This was because of the limited number of tags and the fact that once the epoxy is applied, the tag cannot be removed and reused again.

During the test in the OR, the devices were turned on, but on standby mode, as they were not in use. Although the standard deviations seemed to increase, the maximal reading distances were not affected. To ensure the results of the influence of the devices during a surgery is tested, in later tests, the devices can be used on a simulator while testing the maximal reading distances. The tests performed in the OR were not in-vivo tests, as there was no surgery in progress at the moment of the tests. In-vivo tests can be done to test whether all instruments will be detected during the surgery. It shows realistic movements of the instruments and the orientations of the tags. Furthermore, other influencing factors in the OR that were not tested during the OR test can be taken into account, for example, the use of electrosurgery, where hundreds of kilohertz are applied to the patient through cables which generate a magnetic field. This magnetic field can cause a possible disturbance to the RFID signal [23]. The tests in the OR are performed in the OR at the Reinier de Graaf hospital in Voorburg. Although it was useful to test the set-up in a real OR, it would also be recommended to test the set-up in the OR at the other location of the Reinier de Graaf hospital in Delft. In Delft, the hospital has recently been renewed and the DORA system, working with RFID, is incorporated into every OR. Testing the set-up in combination with the already working DORA system might influence the detection of the tags. Furthermore, every hospital has a different composition of appliances and devices in the operating rooms. Testing in more different hospitals would give a more realistic representation of the expectations of the behaviour of the system when it will be commercially available.

The lab experiments are performed in the clinical lab at the TU Delft. Although this room contains medical appliances, coming close to the final setting for the set-up, the circumstances are not ideal. There are many metal devices and other possibly influencing materials present in the room. Ideally, the first tests would have been performed in an anechoic chamber. An anechoic chamber is a room designed to completely absorb reflections of either sound or electromagnetic waves [20]. This would minimize the external influences of the surroundings.

8.6. Future Work

The first recommendation for future work is, as already mentioned in the limitations, to test the system in the OR in Delft where the DORA system is present. These tests will give insight into whether the DORA system interferes with the set-up and whether the set-up interferes with the DORA system. It is important to know the behaviour of the system for further studies as the test might take place in an OR equipped with a DORA system. Next to testing in the OR in Delft, it is also recommended to test the system in different hospitals before putting it on the market. As earlier mentioned, every OR is different and equipped with different devices. The prediction of the behaviour of the system and the surrounding devices gets more accurate when more different settings are tested. For further research, an attachment of the tag casing from this study to the instrument has to be designed. With this attachment, the instruments can be tagged and the set-up will be ready for in-vivo experiments. In further research, it is also recommended to get more HID tags, to be able to test the layer of epoxy, but also to perform more tests to make the results more reliable.

After the extra tags are available, the protection layer of epoxy is tested and applied, and the attachment to the instruments is made, the next step will be to test the set-up in an OR with devices working on a simulator to see the influences of the devices on the system. If the system functions as desired in the OR with the simulator, the in-vivo tests can start. For the first test, it is recommended that a camera recording is also made, to be able to check whether all instruments are detected. The camera recording creates the possibility to check the system after the surgery as it is not desired to interrupt the surgery to ensure the system works.

8.7. Conclusion

In this study, different approaches are tested to increase the maximal reading distance of RFID 'on-metal' tags to ensure the range is far enough for the technique to be used during a TEP procedure in the OR. For this procedure, a reading distance of 50 cm is desired. The study started with a set of instruments with RFID tags attached to them. In the pilot study, the reading distances were measured and resulted in an average reading distance of 21 cm from the antenna. The next step was to try to use a larger antenna. This resulted in an average reading distance of 32 cm, which is an improvement, but still not the desired 50 cm. Using an even larger antenna was not an option as this would limit the workspace of the medical team. Raising the power of the antenna could also increase the reading distance, but the tests are already performed with the maximally allowed 2 W.

The following step is to take a closer look at the attachment of the RFID tags to the instruments, to see if there are possible improvements to increase the reading distance. First, the basic properties of the metal plates are tested and later on, different casing properties are tested for their influence on the maximal reading distance. The information gathered in these tests is combined to make the final design which will have a higher maximal reading distance than the tags of the instruments in the pilot study. After creating the final design, tests are performed in the lab with the small and large antenna to determine the maximal reading distances. The results of the maximal reading distances with the small antenna are 27 cm: this is still not as far as the desired reading distance. The larger antenna reached an average reading distance of 53 cm in the lab, which is above the desired reading distance. Finally, the improved design of the tag attachment is tested in the OR at the Reinier de Graaf hospital with the large antenna. The reading distances of the tags were sufficient and reading distances in the orientations where the tag was not parallel to the antenna were unexpectedly high. For the last step of this study, the tags are attached to three instruments with a temporary connection to measure the reading distances with the influences of the instruments. No influence of the instruments on the maximal reading distance was detected. The results of this test showed that the desired maximal reading distances can be accomplished with RFID technology.

The main research question was whether it was possible to increase the maximal reading distance of RFID 'on-metal' tags up to 50 cm with the current set-up. It can be concluded from the tests that this is possible. With the final design attached to the instruments in the OR, reading distances with medians between 52.5 cm and 65 cm are achieved. The improvement was not achievable by only changing the set-up, it was the design of the metal plate behind the tag that had to be improved in order to accomplish the desired reading distance. The factors that had an effect on the maximal reading distance were the surface area, a metal plate on the top and bottom of the tag, the type of enclosure surrounding the tag, and finally, the height of the enclosure surrounding the tag.

In conclusion, to achieve the desired reading distance of 50 cm, an improved design was made. With this design, a series of tests was done. The tests showed that the desired reading distance was achieved with the final design both in the lab and in the OR.

A

Safety and Use of RFID

To determine whether RFID can be safely used in healthcare a literature study is performed answering the question: Is it safe to use RFID in hospitals?
First, the different applications of RFID already implemented in healthcare will be briefly mentioned. Second, the challenges and risks of implementing RFID in healthcare are explained. Third, the current laws regarding the safety of RFID are discussed and finally, an answer to the question about whether it is safe to use RFID in a hospital is given.

A.1. Different RFID Applications

As the majority of the work in healthcare is done manually by the employees, there is a considerable risk of human errors. To decrease the number of human errors, hospitals have been trying to reduce the workload by automating parts of the human work for over ten years. One way of reducing the workload is by introducing RFID to the medical sector. RFID is already used in many different medical fields. The applications are widely spread and can be organized into three categories: the first category is RFID applications concerning people, the second category is RFID applications concerning materials, and the last category is RFID in information management.

RFID applications concerning people
RFID applications concerning people are in most cases about tracking and identifying people. This can either be a patient or an employee of the hospital. RFID tags can be worked into a card, shaped like a credit card [5], a wristband (Figure A.1). It can be implemented underneath the skin [24], or it can be incorporated into the clothes [25]. The information can be used to grant access to areas [26], to check on hygiene standards [25], to locate patients [26] or personnel [27], or to get patient records [28].

RFID applications concerning materials
RFID tracking on materials is done in many different applications. The main application is to track equipment throughout the hospital, like beds, wheelchairs, and stretchers [2]. Next, to track the location with RFID, the status of medical devices can also be sent to a central system to give out an alarm when something is not functioning or when a device is scheduled for maintenance [29]. This system is called DORA (Digital Operating Room Assistant) and is initiated at the TU Delft. It is even included in the time-out procedure of the operating rooms (OR) (Figure A.1).
The second application is to manage the inventory. This system manages the inventory and can also track the life cycle of medical devices [5]. In the third application, RFID is used for processes around the OR. For example, counting the surgical sponges [30] and instruments [31] before and after the surgery is usually done by hand, but can also be done using RFID. The fourth application of RFID is to track bags of blood. The background of the blood and the donor can be made visible and by automatically checking if the blood type is correct, the number of human errors can be further reduced [32]. The fifth application is, for example, tracking drugs to prevent counterfeiting and ensuring the authenticity of the drug [33].

Figure A.1: Top left, a baby with RFID tag. (From: https://www.hopelandrfid.com/blog/baby-care-medical-system-with-rfid-technology_b61). Top right, Dora maintenance system. On the left, the screen is green which means no issues are detected. On the right the screen is red, meaning some action has to be taken to solve the issue. (From http://www.medicaldelta.nl/projects/in-love-withdora). Bottom, RFID on a patient's wrist. (From: http://www.rfidwristbandworld.com/)

RFID applications in information management
The final application of RFID is to enhance procedures and to incorporate RFID into the procedure. An example of this is implementing an RFID tag underneath the skin to communicate information to a source outside the body. This is beneficial because there is no need for a line of sight and no intervention has to be done to get the information from the tag [34].

A.2. Challenges and Risks of RFID in Healthcare

Implementing RFID into healthcare introduces challenges for the implementation and potential risks for the hospitals. Three main challenges are frequently mentioned in literature. The most important problem is the costs of an RFID system, followed by the lack of standards and finally the problem is about privacy issues.

Challenges
The cost of an RFID system is an important challenge. Because RFID systems have to be custom made, the costs of the tags, the antennas, and the readers are relatively high compared to the currently used barcodes [26]. When RFID is produced on a large scale, the costs per tag will lower as demonstrated by Walmart [35]. When ordering their suppliers to use RFID, the demand and production increased and thus lowered the prices. The second challenge, the lack of standards, is caused by the multiple frequencies allowed to be used at this moment and the possibility to used any RFID tag and reader. Every tag, antenna, and reader can have a different effect on its surrounding, even though they might operate in the same frequency band [36]. This results in hospitals having to check every different set-up every time a new system is purchased. Third, the problem with privacy issues is related to patients and patient information but also to the staff [37]. Being tracked might be valuable, but nurses can get a feeling of being 'watched' [38]. Properties that make RFID technology attractive for implementation, like the ease of use, no line of sight, and the ability to scan through barriers and objects, also make it vulnerable as the signal can be easily intercepted. There are some solutions to this problem like password protection, RFID tag pseudonyms, or database protection, making it harder to intercept the data and when intercepted, no important information is available for the hackers [39].

Risks

There are several risks mentioned by different studies about the implementation of RFID in a hospital environment. All risks, however, are about the possibility of RFID interfering with the already existing techniques. The studies can be divided into three different categories, the risk of interference with MRI or CT scans, interference with implantable medical devices, and interference with non-implantable medical devices.

For the first category, current techniques like the magnetic resonance imaging (MRI) and computed tomography (CT) scans might encounter problems. It is not only questioned whether the RFID tags influence the current use of the techniques, but also whether the RFID tags are influenced or damaged by the radiation from the MRI or CT scans [40] [41]. Fei et al. [40] found that the RFID tags can still be read properly after being placed in an MRI scan. At a distance of 8 cm, the quality of the images was almost unaffected. Steffen et al. [41] observed the effect of RFID on MRI and MRI on RFID, they also included CT scanning. They found no changes in the RFID tags after MRI and CT scanning. However, some loss in the images was found in the area close to the skin where the tags were placed.

In the second category, the already used active implantable medical devices are thought to be influenced by RFID [42] [43]. It has to be checked whether the implantable devices still work after exposure to RFID as the current treatments should not be interrupted or compromised. Tests have been performed exposing implantable medical devices to an RFID system at different distances. The behaviour and functioning of the devices were tested to see if there was interference. The devices turned out to be functioning normally like before the tests [42]. Seidman et al. [43] also tested implantable devices for electromagnetic interference with different RFID readers and at different frequencies. They found that the implantable devices did respond in some cases to the radio frequencies. They found evidence that justifies the concern for implantable devices with low and high frequencies, but since the FDA has not received any incident reports about this, they don't believe there is an urgent public health risk.

The third category is most important and most mentioned. It is about the risk of electromagnetic interference with medical devices [44–51]. This problem concerns all devices used for treatment in the operating room, but also in other places in the hospital. It is feared that medical devices could operate differently than usual, making them unreliable [45]. Different studies have been conducted to test the interference of RFID on medical devices. For example van der Togt et al. [50] tested two different RFID systems in the proximity of 41 medical devices. The tests were performed at different distances to the devices, while the RFID equipment was moved around the medical devices. They found several reproducible incidents in their tests varying from light to hazardous and most incidents were found with the passive 868 MHz RFID signals. They conclude by saying that the results only apply to the two specific RFID systems they used. In a hospital in Indianapolis [51] another test was conducted in a patient care room with 30 devices, connected to a simulator. Two different RFID systems were used and both were ultrahigh frequency and passive tags. In none of their tests was interference from the RFID devices found. All devices performed as expected. They conclude by saying that RFID systems can be used in general patient care rooms without concern of adverse device performances. But when a new RFID system or component is introduced, additional studies may be necessary to evaluate evolving RFID technology and the impact on medical equipment.

In 2008 the University of Auckland, New Zealand, reproduced parts of the tests from van der Togt et al. [50], by also testing on an infusion pump. They used multiple different readers and even more than one reader at the same time. Interference was only found with one specific reader and when all five readers simultaneously were used. Failures were detected, but not reproducible. They concluded with the notion that high power RFID readers show interference and low power readers did not in their case. They also concluded that their low power tests seem to be safe for now [49]. In Italy, the interference with medical devices is tested on an intensive care unit (ICU) of the children's hospital, with 16 critical care devices that were regularly used at that time. The results of this study show no interference and all devices functioning the same before and after the tests. However, they still advise testing the specific RFID hardware in a new setting. And when new systems are purchased, they should be the most robust over the electromagnetic interference (EMI) [46].

A.3. Safety and Laws of RFID

To evaluate whether RFID is safe to use in a medical environment regarding the electromagnetic interference, more information is needed. The different outcomes of previous work explained in Section

A.2, contradict each other and there is no consensus on whether or not RFID is safe to use in medical care. Some studies found interference, others did not. They do, however, all recommend using RFID as they recognize the benefits of the technique, but with prior on-site testing.

For on-site testing, two standards have been developed, the first for implantable medical devices and the second for non-implantable medical devices. These standards ease the on-site testing and the results of the tests from different hospitals all over the world can be compared to gather information about the safety. In 2011, a standard (ISO 20017) [52] was published with information about implantable medical devices and their interaction with RFID [53]. In 2016, a new standard was released: Medical Electrical Equipment & System Electromagnetic Immunity Test for Exposure to RFID Readers, standard 7351731 [54]. In this standard, manufacturers of medical devices as well as end-users will get guidance on how to evaluate their devices for immunity to electromagnetic interference from RFID systems [55].

In the Netherlands, there are no laws yet about RFID. When applying RFID in a hospital to improve the patient information system, there is, however, an applicable law that has to be obeyed. This is the law for the protection of personal information ("Wet Bescherming Persoonsgegevens", WBP) [51]. The WBP law is from the Netherlands and is the elaboration on the European directive on personal data protection (95/46/EG) [56]. Another Dutch law, "Wet op de medische hulpmiddelen" [57], has to be taken into account. "Wet op de medische hulpmiddelen" can be translated into "Law on Medical Devices". This law applies to instruments, devices, and software that are used for diagnoses, monitoring the patient, treatment, and administering medication. This means for RFID systems that they need to have a CE-mark. Furthermore, the RFID system has to be specifically designed for medical applications and this has to be mentioned in the manual.

A.4. Conclusion

To conclude, there are a lot of benefits to using RFID technology in medical care. For now, the answer to the question regarding the safety of using RFID in healthcare is not possible to give, before testing the system in the real clinical situation. Nor is it known if there are specific circumstances where RFID should or shouldn't be used. Individual on-site tests need to be performed, in every specific situation to make sure there is no harmful interference. After gathering more information about RFID with the new protocols, manufacturers might be able to answer this question and prevent problems when creating a new system.

B

Antenna Arm

For the tests in the OR an arm is made to attach the antenna to the side of the bed. By placing the antenna on the side of the bed, the antenna is close to the surgical area, without adding extra devices on the ground.

The arm of the antenna will be designed as a system with 4 degrees of freedom: translation in the x- and z-direction and rotation about the z- and y-axis, see the axis in Figure B.2. The translation in the x-direction is needed to be able to adjust the distance between the antenna and the surgical site. This way the bed clip can be placed further away from the doctor, leaving more space to perform the surgery. The translation in the z-direction can be used to lower or raise the antenna. This is useful when a patient is larger than average and more space is required. The rotation about the z-axis is to be able to turn the antenna away from the surgical site. This is necessary in case of complications when the doctor needs to be able to reach the patient as the antenna can be turned to the side of the bed. The rotation about the y-axis enables the possibility of tilting the antenna in the right way to be able to focus on the surgical area.

B.1. Connection to the Bed

The arm will be connected to the DIN rail on the side of the bed. The bed clip that will be used is shown in Figure B.1. This clip is specially made for use in hospitals and is usually used to position arm or leg support at the side of the table. The bed clip consists of a part that surrounds the DIN rail and the other part where a round bar can be put through the clip. The bar is secured in height and in rotation by one screw.

B.2. Translation in the X-Direction

To allow a translation in the x-direction, five concepts have been made (Figure B.2). The five concepts are the sliding joint, the telescopic arm, the different bar size, the three-joints, and the zigzag arm.

Sliding joint

In the sliding joint design (Figure B.2a), the arm is connected on the side of the bed. A bar goes vertically up and at the end of the bar, a sliding joint is made. Moving the antenna in the x-direction can be done by moving the horizontal bar through the tube. The bar can be fastened with a screw.

Telescopic arm

In the telescopic arm (Figure B.2b), the arm is connected on the side of the bed, like in the sliding joint design. The vertical bar ends with a 90-degree angle. The horizontal bar consists of different parts that slide over each other. This way the horizontal bar can be elongated.

Different bar sizes

For this design, different bar sizes can be picked (Figure B.2c). The arm is again connected to the side of the bed and the vertical bar ends with a 90-degree angle, like in the telescopic arm. The desired
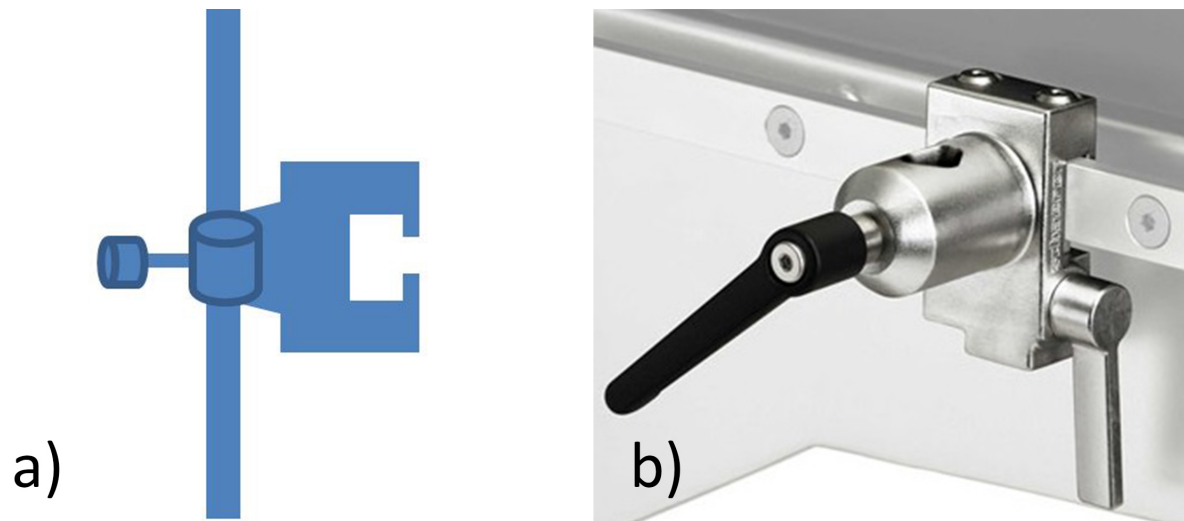
Figure B.1: a) Schematic drawing of the connection to the DIN rail of the surgical bed. b) Rapid-action radial setting clamp (From: http://www.melydsurgical.co.uk/schaerer-clamps/).

length of the arm can be chosen depending on the desired position of the antenna.

Three-joints

For the three-joints design (Figure B.2d), the arm is still connected to the side of the bed and the vertical bar ends with the first joint. One bar is connected to the first and second joint and another bar is connected to the second and third joint. the other side of the third joint is connected to the antenna. The three-joints of this design make sure that the antenna can be placed in different positions. This ensures the translation in the x-direction, but also in the z-direction and a rotation about the y-axis.

Zigzag arm

For the zigzag design (Figure B.2e), the arm is again connected to the side of the bed and a vertical bar goes up. This design provides a translation in the x-direction through the crossing bars. By creating friction in one upper and one lower joint between the bars, the antenna cannot lower or fall down.

B.3. Translation in the Z-Direction

To allow a translation in the z-direction, two different concepts are created. First, the bed clip, and second, the three-joints design from the previous section.

Bed clip

To realize a translation in the z-direction, the clip on the side of the bed can be used (Figure B.1). By moving the bar through the tube and fastening the screw, different positions can be reached. To ensure the arm will not lower during the procedure, an extra ring is attached to the bar above the bed clip. If for some reason the bed clip screw comes loose, the arm will not lower.

Three-joints

As mentioned before, the three-joints can also be used to change the height of the antenna (Figure B.2d). By positioning the antenna higher or lower, with the three-joints, the desired configuration can be accomplished.

B.4. Rotation About the Y-Axis

For the rotation about the y-axis, three concepts are created. The ball-joint, the elongated top/bottom, and the 'Antenna tube', see Figure B.3.
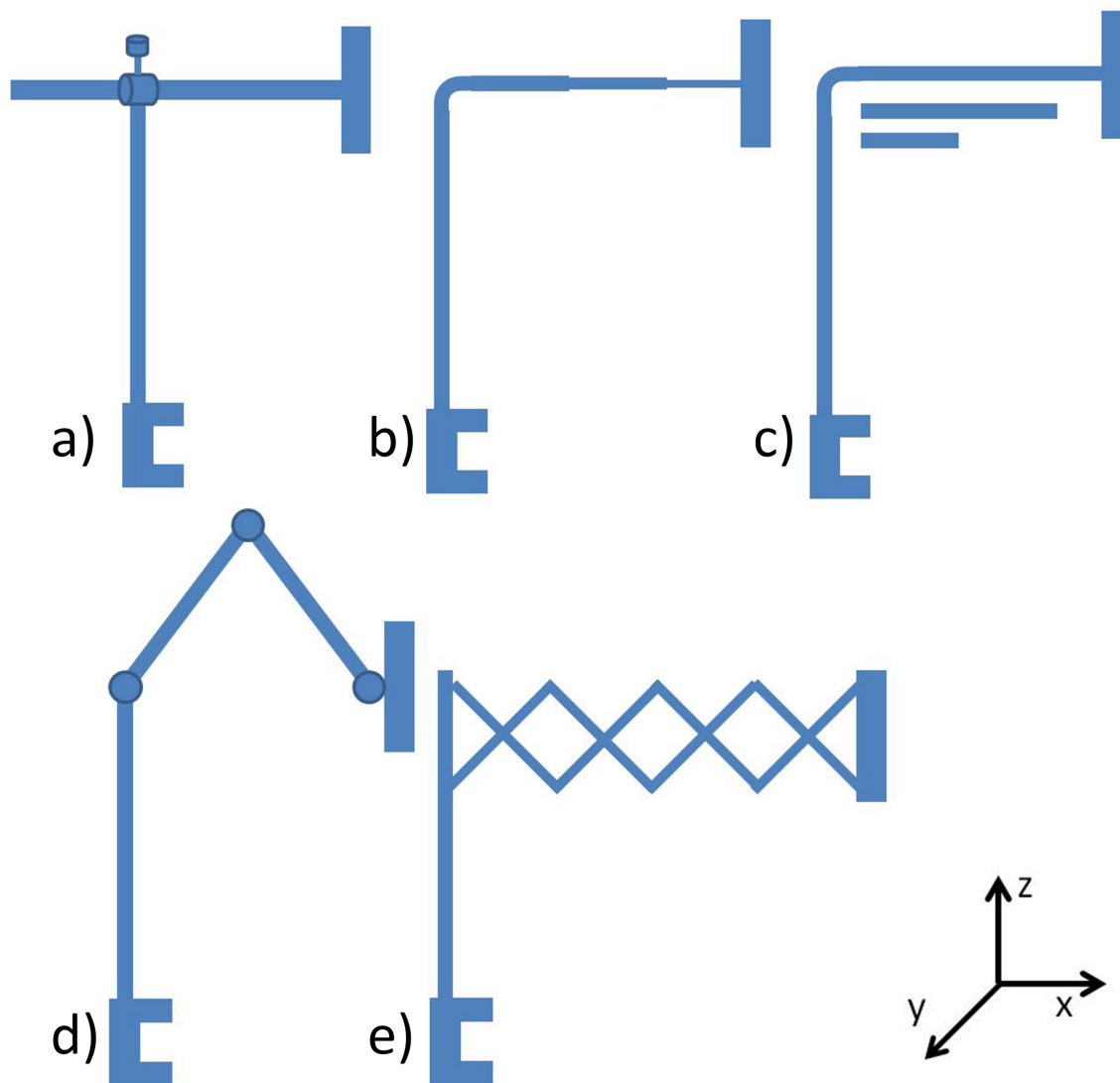
Figure B.2: A schematic drawing of the five designs to allow translation in the x-direction. a) The sliding joint. b) The telescopic arm. c) The different bar sizes. d) The 'three-joints'. e) The zigzag arm.

Ball-joint
In the ball-joint concept, a ball and socket joint is placed at the end of the horizontal bar (Figure B.3a). With this joint, the antenna can move around the x-axis, making it possible to perform small adjustments to point the antenna to the surgical site.

Elongated top/bottom
In the elongated top or bottom concept (Figure B.3b), a plate is placed perpendicular to the horizontal bar at the end of the horizontal bar. The antenna is connected to the plate with screws or small bars. With screws or small steps, the position of the antenna can be adjusted. This way small rotations can be realized.

Antenna tube
At the end of the horizontal bar, a tube is placed for the antenna tube concept (Figure B.3c). The antenna is connected to a bar. This bar goes through the tube and can be rotated, to place the antenna in the right position. By fastening the screw, friction will be created, so the antenna will stay in place.
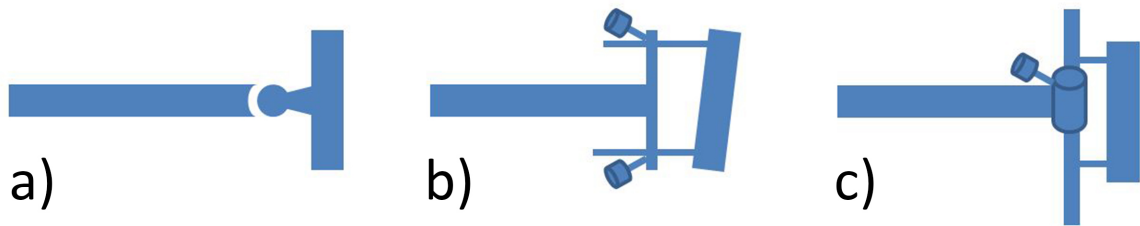
Figure B.3: A schematic drawing of the top view of the three concepts for the rotation about the y-axis. a) The ball joint. b) The elongated top or bottom. c) The antenna tube.

B.5. Rotation About the Z-Axis

Rotation about the z-axis is necessary to be able to point the antenna in the right direction, but also for the surgical team to be able to move the antenna away from the surgical area when it is bothering them. To realize this rotation, two possible concepts are made: the rotation in the bed clip and the rotation at the first joint.

Bed clip

When adjusting the height of the antenna at the bed clip (Figure B.1), the bar can also be rotated in the desired position. If the antenna has to be moved away from the surgical area, this is possible by loosening the screw and rotating the top of the antenna. When the screw is loosened, a little room is created for the bar to be turned.

At the first joint

The rotation about the z-axis can also be accomplished by creating a joint in the first corner where the vertical bar is connected to the horizontal bar, see Figure B.4. In the figure, the concept is combined with the sliding joint concept. The horizontal bar rotates around the vertical bar with the joint. Due to this mechanism, the desired position can be chosen and the arm can be turned away when needed. To fixate the position, a screw can be used.
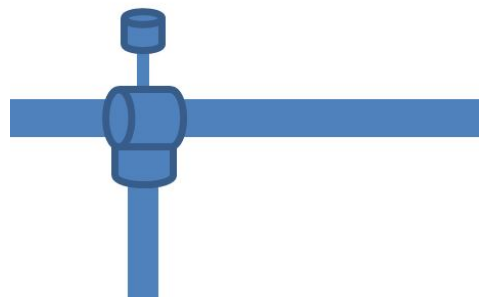
Figure B.4: A schematic drawing of the rotation point at the first joint.

B.6. Combination of the Different Concepts

To finally create an antenna arm, the different concepts are combined into one design, see Figure B.8. To come to this combination, three Harris Profiles are made, one for the translation in the x-direction, and one for each rotation.

Translation X-Direction

To determine which concept will be used to realize the translation in the x-direction, a Harris Profile is made (Figure B.5). The first considered factor is the sterilization of the arm. During the surgery a plastic sleeve can be used to cover the arm of the antenna. This is possible for the sliding joint, the three-joints, and the telescopic arm, but for the zigzag arm and the different bars is this not possible. As the zigzag arm changes in thickness when moving the antenna in the x-direction and for the different bar access to the bars is needed for changing. When looking at the second factor, the ease of use, the sliding joint scores best, because this is easy to adjust by loosening one screw. The telescopic arm is held in place by friction, so to adjust the movement, first the nurse has to overcome the friction, the same goes for the three-joints and the zigzag arm. The different bars is not easy to use as the entire construction needs to be disassembled to make changes in the translation in the x-direction. After adding the third factor, the simplicity, the sliding joint is chosen, because this is a more simple concept than the three-joints.

	'Tube' joint				Telescopic arm				Different bars				Three joints				Zigzag arm			
	++	+	-	--	++	+	-	--	++	+	-	--	++	+	-	--	++	+	-	--
Sterilizable	■	■					■	■			■		■	■					■	
Ease of use	■	■				■					■		■	■				■		
Simplicity	■	■			■	■					■	■	■	■			■	■		

Figure B.5: A Harris Profile comparing the five concepts for the translation in the x-direction.

Translation Z-Direction

The choice of how to realise the translation in the z-direction is done by looking at whether or not the option was already present in the concept. This is the case for the bed clip, which is automatically chosen with the connection to the bed. From the x-direction concepts, the Three joints was not chosen, so for the translation in the z-direction these joints are not added.

Y-Rotation

To determine which concept will be used, a Harris Profile with three factors is made (Figure B.6).The ball joint is easy to use as only one screw needs to be fastened to secure the position of the antenna. The elongated top/bottom is not as easy as two screws are used and the angle of the antenna needs to stay small to prevent the bars on the antenna from breaking. The antenna tube also only requires one screw to be fastened. The ball joint is simple solution, adding minimal extra components to the end of the bar, making this an elegant solution. The elongated top/bottom adds a plate, two screws and elongating bars. This solution makes the tip of the construction bulky. This might interfere with the work flow of the surgeons. The antenna tube also adds extra parts to the tip of the construction, however, less than in the elongated top/bottom. The ball joint is available to order. It is a monitor mounting system. The elongated bottom and antenna tube are not commercially available, but it is possible to make the parts.

Z-Rotation

To determine which concept will be used, a Harris Profile with three factors is made (Figure B.7). As the bed clip is present in all combinations of the antenna arm, it is possible to use this mechanism to rotate the system around the z-axis. However, a rotation at the first joint is also possible in all combinations by simply adding one part. A disadvantage of the bed clip is the possibility of lowering the entire system when only a small rotation is required. This could be prevented with an extra ring

	Ball joint				Elongated top/bottom				Antenna tube			
	++	+	-	--	++	+	-	--	++	+	-	--
Ease of use	🟩	🟩					🟥			🟩		
Simple construction	🟩	🟩					🟥	🟥			🟥	
Availability	🟩	🟩				🟩				🟩		

Figure B.6: A Harris Profile comparing the three concepts for the rotation about the y-axis.

above the bed clip. When the rotation is realised at the first joint, it is impossible for the entire system to lower, when a correction is made. To realise a rotation with the bed clip the entire system needs to be supported. When rotating around the first joint, the bottom part of the system stays supported and only small forces are needed to rotate the antenna.

	Bed clip				At the first joint			
	++	+	-	--	++	+	-	--
Ease of implementation	🟩	🟩				🟩		
Reliability			🟥		🟩	🟩		
Low clamping forces required			🟥		🟩	🟩		

Figure B.7: A Harris Profile comparing the three concepts for the rotation about the z-axis.

B.7. Final Antenna Arm

The final antenna arm is shown in Figure B.8. The top figure shows a schematic drawing of the final antenna arm and the bottom figure shows a photo of the antenna arm in the OR. The translation in the x-direction is made possible by the sliding joint at the top of the vertical bar. The translation in the z-direction is realised at the bedclip. To prevent the entire system from lowering when the clip is loosened, an extra ring is placed on the vertical bar, so the system can not drop unexpectedly. The rotation about the y-axis is done at the end of the horizontal bar with a ball joint close to the antenna, making small adjustments to the position of the antenna possible. The rotation about the z-axis is done at the first joint, this is needed to quickly turn the antenna way during the surgery.
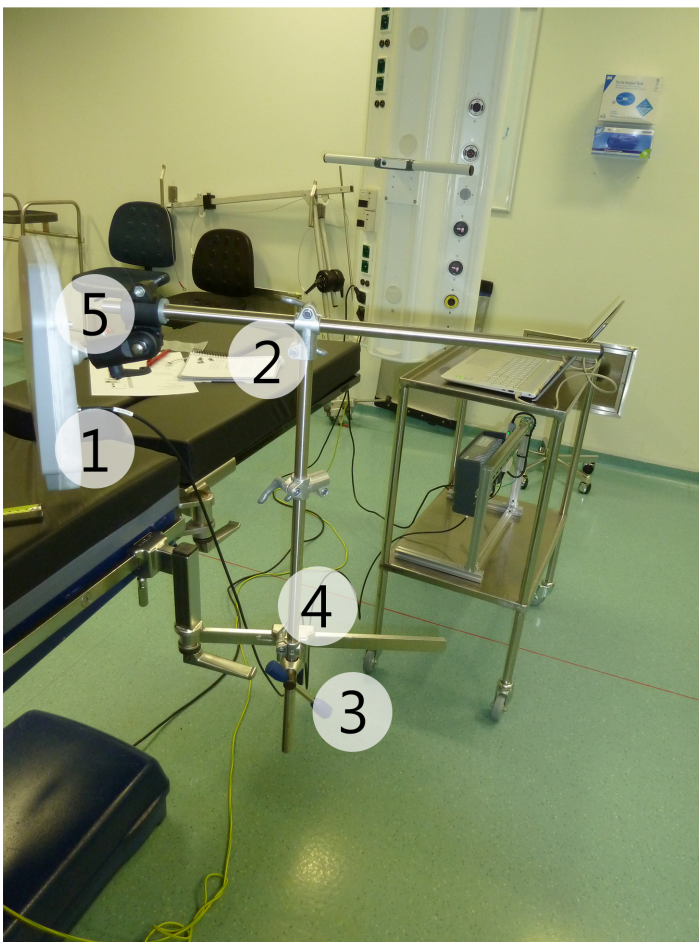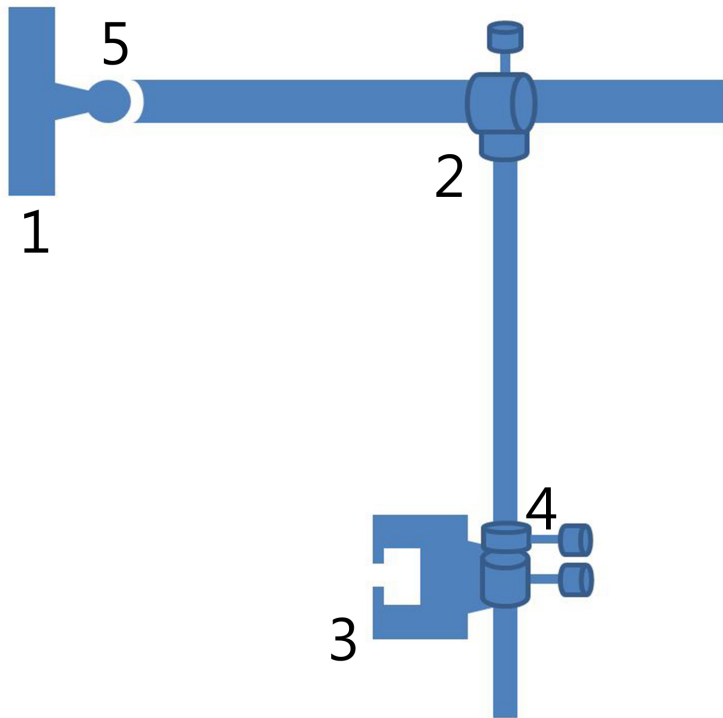
1) Antenna
2) Sliding joint
3) Bed clip
4) Fixating ring
5) Ball joint

Figure B.8: Top: A schematic drawing of the final antenna arm. Bottom: The final antenna arm attached to the bed in the OR. The shown parts in both figures are: 1. The antenna. 2. The sliding joint. 3. The bed clip. 4. The fixating ring. 5. The ball joint.

C

Raw Data

In this Appendix, the raw data of the experiments are given with the averages of the measurements.

C.1. Surface Area

Tables C.1 and C.2 show the maximal reading distance of the Xerafy and the HID tags in centimeters. The last row shows the average maximal reading distance rounded to whole numbers. Per type, three tags are tested on the four different metal plates, with a thickness of 1 mm. The A and B column represent respectively, the test when the tag is facing the antenna and the test with the back of the metal plate facing the antenna.

Table C.1: Maximal reading distances per Xerafy tag on four different plates.

Surface area - Xerafy	10x10mm		20x20mm		30x30mm		40x40mm	
	A	B	A	B	A	B	A	B
E2009A7030091AF000000087	58	44	84	83	73	83	62	88
E2009A7030091AF000000654	74	63	74	93	146	160	77	86
E2009A7030091AF000001016	56	38	81	150	62	59	66	82
Average	63	48	80	109	94	101	68	85

Table C.2: Maximal reading distances per HID tag on four different plates.

Surface area - HID	10x10mm		20x20mm		30x30mm		40x40mm	
	A	B	A	B	A	B	A	B
E280117000000208D0C1DC67	56	56	58	73	101	68	137	84
E280117000000208D0C1E564	59	61	71	77	90	70	148	90
E280117000000208D0C1CD67	61	57	108	75	59	69	136	128
Average	59	58	79	75	83	69	140	101

C.2. Thickness

The maximal reading distances of only the HID tags on the four thicknesses of the 20x20 mm plates are shown in Table C.3 and C.4. Per stainless steel plate, three different HID tags are tested. The A and B column represent respectively, the test when the tag is facing the antenna and the test with the back of the metal plate facing the antenna. These tests are repeated once for the 0.5 mm and the 1 mm plate.

Table C.3: Maximal reading distances for the different thicknesses with the average maximal reading distance, rounded up to whole numbers.

Thickness	0,5 mm		1 mm		2 mm		3 mm	
	A	B	A	B	A	B	A	B
E280117000000208D0C1DC67	76	85	59	70	76	62	79	86
E280117000000208D0C1E564	88	87	73	72	97	81	82	76
E280117000000208D0C1CD67	95	86	87	66	88	56	86	87
Average	86	86	73	69	87	66	82	83

Table C.4: Maximal reading distances for the different thicknesses with the average maximal reading distance, rounded up to whole numbers.

Extra thickness	0,5 mm		1 mm	
	A	B	A	B
E280117000000208D0C1DC67	78	81	90	87
E280117000000208D0C1E564	75	69	104	86
E280117000000208D0C1CD67	103	88	87	89
	85	79	94	87

C.3. Bar Length

The maximal reading distances for the HID tags for the four different bar lengths with a thickness of 1 mm are shown in Tables C.5 and C.6. The last row shows the average maximal reading distance rounded to whole numbers. Table C.5 shows the maximal reading distances with the tag placed on the corner of the bar, as seen in Figure 4.6b. The maximal reading distances with the tag placed in the centre of the bar can be seen in Table C.6. The A and B column represent respectively, the test when the tag is facing the antenna and the test with the back of the metal plate facing the antenna.

Table C.5: Maximal reading distances with the tag on the corner of the bar and the average maximal reading range, rounded up to whole numbers.

Bar - Tag on the corner	10x10mm		10x20mm		10x30mm		10x40mm	
	A	B	A	B	A	B	A	B
E280117000000208D0C1DC67	56	56	56	56	57	56	56	56
E280117000000208D0C1E564	59	61	59	58	59	58	61	57
E280117000000208D0C1CD67	61	57	59	58	61	56	59	58
Average	59	58	58	57	59	57	59	57

C.4. Plate with Cut-Outs

The different maximal reading distances of the three HID tags on the hashtag shaped plate with a thickness of 1 mm can be found in Table C.7. The last row shows the average maximal reading distance rounded to whole numbers.

C.5. Top and Bottom Plate

In Table C.8, the maximal reading distances and the average reading distance of the HID tags are shown when the tag is placed between two 20x20 mm plates of 1 mm thick. The experiment is done with one plate facing the antenna.

Table C.6: Maximal reading distances with the tag in the centre of the bar and the average maximal reading range, rounded up to whole numbers.

Bar - Tag in the centre	10x10mm		10x20mm		10x30mm		10x40mm	
	A	B	A	B	A	B	A	B
E280117000000208D0C1DC67	56	56	58	56	56	56	66	55
E280117000000208D0C1E564	59	61	62	55	64	54	76	75
E280117000000208D0C1CD67	61	57	59	58	63	56	78	75
Average	59	58	60	56	61	55	73	68

Table C.7: Maximal reading distances per tag on plate with cut-outs and the average maximal reading range, rounded up to whole numbers.

Cut-outs plate	20x20mm	
	A	B
E280117000000208D0C1DC67	79	61
E280117000000208D0C1E564	127	118
E280117000000208D0C1CD67	92	78
Average	99	86

C.6. Full Enclosure

Table C.9 shows the maximal reading distances of three different HID tags in centimeters, the first column shows the tag ID's, the second and third column show the maximal reading distance of the bars with a surrounding of 1 mm high. The fourth and fifth column show the results of the bar with a surrounding of 2 mm and the sixth and seventh, of the 3 mm high surrounding. Column A represents the tests performed with the tag facing the antenna and Column B the back of the bar facing the antenna. The last row of the table shows the average reading distances of the three tags.

C.7. Partial Enclosure

Flat pins
The results of the tests with the flat pins on the bars are shown in Table C.10. The maximal reading distances of the three HID tags are shown for the three different bars, with the pins of 1 mm, 2 mm, and 3 mm. The A and B column represent respectively the tag facing the antenna and the back of the bar facing the antenna. The last row of the table shows the average reading distances of the three tags.

Round pins
The results of the tests with the round bars on the bars are shown in Table C.11. The maximal reading distances of the three HID tags are shown for the three different bars, with the pins of 1 mm, 2 mm, and 3 mm. The A and B column represent respectively the tag facing the antenna and the back of the strip facing the antenna. The last row of the table shows the average reading distances of the three tags.

Different corners
The results of the tests with the two and four corners with a height of 1mm on the bars are shown in table XXX. The maximal reading distances of the three HID tags are shown. The A and B column represent respectively the tag facing the antenna and the back of the bar facing the antenna. The last row of the table shows the average reading distances of the three tags.

C.8. Surface

Table C.13 shows the maximal reading distance of three different HID tags in centimeters. The tags are placed on the bar with 2 corners, the surrounding of 1 mm high and the bar with the round pins

Table C.8: Maximal reading distances of the tag between two plates and the average maximal reading range, rounded up to whole numbers.

Top and bottom	20x20mm
E280117000000208D0C1DC67	46
E280117000000208D0C1E564	41
E280117000000208D0C1CD67	37
Average	41

Table C.9: Maximal reading distances in cm per tag with the full enclosure surrounding the tag.

Surrounding	1 mm		2 mm		3 mm	
	A	B	A	B	A	B
E280117000000208D0C1DC67	32	31	0	0	0	0
E280117000000208D0C1E564	45	29	0	0	0	0
E280117000000208D0C1CD67	39	33	20	35	0	0
Average	39	31	7	12	0	0

of 1mm high. This time the tags are not placed within the enclosures, but on the other end of the bar. Column A represents the tests performed with the tag facing the antenna and Column B the back of the bar facing the antenna. The last row of the table shows the average reading distances of the three tags.

C.9. Protection Layer

The results of the test with the three different layers of epoxy held in front of the tags are shown in Table C.14.

C.10. Clinical Lab Measurements with Antenna 1

The results of the measurements with the final design in the clinical lab obtained with Antenna 1 are shown in Table C.15, C.16, C.17, and C.18. Table C.15 shows the results obtained with the short version of the final design in the A and B orientations. The results with the long version of the final design are shown in Table C.16. The results of the measurements performed in the other four orientations C, D, E, and F for the short and long version of the final design are, respectively, shown in Table C.17 and C.18.

Table C.10: Maximal reading distances in cm per tag with flat pins surrounding the tag.

Flat pins	1 mm		2 mm		3 mm	
	A	B	A	B	A	B
E28011700000208D0C1DC67	54	50	49	47	39	33
E28011700000208D0C1E564	57	52	57	52	0	0
E28011700000208D0C1CD67	54	54	52	48	36	39
Average	55	52	53	49	25	24

Table C.11: Maximal reading distances in cm per tag with round pins surrounding the tag.

Round pins	1 mm		2 mm		3 mm	
	A	B	A	B	A	B
E28011700000208D0C1DC67	51	50	52	46	0	0
E28011700000208D0C1E564	56	52	56	51	56	37
E28011700000208D0C1CD67	54	52	50	50	46	49
Average	54	51	53	49	34	29

C.11. Clinical Lab Measurements with Antenna 2

The results of the measurements with the final design in the clinical lab obtained with Antenna 2 are shown in Table C.19, C.20, C.21, and C.22. Table C.19 shows the results obtained with the short version of the final design in the A and B orientations. The results with the long version of the final design are shown in Table C.20. The results of the measurements performed in the other four orientations C, D, E, and F for the short and long version of the final design are, respectively, shown in Table C.21 and C.22.

Table C.12: Maximal reading distances in cm per tag with the tag enclosed by two and four corners

Corners	Two		Four	
	A	B	A	B
E280117000000208D0C1DC67	60	52	54	50
E280117000000208D0C1E564	55	51	58	50
E280117000000208D0C1CD67	54	52	56	53
Average	56	52	56	51

Table C.13: Maximal reading distance in cm per tag on uneven ground of three different bars.

Uneven ground	Corners		Surrounding		Round pins	
	A	B	A	B	A	B
E280117000000208D0C1DC67	59	56	59	53	59	53
E280117000000208D0C1E564	58	56	61	54	58	53
E280117000000208D0C1CD67	59	56	58	56	59	57
Average	59	56	59	54	59	54

C.12. Operating Room Measurements with Antenna 2

The results of the measurements with the final design in the OR at the Reinier de Graaf hospital obtained with Antenna 2 are shown in Table C.23, C.24, C.25, and C.26. Table C.23 shows the results obtained with the short version of the final design in the A and B orientations. The results with the long version of the final design are shown in Table C.24. The results of the measurements performed in the other four orientations C, D, E, and F for the short and long version of the final design are, respectively, shown in Table C.25 and C.26. Finally, Table C.27 shows the results of the measurements in the OR with short version of the final design attached to the instruments.

Table C.14: Maximal reading distance in cm per tag with different layer of epoxy in front of the tag.

Epoxy	Thin layer		Thick layer		Cup	
	A	B	A	B	A	B
E280117000000208D0C1DC67	55	53	52	53	53	53
E280117000000208D0C1E564	59	56	59	59	60	59
E280117000000208D0C1CD67	59	58	60	57	60	59
Average	58	56	57	56	58	57

Table C.15: Maximal reading distance in cm per tag of the short version of the final design in the clinical lab with Antenna 1.

Final design - short Clinical lab - Antenna 1	Experiment 1		Experiment 2		Experiment 3	
	A	B	A	B	A	B
E280117000000208D0C1DC67	28	29	29	28	30	22
E280117000000208D0C1E564	29	28	27	32	32	29
E280117000000208D0C1CD67	31	29	32	29	31	31
Average	29	29	29	30	31	27

Table C.16: Maximal reading distance in cm per tag of the long version of the final design in the clinical lab with Antenna 1.

Final design - long Clinical lab - Antenna 1	Experiment 1		Experiment 2		Experiment 3	
	A	B	A	B	A	B
E280117000000208D0C1DC67	18	19	28	18	29	20
E280117000000208D0C1E564	31	19	31	18	32	26
E280117000000208D0C1CD67	29	16	28	28	29	21
Average	26	18	29	21	30	22

Table C.17: Maximal reading distance in cm per tag of the short version of the final design in the clinical lab with Antenna 1 in the C, D, E, and F orientations.

Orientations - short Clinical lab - Antenna 1	C	D	E	F
E280117000000208D0C1DC67	78	80	49	57
E280117000000208D0C1E564	85	79	25	33
E280117000000208D0C1CD67	80	82	48	33
Average	81	80	41	41

Table C.18: Maximal reading distance in cm per tag of the long version of the final design in the clinical lab with Antenna 1 in the C, D, E, and F orientations.

Orientations - long Clinical lab - Antenna 1	C	D	E	F
E280117000000208D0C1DC67	80	79	15	13
E280117000000208D0C1E564	61	65	46	24
E280117000000208D0C1CD67	82	80	30	24
Average	74	75	30	20

Table C.19: Maximal reading distance in cm per tag of the short version of the final design in the clinical lab with Antenna 2.

Final design - short Clinical lab - Antenna 2	Experiment 1		Experiment 2		Experiment 3	
	A	B	A	B	A	B
E280117000000208D0C1DC67	53	48	54	52	54	51
E280117000000208D0C1E564	55	51	54	53	53	55
E280117000000208D0C1CD67	56	54	53	53	53	51
Average	55	51	54	53	53	52

Table C.20: Maximal reading distance in cm per tag of the long version of the final design in the clinical lab with Antenna 2.

Final design - long Clinical lab - Antenna 2	Experiment 1		Experiment 2		Experiment 3	
	A	B	A	B	A	B
E280117000000208D0C1DC67	52	53	52	50	54	52
E280117000000208D0C1E564	54	52	53	54	56	54
E280117000000208D0C1CD67	56	55	53	56	53	54
Average	54	53	53	53	54	53

Table C.21: Maximal reading distance in cm per tag of the short version of the final design in the clinical lab with Antenna 2 in the C, D, E, and F orientations.

Orientations - short Clinical lab - Antenna 2	C	D	E	F
E280117000000208D0C1DC67	92	90	67	81
E280117000000208D0C1E564	91	90	81	84
E280117000000208D0C1CD67	94	87	82	79
Average	92	89	77	81

Table C.22: Maximal reading distance in cm per tag of the long version of the final design in the clinical lab with Antenna 2 in the C, D, E, and F orientations.

Orientations - long Clinical lab - Antenna 2	C	D	E	F
E280117000000208D0C1DC67	89	81	80	81
E280117000000208D0C1E564	98	93	65	133
E280117000000208D0C1CD67	104	90	76	83
Average	97	88	74	99

Table C.23: Maximal reading distance in cm per tag of the short version of the final design in the OR with Antenna 2.

Final design - short OR	Experiment 1 A	B	Experiment 2 A	B	Experiment 3 A	B
E280117000000208D0C1DC67	46	44	49	47	47	48
E280117000000208D0C1E564	50	49	72	47	65	51
E280117000000208D0C1CD67	52	67	73	68	71	64
Average	49	53	65	54	61	54

Table C.24: Maximal reading distance in cm per tag of the long version of the final design in the OR with Antenna 2.

Final design - long OR	Experiment 1 A	B	Experiment 2 A	B	Experiment 3 A	B
E280117000000208D0C1DC67	49	46	50	49	52	48
E280117000000208D0C1E564	68	61	67	70	73	49
E280117000000208D0C1CD67	56	46	63	69	54	62
Average	58	51	60	63	60	53

Table C.25: Maximal reading distance in cm per tag of the short version of the final design in the OR with Antenna 2 in the C, D, E, and F orientations.

Orientations - short OR	C	D	E	F
E280117000000208D0C1DC67	107	112	132	120
E280117000000208D0C1E564	116	122	96	74
E280117000000208D0C1CD67	128	127	104	100
Average	117	120	111	98

Table C.26: Maximal reading distance in cm per tag of the long version of the final design in the OR with Antenna 2 in the C, D, E, and F orientations.

Orientations - long OR	C	D	E	F
E280117000000208D0C1DC67	109	97	112	125
E280117000000208D0C1E564	106	73	132	136
E280117000000208D0C1CD67	136	125	133	122
Average	117	98	126	128

Table C.27: Maximal reading distance in cm per tag of the short version of the final design in the OR with Antenna 2 attached to the three instruments.

Final design Short on instrument	Laparoscopic A	B	Spreader A	B	Clamp A	B
E280117000000208D0C1DC67	49	46	50	49	52	48
E280117000000208D0C1E564	68	61	67	70	73	49
E280117000000208D0C1CD67	56	46	63	69	54	62
Average	58	51	60	63	60	53

D

Extra Experiments

Another test has been carried out to see if different shapes of the tip of the bar influence the reading range of the tags. This was done in case the different casings all blocked the signal and the tag had to be held in place by the epoxy layer. The different tips of the bar are designed so that the epoxy layer is form-locked and it would not come loose during the surgery. The dependent variable that will be measured is still the maximal reading distance. The independent variable is:

- Different tips of the bar

D.1. Different Tips of the Bar

In case the metal parts on the bars block the signal partially or entirely, limiting the reading range, three flat designs are made. These designs would be used in case the other designs do not function as desired. Figure D.1 shows from top to bottom, the outer part of the metal bars with corners on the side of the bar, a T-shape at the top of the bar, and a tapered top of the bar. These designs will not ensure the exact placing of the tags, but when the tags and top of the bars are covered in epoxy, these designs will ensure that the epoxy is form-locked on the bar, reducing the possibility of the tag and epoxy layer coming off.
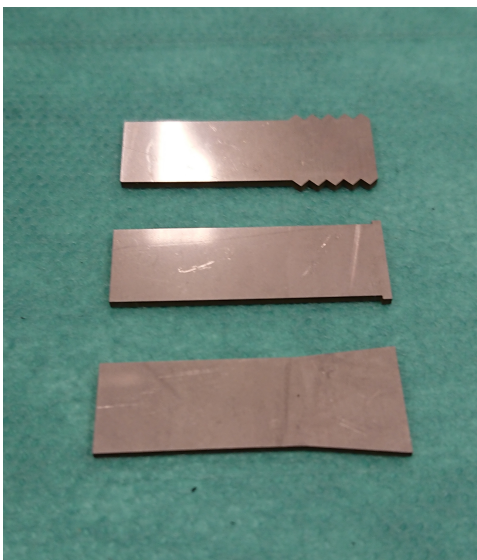
Figure D.1: Three different tips of the bar; from top to bottom, the corners on the side of the bar, a T-shape at the top of the bar, and a tapered top of the bar.

D.2. Results

The results of the tests with the different tips of the strips are shown in Table D.1. The maximal reading distances of the three HID tags are shown for the three different strips, with the tapered end, the T-shaped end, and the corners on the side of the strip. The A and B column represent respectively the tag facing the antenna and the back of the strip facing the antenna. The last row of the table shows the average reading distances of the three tags.

Table D.1: Maximal reading distances in cm per tag with different tips of the metal strips.

Top	Tapered		T-shape		Corners	
	A	B	A	B	A	B
E280117000000208D0C1DC67	55	48	54	52	53	53
E280117000000208D0C1E564	52	52	58	58	56	53
E280117000000208D0C1CD67	56	55	69	68	56	53
Average	54	52	60	59	55	53

E
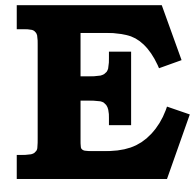
Detailed Drawing

In this appendix, the detailed drawing of the two versions of the final design is shown. Note that the designs are similar except for the elongated part. The corners are relative to the top of the drawing the same. The holes at the bottom of the parts are the same relative to the bottom of the part. The sizes are given in mm. First, the drawing of the short version is given and second, the drawing of the long version is given.

Dimensions (mm)

- 1
- 1
- 1,45
- 2
- 1
- 1,45
- 1,45
- R1
- 6,55
- 15
- 1
- 2
- 3
- 1
- 1
- 2
- 3
- 10
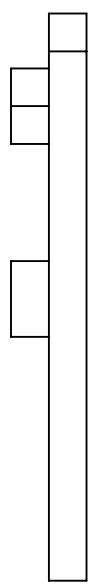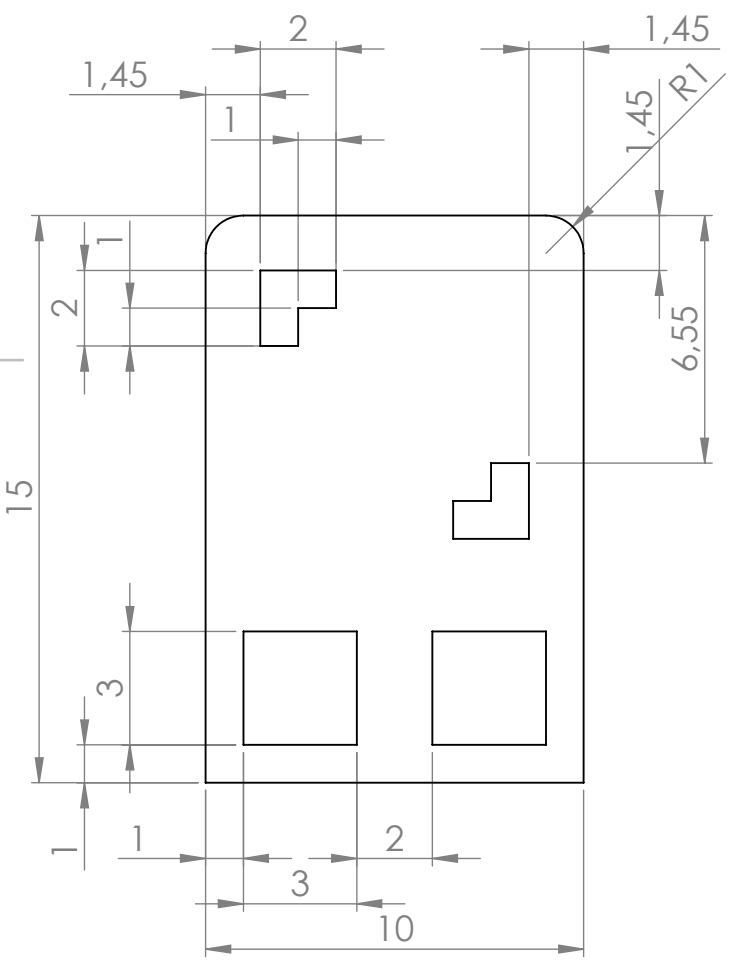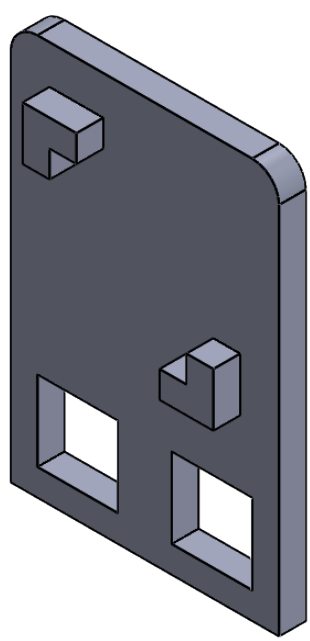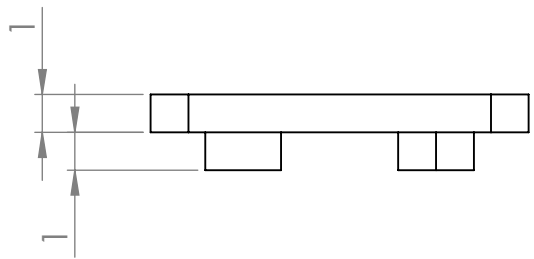
NAME	Mariëlle Haring
Student number	4126440

DIMENSIONS ARE IN MILLIMETERS

TUDelft

MATERIAL:
Stainless steel

WEIGHT:

TITLE:

Final Design - Long

DWG NO.
02

A4

SCALE:5:1   SHEET 1 OF 1
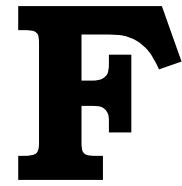
F
Matlab Code

This appendix consists of three Matlab codes. The first code is used for the results of the pilot study. The second code is used on the results of the experiments in the Lab. And finally the third code is used on the results in the operating room.

F.1. Matlab File - Pilot Study

```matlab
%% ================================ %%
%                 Start
% ================================ %%
clc
clear all
close all


%% ================================ %%
%            VanStraten test
% ================================ %%

% Maximal reading distances of the instruments
% Small reader
I_(01) = 30;       I_(02) = 4;        I_(03) = 26;
I_(04) = 4;        I_(05) = 20;       I_(06) = 13;
I_(07) = 10;       I_(08) = 10;       I_(09) = 20;
I_(10) = 20;       I_(11) = 3;        I_(12) = 2;
I_(13) = 3;        I_(14) = 40;       I_(15) = 64;
I_(16) = 3;        I_(17) = 65;       I_(18) = 10;
I_(19) = 31;       I_(20) = 60;       I_(21) = 37;
I_(22) = 10;       I_(23) = 8;        I_(24) = 0.5;
I_(25) = 62;       I_(26) = 10;       I_(27) = 8;
I_(28) = 20;       I_(29) = 31;       I_(30) = 8;

% Maximal reading distances of the instruments
% Large reader
LI_(01) = 38;      LI_(02) = 16;      LI_(03) = 53;
LI_(04) = 8;       LI_(05) = 29;      LI_(06) = 31;
LI_(07) = 26;      LI_(08) = 21;      LI_(09) = 34;
LI_(10) = 28;      LI_(11) = 6;       LI_(12) = 17;
LI_(13) = 26;      LI_(14) = 22;      LI_(15) = 38;
LI_(16) = 20;      LI_(17) = 85;      LI_(18) = 36;
LI_(19) = 81;      LI_(20) = 53;      LI_(21) = 66;
LI_(22) = 24;      LI_(23) = 19;      LI_(24) = 9;
```

```matlab
35  LI_(25) = NaN;        LI_(26) = 29;        LI_(27) = 49;
36  LI_(28) = 46;         LI_(29) = 45;        LI_(30) = 16;
37  %LI_(25) = 227;
38
39  %% ================================= %%
40  %  Plot distances - Small antenna
41  %  ================================= %%
42  subplot(1,2,1)
43  set(gcf,'position',[0 0 900 500])
44
45  stem(I_)
46      xlabel('Instrument number')
47      ylabel('Maximal reading distance [cm]')
48      title('Van Straten instruments - Antenna 1')
49      ylim([0 90])
50  hold on
51      mu = mean(I_);
52      hline = refline([0 mu]);
53      hline.Color = 'r';
54      hline = refline([0 50]);
55      hline.Color = 'g';
56  legend('Measurement', 'Average', 'Desired','Location','northwest')
57  hold off
58
59  %% ================================= %%
60  %  Plot distances - Large antenna
61  %  ================================= %%
62  subplot(1,2,2)
63  stem(LI_)
64      xlabel('Instrument number')
65      ylabel('Maximal reading distance [cm]')
66      title('Van Straten instruments - Antenna 2')
67      ylim([0 90])
68  hold on
69      Lmu = mean(LI_, 'omitnan');
70      hline = refline([0 Lmu]);
71      hline.Color = 'r';
72      hline = refline([0 50]);
73      hline.Color = 'g';
74  legend('Measurement', 'Average', 'Desired','Location','northwest')
75  hold off
76
77  %% ================================= %%
78  %  Sigma for outliers - Small Antenna
79  %  ================================= %%
80  S_sigma = std(I_);
81  SSigma3 = S_sigma*3;
82  OutlierS_top = mu + SSigma3;
83  OutlierS_bottom = mu - SSigma3;
84
85
86  %% ================================= %%
87  %  Sigma for outliers - Large Antenna
88  %  ================================= %%
89  L_sigma = std(LI_, 'omitnan');
90  Sigma3 = L_sigma*3;
```

```matlab
91  Outlier_top = Lmu + Sigma3;
92  Outlier_bottom = Lmu - Sigma3;
93
94  %% =============================== %%
95  % Statistics
96  % =============================== %%
97  [h,p] = ttest2(I_,LI_);
```

F.2. Matlab File - Lab Experiments

```matlab
1  %% ===================================== %%
2  %  Start − Lab experiments
3  %  ===================================== %%
4  clear all
5  close all
6  clc
7
8  %% ===================================== %%
9  %  Import data from spreadsheet
10 %  ===================================== %%
11 % Script for importing data from the following spreadsheet:
12 %    Workbook: C:\Users\marie\Dropbox\Afstuderen_Marielle\Tests\VoorMatlab
       .xlsx
13 %    Worksheet: Blad1
14
15 % Import the data
16 [~, ~, raw] = xlsread('C:\Users\marie\Dropbox\Afstuderen_Marielle\Tests\
       VoorMatlab.xlsx','Blad1','A2:CI4');
17
18 %% Create output variable
19 data = reshape([raw{:}],size(raw));
20
21 %% Allocate imported array to column variable names
22 SAX1010A = data(:,1);
23 SAX1010B = data(:,2);
24 SAX2020A = data(:,3);
25 SAX2020B = data(:,4);
26 SAX3030A = data(:,5);
27 SAX3030B = data(:,6);
28 SAX4040A = data(:,7);
29 SAX4040B = data(:,8);
30 SAH1010A = data(:,9);
31 SAH1010B = data(:,10);
32 SAH2020A = data(:,11);
33 SAH2020B = data(:,12);
34 SAH3030A = data(:,13);
35 SAH3030B = data(:,14);
36 SAH4040A = data(:,15);
37 SAH4040B = data(:,16);
38 THI05A = data(:,17);
39 THI05B = data(:,18);
40 THI1A = data(:,19);
41 THI1B = data(:,20);
42 THI2A = data(:,21);
43 THI2B = data(:,22);
44 THI3A = data(:,23);
45 THI3B = data(:,24);
46 BOC1010A = data(:,25);
47 BOC1010B = data(:,26);
48 BOC1020A = data(:,27);
49 BOC1020B = data(:,28);
50 BOC1030A = data(:,29);
51 BOC1030B = data(:,30);
52 BOC1040A = data(:,31);
```

```
53  BOC1040B = data(:,32);
54  BIC1010A = data(:,33);
55  BIC1010B = data(:,34);
56  BIC1020A = data(:,35);
57  BIC1020B = data(:,36);
58  BIC1030A = data(:,37);
59  BIC1030B = data(:,38);
60  BIC1040A = data(:,39);
61  BIC1040B = data(:,40);
62  HT2020A = data(:,41);
63  HT2020B = data(:,42);
64  SC2020 = data(:,43);
65  TOPTapA = data(:,44);
66  TOPTapB = data(:,45);
67  TOPTshA = data(:,46);
68  TOPTshB = data(:,47);
69  TOPcorA = data(:,48);
70  TOPcorB = data(:,49);
71  COR2A = data(:,50);
72  COR2B = data(:,51);
73  COR4A = data(:,52);
74  COR4B = data(:,53);
75  RB1A = data(:,54);
76  RB1B = data(:,55);
77  RB2A = data(:,56);
78  RB2B = data(:,57);
79  RB3A = data(:,58);
80  RB3B = data(:,59);
81  FB1A = data(:,60);
82  FB1B = data(:,61);
83  FB2A = data(:,62);
84  FB2B = data(:,63);
85  FB3A = data(:,64);
86  FB3B = data(:,65);
87  SUR1A = data(:,66);
88  SUR1B = data(:,67);
89  SUR2A = data(:,68);
90  SUR2B = data(:,69);
91  SUR3A = data(:,70);
92  SUR3B = data(:,71);
93  HTT05A = data(:,72);
94  HTT05B = data(:,73);
95  HTT1A = data(:,74);
96  HTT1B = data(:,75);
97  TOUcorA = data(:,76);
98  TOUcorB = data(:,77);
99  TOUsurA = data(:,78);
100 TOUsurB = data(:,79);
101 TOUbarA = data(:,80);
102 TOUbarB = data(:,81);
103 TTOup1A = data(:,82);
104 TTOup1B = data(:,83);
105 TTOdo1A = data(:,84);
106 TTOdo1B = data(:,85);
107 TTOup2A = data(:,86);
108 TTOup2B = data(:,87);
```

```
109
110  %% Clear temporary variables
111  clearvars data raw;
112
113  %% Import data from spreadsheet − Extra thickness tests
114  % Script for importing data from the following spreadsheet:
115  %
116  %    Workbook: C:\Users\marie\Dropbox\Afstuderen_Marielle\Tests\
            VoorMatlab_ExtraThick.xlsx
117  %    Worksheet: Blad1
118
119  %% Import the data
120  [~, ~, raw] = xlsread('C:\Users\marie\Dropbox\Afstuderen_Marielle\Tests\
            VoorMatlab_ExtraThick.xlsx','Blad1','B2:E4');
121
122  %% Create output variable
123  data = reshape([raw{:}],size(raw));
124
125  %% Allocate imported array to column variable names
126  ETH05A = data(:,1);
127  ETH05B = data(:,2);
128  ETH1A = data(:,3);
129  ETH1B = data(:,4);
130
131  %% Clear temporary variables
132  clearvars data raw;
133
134  %% ==================================== %%
135  %  Surface area − Xerafy tags
136  %  ==================================== %%
137  mmX1010 = [SAX1010A; SAX1010B];
138  mmX2020 = [SAX2020A; SAX2020B];
139  mmX3030 = [SAX3030A; SAX3030B];
140  mmX4040 = [SAX4040A; SAX4040B];
141
142  CSAX = [mmX1010; mmX2020; mmX3030; mmX4040];
143  grpSAX = [zeros(6,1); ones(6,1); ones(6,1)*2; ones(6,1)*3];
144
145  % Make boxplot
146  figure(1)
147  subplot(1,2,1)
148  set(gcf,'position',[0 0 900 500])
149  boxplot(CSAX,grpSAX, 'labels', {'10x10', '20x20', '30x30', '40x40'})
150      title('Xerafy tags')
151      xlabel('Surface area [mm^2]')
152      ylabel('Maximal reading distance [cm]')
153      ylim([0 180])
154
155  % statistics
156  [hX1,pX1] = ttest2(mmX1010,mmX2020);
157  [hX2,pX2] = ttest2(mmX2020,mmX3030);
158  [hX3,pX3] = ttest2(mmX3030,mmX4040);
159  [hX4,pX4] = ttest2(mmX1010,mmX4040);
160
161  %% ==================================== %%
162  %  Surface area − HID tags
```

```matlab
163 % ===================================== %%%
164 mm1010 = [SAH1010A; SAH1010B];
165 mm2020 = [SAH2020A; SAH2020B; THI1A; THI1B; TTOup1A; TTOup1B; TTOdo1A;
        TTOdo1B; TTOup2A; TTOup2B];
166 mm3030 = [SAH3030A; SAH3030B];
167 mm4040 = [SAH4040A; SAH4040B];
168
169 CSA = [mm1010; mm2020; mm3030; mm4040];
170 grpSA = [zeros(6,1); ones(30,1); ones(6,1)*2; ones(6,1)*3];
171
172 % Make boxplot
173 subplot(1,2,2)
174 boxplot(CSA,grpSA, 'labels', {'10x10', '20x20', '30x30', '40x40'})
175 title('HID tags')
176 xlabel('Surface area [mm^2]')
177 ylabel('Maximal reading distance [cm]')
178 ylim([0 180])
179
180 % Make a 2nd order line fit
181 % x = x data, y = y data, 1 = order of the polynomial i.e a straight line
182 figure(7)
183 subplot(1,2,1)
184 set(gcf,'position',[0 0 900 500])
185 grpSA2 = [100; 100; 100; 100; 100; 100; 400; 400; 400; 400; 400; 400; 400;
        400; 400; 400; 400; 400; 400; 400; 400; 400; 400; 400; 400; 400; 400;
      400; 400; 400; 400; 400; 400; 400; 400; 400; 900; 900; 900; 900; 900;
      900; 1600; 1600; 1600; 1600; 1600; 1600];
186 xA = grpSA2;
187 yA = CSA;
188 Fit = polyfit(xA,yA,2);
189 plot(100:1:2000,polyval(Fit,100:1:2000))
190 hold on
191 plot(xA,yA,'o')
192     ylim([0 200])
193     xlim([0 2000])
194     title('Surface area - HID tags')
195     xlabel('Surface area [mm^2]')
196     ylabel('Maximal reading distance [cm]')
197 hold off
198
199 % statistics
200 [h1,p1] = ttest2(mm1010,mm2020);
201 [h2,p2] = ttest2(mm2020,mm3030);
202 [h3,p3] = ttest2(mm3030,mm4040);
203 [h4,p4] = ttest2(mm1010,mm4040);
204 [h5,p5] = ttest2(mm3030,mm1010);
205 [h6,p6] = ttest2(mm2020,mm4040);
206
207 % between Xerafy and HID
208 [hXH1,pXH1] = ttest2(mmX1010,mm1010);
209 [hXH2,pXH2] = ttest2(mmX2020,mm2020);
210 [hXH3,pXH3] = ttest2(mmX3030,mm3030);
211 [hXH4,pXH4] = ttest2(mmX1010,mm4040);
212
213 % A and B orientation Surface Area HID tags
214 SurfArA = [SAH1010A; SAH2020A; SAH3030A; SAH4040A; THI1A; TTOup1A; TTOdo1A
```

```matlab
     ; TTOup2A];
215  SurfArB = [SAH1010B; SAH2020B; SAH3030B; SAH4040B; THI1B; TTOup1B; TTOdo1B
         ; TTOup2B];
216
217  CorSA = [SurfArA; SurfArB];
218  grporSA = [zeros(24,1); ones(24,1)];
219
220  % Make boxplot
221  subplot(1,2,2)
222  boxplot(CorSA,grporSA, 'labels', {'A', 'B'})
223  title('Orientation - HID tags')
224  xlabel('Orientation')
225  ylabel('Maximal reading distance [cm]')
226  ylim([0 200])
227
228  % statistics
229  [hsurf1,psurf1] = ttest2(SurfArA,SurfArB);
230
231  % Standard deviations
232  S_surforA = std(SurfArA);
233  S_surforB = std(SurfArB);
234
235  %% ===================================== %%
236  %  Bar length
237  % ===================================== %%
238  bar1 = [BOC1010A; BOC1010B; BIC1010A; BIC1010B];
239  bar2 = [BOC1020A; BOC1020B; BIC1020A; BIC1020B];
240  bar3 = [BOC1030A; BOC1030B; BIC1030A; BIC1030B];
241  bar4 = [BOC1040A; BOC1040B; BIC1040A; BIC1040B];
242
243  Cb = [bar1; bar2; bar3; bar4];
244  grpb = [zeros(12,1); ones(12,1); ones(12,1)*2; ones(12,1)*3];
245
246  % Make boxplot
247  figure(2)
248  subplot(1,2,1)
249  set(gcf,'position',[0 0 900 500])
250  boxplot(Cb,grpb, 'labels', {'10', '20', '30', '40'})
251      title('Bar length')
252      xlabel('Length of the bar [mm]')
253      ylabel('Maximal reading distance [cm]')
254      ylim([0 100])
255
256  % Standard deviations
257  S_bar1 = std(bar1);
258  S_bar2 = std(bar2);
259  S_bar3 = std(bar3);
260  S_bar4 = std(bar4);
261
262  % statistics
263  [h_bar_1,p_bar_1] = ttest2(bar1,bar2);
264  [h_bar_2,p_bar_2] = ttest2(bar1,bar3);
265  [h_bar_3,p_bar_3] = ttest2(bar1,bar4);
266  [h_bar_4,p_bar_4] = ttest2(bar3,bar2);
267  [h_bar_5,p_bar_5] = ttest2(bar4,bar2);
268  [h_bar_6,p_bar_6] = ttest2(bar3,bar4);
```

```matlab
269
270
271   %%% ===================================== %%%
272   %   Bar length Centre VS End of the bar
273   %   ===================================== %%%
274   bar_end     = [BOC1010A; BOC1010B; BOC1020A; BOC1020B; BOC1030A; BOC1030B;
          BOC1040A; BOC1040B];
275   bar_centre  = [BIC1010A; BIC1010B; BIC1020A; BIC1020B; BIC1030A; BIC1030B;
          BIC1040A; BIC1040B];
276
277   CbCE    = [bar_end; bar_centre];
278   grpbCE  = [zeros(24,1); ones(24,1)];
279
280   % Make boxplot
281   subplot(1,2,2)
282   boxplot(CbCE,grpbCE, 'labels', {'End', 'Centre'})
283       title('Tag placement')
284       xlabel('Tag placement on the bar')
285       ylabel('Maximal reading distance [cm]')
286       ylim([0 100])
287
288   % Standard deviations
289   S_barend    = std(bar_end);
290   S_barcentre = std(bar_centre);
291
292   % statistics
293   [h_bar_place_1,p_bar_place_1] = ttest2(bar_end,bar_centre);
294
295   %%% ===================================== %%%
296   %   Thickness
297   %   ===================================== %%%
298   Thick05 = [THI05A; THI05B; ETH05A; ETH05B];
299   Thick1  = [THI1A; THI1B; ETH1A; ETH1B];
300   Thick2  = [THI2A; THI2B];
301   Thick3  = [THI3A; THI3B];
302
303   % == A and B Orientation ==%
304   ThickA = [THI05A; ETH05A; THI1A; ETH1A; THI2A; THI3A];
305   ThickB = [THI05B; ETH05B; THI1B; ETH1B; THI2B; THI3B];
306
307   CTHor    = [ThickA; ThickB];
308   grpTHor  = [zeros(18,1); ones(18,1)];
309
310   % Make boxplot
311   figure(3)
312   subplot(1,2,2)
313   set(gcf,'position',[0 0 900 500])
314   boxplot(CTHor,grpTHor, 'labels', {'A', 'B'})
315   title('Orientation − Thickness')
316   xlabel('Orientation')
317   ylabel('Maximal reading distance [cm]')
318   ylim([0 180])
319
320   % statistics
321   [hTHor1,pTHor1] = ttest2(ThickA,ThickB);
322
```

```matlab
323  % Standard deviations
324  S_THorA = std(ThickA);
325  S_THorB = std(ThickB);
326
327  % == Comparing the thicknesses ==%
328  CTH     = [Thick05; Thick1; Thick2; Thick3];
329  grpTH   = [zeros(12,1); ones(12,1); ones(6,1)*2; ones(6,1)*3];
330
331  % Make boxplot
332  subplot(1,2,1)
333  boxplot(CTH,grpTH, 'labels', {'0.5', '1', '2', '3'})
334      title('Plate thickness 20x20 mm')
335      xlabel('Thickness of the plate [mm]')
336      ylabel('Maximal reading distance [cm]')
337      ylim([0 180])
338
339  % Standard deviations
340  S_thick05   = std(Thick05);
341  S_thick1    = std(Thick1);
342  S_thick2    = std(Thick2);
343  S_thick3    = std(Thick3);
344
345  % statistics
346  [h_thick_1,p_thick_1] = ttest2(Thick05,Thick1);
347  [h_thick_2,p_thick_2] = ttest2(Thick05,Thick2);
348  [h_thick_3,p_thick_3] = ttest2(Thick05,Thick3);
349  [h_thick_4,p_thick_4] = ttest2(Thick2,Thick1);
350  [h_thick_5,p_thick_5] = ttest2(Thick3,Thick1);
351  [h_thick_6,p_thick_6] = ttest2(Thick2,Thick3);
352
353  %% ====================================== %%
354  %  Hash tag, sandwich and normal
355  %  ====================================== %%
356  Normaal_    = [SAH2020A; SAH2020B; THI1A; THI1B; TTOup1A; TTOup1B; TTOdo1A
           ; TTOdo1B; TTOup2A; TTOup2B];
357  Hashtag     = [HT2020A; HT2020B];
358  Sandwich    = [SC2020];
359
360  CbH = [Normaal_; Hashtag; Sandwich];
361  grpbH = [ones(30,1); ones(6,1)*2; ones(3,1)*3];
362
363  % Make boxplot
364  figure(8)
365  boxplot(CbH,grpbH, 'labels', {'Reference', 'Cut-outs', 'Top and bottom'})
366      title('Different shapes 20x20 mm')
367      xlabel('Type of shape')
368      ylabel('Maximal reading distance [cm]')
369      ylim([0 200])
370
371  % Standard deviations
372  S_normaal = std(Normaal_);
373  S_Hashtag = std(Hashtag);
374  S_Sandwich = std(Sandwich);
375
376  % statistics
377  [h_Shapes_1,p_Shapes_1] = ttest2(Normaal_,Hashtag);
```

```matlab
378  [h_Shapes_2,p_Shapes_2] = ttest2(Normaal_,Sandwich);
379  [h_Shapes_3,p_Shapes_3] = ttest2(Sandwich,Hashtag);
380
381
382  %% ===================================== %%
383  %  Combination of all A and B groups
384  %  ===================================== %%
385  % All A groups
386  A_all_under = [SAX1010A; SAX2020A; SAX3030A; SAX4040A; SAH1010A; SAH2020A;
            SAH3030A; SAH4040A; THI05A; THI1A; THI2A; THI3A; BOC1010A; BOC1020A;
         BOC1030A; BOC1040A; BIC1010A; BIC1020A; BIC1030A; BIC1040A; HT2020A;
         TOPTapA; TOPTshA; TOPcorA; COR2A; COR4A; RB1A; RB2A; RB3A; FB1A; FB2A;
         FB3A; SUR1A; SUR2A; SUR3A; HTT05A; HTT1A; TOUcorA; TOUsurA; TOUbarA;
         TTOup1A; TTOdo1A; TTOup2A];
387
388  % All B groups
389  B_all_under = [SAX1010B; SAX2020B; SAX3030B; SAX4040B; SAH1010B; SAH2020B;
            SAH3030B; SAH4040B; THI05B; THI1B; THI2B; THI3B; BOC1010B; BOC1020B;
         BOC1030B; BOC1040B; BIC1010B; BIC1020B; BIC1030B; BIC1040B; HT2020B;
         TOPTapB; TOPTshB; TOPcorB; COR2B; COR4B; RB1B; RB2B; RB3B; FB1B; FB2B;
         FB3B; SUR1B; SUR2B; SUR3B; HTT05B; HTT1B; TOUcorB; TOUsurB; TOUbarB;
         TTOup1B; TTOdo1B; TTOup2B];
390
391  %% ===================================== %%
392  %  Open/closed - Full/partial enclosure
393  %  ===================================== %%
394
395  Open    = [COR2A; COR2B; COR4A; COR4B; RB1A; RB1B; RB2A; RB2B; RB3A; RB3B;
            FB1A; FB1B; FB2A; FB2B; FB3A; FB3B];
396  Closed  = [SUR1A; SUR1B; SUR2A; SUR2B; SUR3A; SUR3B];
397
398  C = [Open; Closed];
399  grp = [zeros(48,1); ones(18,1)];
400
401  % Make boxplot
402  figure(4)
403  subplot(1,2,1)
404  set(gcf,'position',[0 0 900 500])
405  boxplot(C,grp, 'labels', {'Partial', 'Full'})
406      title('Partial or full enclosure')
407      xlabel('Enclosure around the tag')
408      ylabel('Maximal reading distance [cm]')
409      ylim([0 100])
410
411  % Standard deviations
412  S_open      = std(Open);
413  S_closed    = std(Closed);
414
415  % statistics
416  [h_fpenclose_1,p_fpenclose_1] = ttest2(Open,Closed);
417
418
419  %% ===================================== %%
420  %  flat, round pins, corners
421  %  additions 1 mm height
422  %  ===================================== %%
```

```matlab
423  flat    = [FB1A; FB1B];
424  round   = [RB1A; RB1B];
425  corners = [COR2A; COR2B; COR4A; COR4B];
426
427  adds_pins  = [flat; round; corners];
428  grp_adds   = [zeros(6,1); ones(6,1); ones(12,1)*2];
429
430  % Make boxplot
431  subplot(1,2,2)
432  boxplot(adds_pins,grp_adds, 'labels', {'Flat', 'Round', 'Corners'})
433      title('1 mm high enclosures')
434      xlabel('Type of partial enclosure on the bar')
435      ylabel('Maximal reading distance [cm]')
436      ylim([0 100])
437
438  % statistics
439  [h_1high_1,p_1high_1] = ttest2(flat,round);
440  [h_1high_2,p_1high_2] = ttest2(flat,corners);
441  [h_1high_3,p_1high_3] = ttest2(corners,round);
442
443
444  %% ===================================== %%
445  %  1, 2, 3 mm additions
446  % ===================================== %%
447  MM1 = [RB1A; RB1B; FB1A; FB1B; SUR1A; SUR1B];
448  MM2 = [RB2A; RB2B; FB2A; FB2B; SUR2A; SUR2B];
449  MM3 = [RB3A; RB3B; FB3A; FB3B; SUR3A; SUR3B];
450
451  Height123 = [MM1 MM2 MM3];
452
453  % Make boxplot
454  figure(5)
455  subplot(1,2,1)
456  set(gcf,'position',[0 0 900 500])
457  boxplot(Height123, {'1', '2', '3'})
458      title('Enclosure heights')
459      xlabel('Height of the enclosure [mm]')
460      ylabel('Maximal reading distance [cm]')
461      ylim([0 100])
462
463  % Standard deviations
464  S_mm1 = std(MM1);
465  S_mm2 = std(MM2);
466  S_mm3 = std(MM3);
467
468  % statistics
469  [h_height_1,p_height_1] = ttest2(MM1,MM2);
470  [h_height_2,p_height_2] = ttest2(MM1,MM3);
471  [h_height_3,p_height_3] = ttest2(MM3,MM2);
472
473
474  %% ===================================== %%
475  %  Uneven surface
476  % ===================================== %%
477  Even    = [BOC1030A; BOC1030B];
478  uneven  = [TOUcorA; TOUcorB; TOUsurA; TOUsurB; TOUbarA; TOUbarB];
```

```
479
480  EvenUneven = [Even; uneven];
481  grp_even   = [zeros(6,1); ones(18,1)];
482
483  % Make boxplot
484  subplot(1,2,2)
485  boxplot(EvenUneven,grp_even, 'labels', {'Smooth surface', '3D printed
         surface'})
486      title('Surface smoothness')
487      xlabel('Surface type')
488      ylabel('Maximal reading distance [cm]')
489      ylim([0 100])
490
491  % Standard deviations
492  S_even      = std(Even);
493  S_uneven    = std(uneven);
494
495  % statistics
496  [h_Surface_1,p_Surface_1] = ttest2(Even,uneven);
497
498  %% ==================================== %%
499  %   Boxplots AB Orientations
500  %  ==================================== %%
501  Both_AB = [A_all_under B_all_under];
502
503  % Make boxplot
504  figure(6)
505  subplot(1,2,1)
506  set(gcf,'position',[0 0 900 500])
507  boxplot(Both_AB, {'Front', 'Back'})
508      title('Side facing the antenna')
509      xlabel('Side facing the antenna')
510      ylabel('Maximal reading distance [cm]')
511      ylim([0 180])
512
513  % Standard deviations
514  S_Front = std(A_all_under);
515  S_Back  = std(B_all_under);
516
517  % statistics
518  [h_Orient_1,p_Orient_1] = ttest2(A_all_under,B_all_under);
519
520  %% ==================================== %%
521  %   Meaning of the symbols
522  %  ==================================== %%
523  % SAX    Surface area - Xerafy
524  % SAH    Surface area - HID
525  % THI    Thickness
526  % BOC    Bar - Tag on the corner
527  % BIC    Bar - Tag in the centre
528  % HT     Hash tag shaped plate
529  % SC     Sandwich configuration
530  % TOP    Top
531  % COR    Corners
532  % RB     Round bars
533  % FB     Flat bars
```

```matlab
534   % SUR      Surrounding
535   % HTT      HID 20x20mm
536   % TOU      Tag on uneven ground
537   % TTO      20x20x1 mm
538
539   %% ==================================== %%
540   %  Import data from spreadsheet
541   %  ==================================== %%
542   % Script for importing data from the following spreadsheet:
543   %     Workbook: C:\Users\marie\Dropbox\Afstuderen_Marielle\Tests\
            VoorMatlab_Epoxy.xlsx
544   %       Worksheet: Blad1
545
546   % Import the data
547   [~, ~, raw] = xlsread('C:\Users\marie\Dropbox\Afstuderen_Marielle\Tests\
            VoorMatlab_Epoxy.xlsx','Blad1','B2:G4');
548
549   %% Create output variable
550   data = reshape([raw{:}],size(raw));
551
552   %% Allocate imported array to column variable names
553   EpDunA  = data(:,1);
554   EpDunB  = data(:,2);
555   EpDikA  = data(:,3);
556   EpDikB  = data(:,4);
557   EpKuipA = data(:,5);
558   EpKuipB = data(:,6);
559
560   %% Clear temporary variables
561   clearvars data raw;
562
563   %% ==================================== %%
564   %  Boxplots with different epoxy layers
565   %  and reference group
566   %  ==================================== %%
567   Ep_dun  = [EpDunA; EpDunB];
568   Ep_dik  = [EpDikA; EpDikB];
569   Ep_kuip = [EpKuipA; EpKuipB];
570
571   Epoxy   = [uneven; Ep_dun; Ep_dik; Ep_kuip];
572   grp_Ep  = [zeros(18,1); ones(6,1); ones(6,1)*2; ones(6,1)*3];
573
574   % Make boxplot
575   subplot(1,2,2)
576   boxplot(Epoxy,grp_Ep, 'labels', {'None', 'Thin', 'Thick', 'Bowl'})
577       title('Protection layer')
578       xlabel('Type of epoxy layer')
579       ylabel('Maximal reading distance [cm]')
580       ylim([0 180])
581
582   % Standard deviations
583   S_dun  = std(Ep_dun);
584   S_dik  = std(Ep_dik);
585   S_kuip = std(Ep_kuip);
586
587   % statistics
```

```
588  [h_Ep_1,p_Ep_1] = ttest2(Ep_dun,Ep_dik);
589  [h_Ep_2,p_Ep_2] = ttest2(Ep_dun,Ep_kuip);
590  [h_Ep_3,p_Ep_3] = ttest2(Ep_dun,uneven);
591  [h_Ep_4,p_Ep_4] = ttest2(Ep_kuip,Ep_dik);
592  [h_Ep_5,p_Ep_5] = ttest2(uneven,Ep_dik);
593  [h_Ep_6,p_Ep_6] = ttest2(Ep_kuip,uneven);
```

F.3. Matlab File - Final Design Experiments

```matlab
1  %% ===================================== %%
2  %  Start - Final Design
3  %  ===================================== %%
4  clc
5  clear all
6  close all
7
8  %% ===================================== %%
9  %  Import data from spreadsheet
10 %  ===================================== %%
11 % Script for importing data from the following spreadsheet:
12 %
13 %    Workbook: C:\Users\marie\Dropbox\Afstuderen_Marielle\Tests\
          VoorMatlab_OKFinal.xlsx
14 %    Worksheet: Blad1
15
16 %% Import the data
17 [~, ~, raw] = xlsread('C:\Users\marie\Dropbox\Afstuderen_Marielle\Tests\
          VoorMatlab_OKFinal.xlsx','Blad1','B2:AA4');
18
19 %% Create output variable
20 data = reshape([raw{:}],size(raw));
21
22 %% Allocate imported array to column variable names
23 OK_SA1 = data(:,1);
24 OK_SB1 = data(:,2);
25 OK_SA2 = data(:,3);
26 OK_SB2 = data(:,4);
27 OK_SA3 = data(:,5);
28 OK_SB3 = data(:,6);
29 OK_LA1 = data(:,7);
30 OK_LB1 = data(:,8);
31 OK_LA2 = data(:,9);
32 OK_LB2 = data(:,10);
33 OK_LA3 = data(:,11);
34 OK_LB3 = data(:,12);
35 OK_LC = data(:,13);
36 OK_LD = data(:,14);
37 OK_LE = data(:,15);
38 OK_LF = data(:,16);
39 OK_SC = data(:,17);
40 OK_SD = data(:,18);
41 OK_SE = data(:,19);
42 OK_SF = data(:,20);
43 OK_SlapA = data(:,21);
44 OK_SlapB = data(:,22);
45 OK_SsprA = data(:,23);
46 OK_SsprB = data(:,24);
47 OK_SCLA = data(:,25);
48 OK_SCLB = data(:,26);
49
50 %% Clear temporary variables
51 clearvars data raw;
52
```

```matlab
53  %% ====================================== %%
54  %  Start Final Design Lab
55  %  ====================================== %%
56
57  %% Import data from spreadsheet
58  % Script for importing data from the following spreadsheet:
59  %
60  %    Workbook: C:\Users\marie\Dropbox\Afstuderen_Marielle\Tests\
        VoorMatlab_2.xlsx
61  %    Worksheet: Blad1
62
63  %% Import the data
64  [~, ~, raw] = xlsread('C:\Users\marie\Dropbox\Afstuderen_Marielle\Tests\
        VoorMatlab_2.xlsx','Blad1','B2:U4');
65
66  %% Create output variable
67  data = reshape([raw{:}],size(raw));
68
69  %% Allocate imported array to column variable names
70  FK1_A = data(:,1);
71  FK1_B = data(:,2);
72  FK2_A = data(:,3);
73  FK2_B = data(:,4);
74  FK3_A = data(:,5);
75  FK3_B = data(:,6);
76  FL1_A = data(:,7);
77  FL1_B = data(:,8);
78  FL2_A = data(:,9);
79  FL2_B = data(:,10);
80  FL3_A = data(:,11);
81  FL3_B = data(:,12);
82  L_C = data(:,13);
83  L_D = data(:,14);
84  L_E = data(:,15);
85  L_F = data(:,16);
86  K_C = data(:,17);
87  K_D = data(:,18);
88  K_E = data(:,19);
89  K_F = data(:,20);
90
91  %% Clear temporary variables
92  clearvars data raw;
93
94  %% Import data from spreadsheet
95  %    Workbook: C:\Users\marie\Dropbox\Afstuderen_Marielle\Tests\
        VoorMatlab_Final_Klein.xlsx
96  %    Worksheet: Blad1
97
98  %% Import the data
99  [~, ~, raw] = xlsread('C:\Users\marie\Dropbox\Afstuderen_Marielle\Tests\
        VoorMatlab_Final_Klein.xlsx','Blad1','B2:U4');
100
101 %% Create output variable
102 data = reshape([raw{:}],size(raw));
103
104 %% Allocate imported array to column variable names
```

```matlab
105  FKK_1A = data(:,1);
106  FKK_1B = data(:,2);
107  FKK_2A = data(:,3);
108  FKK_2B = data(:,4);
109  FKK_3A = data(:,5);
110  FKK_3B = data(:,6);
111  FKL_1A = data(:,7);
112  FKL_1B = data(:,8);
113  FKL_2A = data(:,9);
114  FKL_2B = data(:,10);
115  FKL_3A = data(:,11);
116  FKL_3B = data(:,12);
117  FKK_C = data(:,13);
118  FKK_D = data(:,14);
119  FKK_E = data(:,15);
120  FKK_F = data(:,16);
121  FKL_C = data(:,17);
122  FKL_D = data(:,18);
123  FKL_E = data(:,19);
124  FKL_F = data(:,20);
125
126  %% Clear temporary variables
127  clearvars data raw;
128
129  %% ==================================== %%
130  % Long short -  small Antenna (1) - Lab
131  % ==================================== %%
132  Short_small = [FKK_1A; FKK_1B; FKK_2A; FKK_2B; FKK_3A; FKK_3B];
133  Long_small = [FKL_1A; FKL_1B; FKL_2A; FKL_2B; FKL_3A; FKL_3B];
134
135  Cb = [Long_small; Short_small];
136  grpb = [zeros(18,1); ones(18,1)];
137
138  figure(1)
139  subplot(1,2,1)
140  set(gcf,'position',[0 0 900 500])
141  boxplot(Cb,grpb, 'labels', {'Long', 'Short'})
142      title('Clinical lab - Antenna 1')
143      xlabel('Length of the bar')
144      ylabel('Maximal reading distance [cm]')
145      ylim([0 100])
146
147  % Standard deviations
148  S_small_long = std(Long_small);
149  S_small_short = std(Short_small);
150
151  % statistics
152  [h_smallLS_1,p_smallLS_1] = ttest2(Short_small,Long_small);
153
154  %% ==================================== %%
155  % Long short - Large Antenna (2) - Lab
156  % ==================================== %%
157  Short = [FK1_A; FK1_B; FK2_A; FK2_B; FK3_A; FK3_B];
158  Long = [FL1_A; FL1_B; FL2_A; FL2_B; FL3_A; FL3_B];
159
160  Cb2 = [Long; Short];
```

```matlab
161  grpb2 = [zeros(18,1); ones(18,1)];
162
163  subplot(1,2,2)
164  boxplot(Cb2,grpb2, 'labels', {'Long', 'Short'})
165      title('Clinical lab - Antenna 2')
166      xlabel('Length of the bar')
167      ylabel('Maximal reading distance [cm]')
168      ylim([0 100])
169
170  % Standard deviations
171  S_lab_long = std(Long);
172  S_lab_short = std(Short);
173
174  % statistics
175  [h_LSlab_1,p_LSlab_1] = ttest2(Long,Short);
176
177  % statistics between Antenna 1 and 2
178  [h_ant_1,p_ant_1] = ttest2(Long_small,Long);
179  [h_ant_2,p_ant_2] = ttest2(Short_small,Short);
180  [h_ant_3,p_ant_3] = ttest2(Long_small,Short);
181  [h_ant_4,p_ant_4] = ttest2(Short_small,Long);
182
183  %% ====================================== %%
184  %  Orientation - Small Antenne (1) - Lab
185  %  ====================================== %%
186  OR_small_A = [FKL_1A; FKK_1A; FKL_2A; FKK_2A; FKL_3A; FKK_3A];
187  OR_small_B = [FKL_1B; FKK_1B; FKL_2B; FKK_2B; FKL_3B; FKK_3B];
188  OR_small_C = [FKL_C; FKK_C];
189  OR_small_D = [FKL_D; FKK_D];
190  OR_small_E = [FKL_E; FKK_E];
191  OR_small_F = [FKL_F; FKK_F];
192
193  Cor_small = [OR_small_A; OR_small_B; OR_small_C; OR_small_D; OR_small_E;
         OR_small_F];
194  grpor_small = [zeros(18,1); ones(18,1); ones(6,1)*2; ones(6,1)*3; ones
         (6,1)*4; ones(6,1)*5];
195
196  figure(2)
197  subplot(1,2,1)
198  set(gcf,'position',[0 0 900 500])
199  boxplot(Cor_small,grpor_small, 'labels', {'A', 'B','C', 'D', 'E', 'F'})
200      title('Clinical lab - Antenna 1')
201      xlabel('Orientation')
202      ylabel('Maximal reading distance [cm]')
203      ylim([0 140])
204
205  % Standard deviations
206  S_small_A = std(OR_small_A);
207  S_small_B = std(OR_small_B);
208  S_small_C = std(OR_small_C);
209  S_small_D = std(OR_small_D);
210  S_small_E = std(OR_small_E);
211  S_small_F = std(OR_small_F);
212
213  % statistics
214  [h_small_1,p_small_1] = ttest2(OR_small_C,OR_small_D);
```

```matlab
215 [h_small_2,p_small_2] = ttest2(OR_small_C,OR_small_E);
216 [h_small_3,p_small_3] = ttest2(OR_small_C,OR_small_F);
217 [h_small_4,p_small_4] = ttest2(OR_small_D,OR_small_E);
218 [h_small_5,p_small_5] = ttest2(OR_small_D,OR_small_F);
219 [h_small_6,p_small_6] = ttest2(OR_small_E,OR_small_F);
220 [h_small_7,p_small_7] = ttest2(OR_small_A,OR_small_D);
221 [h_small_8,p_small_8] = ttest2(OR_small_A,OR_small_E);
222 [h_small_9,p_small_9] = ttest2(OR_small_A,OR_small_F);
223 [h_small_10,p_small_10] = ttest2(OR_small_A,OR_small_C);
224 [h_small_11,p_small_11] = ttest2(OR_small_B,OR_small_D);
225 [h_small_12,p_small_12] = ttest2(OR_small_B,OR_small_E);
226 [h_small_13,p_small_13] = ttest2(OR_small_B,OR_small_F);
227 [h_small_14,p_small_14] = ttest2(OR_small_B,OR_small_C);
228 [h_small_15,p_small_15] = ttest2(OR_small_B,OR_small_A);
229
230
231 %% ==================================== %%
232 %  Orientation - Large Antenne (2) - Lab
233 %  ==================================== %%
234 OR_A = [FK1_A; FL1_A; FK2_A; FL2_A; FK3_A; FL3_A];
235 OR_B = [FK1_B; FL1_B; FK2_B; FL2_B; FK3_B; FL3_B];
236 OR_C = [L_C; K_C];
237 OR_D = [L_D; K_D];
238 OR_E = [L_E; K_E];
239 OR_F = [L_F; K_F];
240
241 Cor = [OR_A; OR_B; OR_C; OR_D; OR_E; OR_F];
242 grpor = [zeros(18,1); ones(18,1); ones(6,1)*2; ones(6,1)*3; ones(6,1)*4;
         ones(6,1)*5];
243
244 subplot(1,2,2)
245 boxplot(Cor,grpor, 'labels', {'A', 'B','C', 'D', 'E', 'F'})
246     title('Clinical lab - Antenna 2')
247     xlabel('Orientation')
248     ylabel('Maximal reading distance [cm]')
249     ylim([0 140])
250
251 % Standard deviations
252 S_ORlab_A = std(OR_A);
253 S_ORlab_B = std(OR_B);
254 S_ORlab_C = std(OR_C);
255 S_ORlab_D = std(OR_D);
256 S_ORlab_E = std(OR_E);
257 S_ORlab_F = std(OR_F);
258
259 % statistics
260 [h_OrLab_1,p_OrLab_1] = ttest2(OR_C,OR_D);
261 [h_OrLab_2,p_OrLab_2] = ttest2(OR_C,OR_E);
262 [h_OrLab_3,p_OrLab_3] = ttest2(OR_C,OR_F);
263 [h_OrLab_4,p_OrLab_4] = ttest2(OR_D,OR_E);
264 [h_OrLab_5,p_OrLab_5] = ttest2(OR_D,OR_F);
265 [h_OrLab_6,p_OrLab_6] = ttest2(OR_E,OR_F);
266 [h_OrLab_7,p_OrLab_7] = ttest2(OR_A,OR_B);
267 [h_OrLab_8,p_OrLab_8] = ttest2(OR_A,OR_C);
268 [h_OrLab_9,p_OrLab_9] = ttest2(OR_A,OR_D);
269 [h_OrLab_10,p_OrLab_10] = ttest2(OR_A,OR_E);
```

```matlab
270  [h_OrLab_11,p_OrLab_11] = ttest2(OR_A,OR_F);
271  [h_OrLab_12,p_OrLab_12] = ttest2(OR_B,OR_C);
272  [h_OrLab_13,p_OrLab_13] = ttest2(OR_B,OR_D);
273  [h_OrLab_14,p_OrLab_14] = ttest2(OR_B,OR_E);
274  [h_OrLab_15,p_OrLab_15] = ttest2(OR_B,OR_F);
275
276  % statistics between Antenna 1 and 2
277  [h_Or_small_1,p_Or_small_1] = ttest2(OR_small_C,OR_C);
278  [h_Or_small_2,p_Or_small_2] = ttest2(OR_small_D,OR_D);
279  [h_Or_small_3,p_Or_small_3] = ttest2(OR_small_E,OR_E);
280  [h_Or_small_4,p_Or_small_4] = ttest2(OR_small_F,OR_F);
281
282  %% ====================================== %%
283  % Long short - Large Antenne (2) - OR
284  % ====================================== %%
285  LongOK = [OK_LA1; OK_LB1; OK_LA2; OK_LB2; OK_LA3; OK_LB3];
286  ShortOK = [OK_SA1; OK_SB1; OK_SA2; OK_SB2; OK_SA3; OK_SB3];
287
288  CbOK = [LongOK; ShortOK];
289  grpbOK = [zeros(18,1); ones(18,1)];
290
291  figure(3)
292  subplot(1,2,1)
293  set(gcf,'position',[0 0 900 500])
294  boxplot(CbOK,grpbOK, 'labels', {'Long', 'Short'})
295      title('Long vs Short - OR')
296      xlabel('Length of the bar')
297      ylabel('Maximal reading distance [cm]')
298      ylim([0 140])
299
300  % Standard deviations
301  S_OR_long = std(LongOK);
302  S_OR_short = std(ShortOK);
303
304  % statistics
305  [h_LSOK_1,p_LSOK_1] = ttest2(LongOK,ShortOK);
306
307  % statistics between OR and lab
308  [h_labOR_1,p_labOR_1] = ttest2(LongOK,Long);
309  [h_labOR_2,p_labOR_2] = ttest2(ShortOK,Short);
310  [h_labOR_3,p_labOR_3] = ttest2(LongOK,Short);
311  [h_labOR_4,p_labOR_4] = ttest2(ShortOK,Long);
312
313  %% ====================================== %%
314  % Orientation - Large Antenne (2) - OR
315  % ====================================== %%
316  OROK_A = [OK_SA1; OK_SA2; OK_SA3; OK_LA1; OK_LA2; OK_LA3];
317  OROK_B = [OK_SB1; OK_SB2; OK_SB3; OK_LB1; OK_LB2; OK_LB3];
318  OROK_C = [OK_LC; OK_SC];
319  OROK_D = [OK_LD; OK_SD];
320  OROK_E = [OK_LE; OK_SE];
321  OROK_F = [OK_LF; OK_SF];
322
323  CorOK = [OROK_A; OROK_B; OROK_C; OROK_D; OROK_E; OROK_F];
324  grporOK = [zeros(18,1); ones(18,1); ones(6,1)*2; ones(6,1)*3; ones(6,1)*4;
         ones(6,1)*5];
```

```
325
326  subplot(1,2,2)
327  set(gcf,'position',[0 0 900 500])
328  boxplot(CorOK,grporOK, 'labels', {'A', 'B', 'C', 'D', 'E', 'F'})
329      title('Orientations − OR')
330      xlabel('Orientation')
331      ylabel('Maximal reading distance [cm]')
332      ylim([0 140])
333
334  % Standard deviations
335  S_OROK_A = std(OROK_A);
336  S_OROK_B = std(OROK_B);
337  S_OROK_C = std(OROK_C);
338  S_OROK_D = std(OROK_D);
339  S_OROK_E = std(OROK_E);
340  S_OROK_F = std(OROK_F);
341
342  % statistics
343  [h_OrOK_1,p_OrOK_1] = ttest2(OROK_C,OROK_D);
344  [h_OrOK_2,p_OrOK_2] = ttest2(OROK_C,OROK_E);
345  [h_OrOK_3,p_OrOK_3] = ttest2(OROK_C,OROK_F);
346  [h_OrOK_4,p_OrOK_4] = ttest2(OROK_D,OROK_E);
347  [h_OrOK_5,p_OrOK_5] = ttest2(OROK_D,OROK_F);
348  [h_OrOK_6,p_OrOK_6] = ttest2(OROK_E,OROK_F);
349  [h_OrOK_7,p_OrOK_7] = ttest2(OROK_A,OROK_B);
350  [h_OrOK_8,p_OrOK_8] = ttest2(OROK_A,OROK_C);
351  [h_OrOK_9,p_OrOK_9] = ttest2(OROK_A,OROK_D);
352  [h_OrOK_10,p_OrOK_10] = ttest2(OROK_A,OROK_E);
353  [h_OrOK_11,p_OrOK_11] = ttest2(OROK_A,OROK_F);
354  [h_OrOK_12,p_OrOK_12] = ttest2(OROK_B,OROK_C);
355  [h_OrOK_13,p_OrOK_13] = ttest2(OROK_B,OROK_D);
356  [h_OrOK_14,p_OrOK_14] = ttest2(OROK_B,OROK_E);
357  [h_OrOK_15,p_OrOK_15] = ttest2(OROK_B,OROK_F);
358
359  % statistics between lab and OR
360  [h_Or_1,p_Or_1] = ttest2(OROK_C,OR_C);
361  [h_Or_2,p_Or_2] = ttest2(OROK_D,OR_D);
362  [h_Or_3,p_Or_3] = ttest2(OROK_E,OR_E);
363  [h_Or_4,p_Or_4] = ttest2(OROK_F,OR_F);
364
365  %% ==================================== %%
366  %  OR − Final Design on Instruments
367  %  ==================================== %%
368  %  Import data from spreadsheet
369  %     Workbook: C:\Users\marie\Dropbox\Afstuderen_Marielle\Tests\
         VoorMatlab_OKInstruments.xlsx
370  %     Worksheet: Blad1
371
372  %% Import the data
373  [~, ~, raw] = xlsread('C:\Users\marie\Dropbox\Afstuderen_Marielle\Tests\
         VoorMatlab_OKInstruments.xlsx','Blad1','B2:G4');
374
375  %% Create output variable
376  data = reshape([raw{:}],size(raw));
377
378  %% Allocate imported array to column variable names
```

```matlab
379  IN_lapA = data(:,1);
380  IN_lapB = data(:,2);
381  IN_sprA = data(:,3);
382  IN_sprB = data(:,4);
383  IN_clA = data(:,5);
384  IN_clB = data(:,6);
385
386  %% Clear temporary variables
387  clearvars data raw;
388
389  % IN_lap       Laparoscopic tool − short = Tool 3 = C
390  % IN_spr       Spreader − short         = Tool 2 = B
391  % IN_cl     Clamp − short               = Tool 1 = A
392
393  Instr_lap = [IN_lapA; IN_lapB];
394  Instr_spr = [IN_sprA; IN_sprB];
395  Instr_cl = [IN_clA; IN_clB];
396
397  C_instr = [Instr_cl; Instr_spr; Instr_lap];
398  grp_instr = [zeros(6,1); ones(6,1); ones(6,1)*2];
399
400  figure(4)
401  boxplot(C_instr,grp_instr, 'labels', {'Instrument A', 'Instrument B', '
         Instrument C'})
402      title('Final Design on instruments in the OR')
403      ylabel('Maximal reading distance [cm]')
404      ylim([0 100])
405
406  % Standard deviations
407  S_instr_lap = std(Instr_lap);
408  S_instr_spr = std(Instr_spr);
409  S_instr_cl = std(Instr_cl);
410
411  % statistics
412  [h_instr_1,p_instr_1] = ttest2(Instr_lap,Instr_spr);
413  [h_instr_2,p_instr_2] = ttest2(Instr_lap,Instr_cl);
414  [h_instr_3,p_instr_3] = ttest2(Instr_spr,Instr_cl);
```

Bibliography

[1] M. Kaur, M. Sandhu, N. Mohan, and P. S. Sandhu, *Rfid technology principles, advantages, limitations & its applications,* International Journal of Computer and Electrical Engineering **3**, 151 (2011).

[2] J. Cox, *Rfid, radio location services use soaring at hospitals,* Network world (2008).

[3] C. Becker, *A new game of leapfrog? rfid is rapidly changing the product-tracking process. some say the technology–once costs drop–could displace bar-coding.* Modern healthcare **34**, 38 (2004).

[4] M. Kranzfelder, A. Schneider, A. Fiolka, E. Schwan, S. Gillen, D. Wilhelm, R. Schirren, S. Reiser, B. Jensen, and H. Feussner, *Real-time instrument detection in minimally invasive surgery using radiofrequency identification technology,* journal of surgical research **185**, 704 (2013).

[5] J. Crayton, *Incorporating radio frequency identification technology into the health care sector,* Infohealth Management Corp., available at: www. infohealth. net (2004).

[6] M. Kranzfelder, C. Staub, A. Fiolka, A. Schneider, S. Gillen, D. Wilhelm, H. Friess, A. Knoll, and H. Feussner, *Toward increased autonomy in the surgical or: needs, requests, and expectations,* Surgical endoscopy **27**, 1681 (2013).

[7] S.-A. Ahmadi, T. Sielhorst, R. Stauder, M. Horn, H. Feussner, and N. Navab, *Recovery of surgical workflow without explicit models,* in *International Conference on Medical Image Computing and Computer-Assisted Intervention* (Springer, 2006) pp. 420–428.

[8] J. Wayne and M. Guglielmo, *Cameras in the operating room: A new problem for docs?* Medscape (2015).

[9] S. Iyer, *Rfid: technology and applications,* in *Eleventh National Conference On Communications* (2005) pp. 28–30.

[10] S. Li, J. K. Visich, B. M. Khumawala, and C. Zhang, *Radio frequency identification technology: applications, technical challenges and strategies,* Sensor Review **26**, 193 (2006).

[11] M. Ward, R. Van Kranenburg, and G. Backhouse, *Rfid: Frequency, standards, adoption and innovation,* JISC Technology and Standards Watch **5** (2006).

[12] S. A. Ahson and M. Ilyas, *RFID handbook: applications, technology, security, and privacy* (CRC press, 2008).

[13] D. M. Dobkin and S. M. Weigand, *Environmental effects on rfid tag antennas,* in *IEEE MTT-S International Microwave Symposium Digest*, Vol. 2005 (2005) pp. 135–138.

[14] HID Global Corporation, *RFID Tag Fixation Guide (white paper)* (HID Global Corporation, 2007).

[15] F. Brunicardi, D. Andersen, T. Billiar, D. Dunn, J. Hunter, J. Matthews, and R. Pollock, *Schwartz's principles of surgery, 10e* (McGraw-Hill, 2014).

[16] R. Lehmann, *3 σ-rule for outlier detection from the viewpoint of geodetic adjustment,* Journal of Surveying Engineering **139**, 157 (2013).

[17] HID Global Corporation, *HID Global Industrial RFID & BLE Tags: What to Use When (white paper)* (HID Global Corporation, 2018).

[18] Everything RF, *What is a grid antenna?* EverythingRF.com, Retrieved from https://www.everythingrf.com/community/what-is-a-grid-antenna, Accessed: 2018-06-13 (2017).

[19] Xerafy, *Xerafy XS Series, EPC UHF RFID-On-Metal Tags (white paper)* (Xerafy.com, 2016).

[20] G. Dash and L. Ampyx, *How rf anechoic chambers work,* glendash.com (2005).

[21] S.-L. Chen and K.-H. Lin, *A slim rfid tag antenna design for metallic object applications,* IEEE Antennas and Wireless Propagation Letters **7**, 729 (2008).

[22] L. Ukkonen, D. Engels, L. Sydanheimo, and M. Kivikoski, *Planar wire-type inverted-f rfid tag antenna mountable on metallic objects,* in *Antennas and Propagation Society International Symposium, 2004. IEEE*, Vol. 1 (IEEE, 2004) pp. 101–104.

[23] M. Fernández Chimeno and F. Silva Martínez, *Rfid systems in medical environment: Emc issues,* in *9th International Symposium on EMC* (2010).

[24] In-PharmaTechnologist.com, *Fda clears rfid chip for humans,* In-Pharmatechnologist.com, Retrieved from https://www.in-pharmatechnologist.com/Article/2004/10/18/FDA-clears-RFID-chip-for-humans, Accessed: 2017-10-30 (2004).

[25] T. Zhao, X. Zhang, L. Zeng, S. Xia, A. O. Hinton, and X. Li, *Applications for radio-frequency identification technology in the perioperative setting,* AORN journal **99**, 764 (2014).

[26] A. M. Wicks, J. K. Visich, and S. Li, *Radio frequency identification applications in hospital environments,* Hospital topics **84**, 3 (2006).

[27] J. Britton, *An investigation into the feasibility of locating portable medical devices using radio frequency identification devices and technology,* Journal of medical engineering & technology **31**, 450 (2007).

[28] N. M. Davis, *Application guide for radio frequency identification in electronic medical records,* partial fulfillment of the requirements for the degree. Masters in Communication Technology and Policy in the faculty of the College of Communication of Ohio University USA (2004).

[29] A. Guédon, L. Wauben, D. De Korne, M. Overvelde, J. Dankelman, and J. van Den Dobbelsteen, *A rfid specific participatory design approach to support design and implementation of real-time location systems in the operating room,* Journal of medical systems **39**, 168 (2015).

[30] A. Coustasse, S. Tomblin, and C. Slack, *Impact of radio-frequency identification (rfid) technologies on the hospital supply chain: a literature review,* Perspectives in Health Information Management **10** (2013).

[31] K. Kusuda, K. Yamashita, A. Ohnishi, K. Tanaka, M. Komino, H. Honda, S. Tanaka, T. Okubo, J. Tripette, and Y. Ohta, *Management of surgical instruments with radio frequency identification tags: A 27-month in hospital trial,* International journal of health care quality assurance **29**, 236 (2016).

[32] A. Coustasse, B. Cunningham, S. Deslich, E. Willson, and P. Meadows, *Benefits and barriers of implementation and utilization of radio-frequency identification (rfid) systems in transfusion medicine,* Perspectives in health information management **12** (2015).

[33] F. Wu, F. Kuo, and L.-W. Liu, *The application of rfid on drug safety of inpatient nursing healthcare,* in *Proceedings of the 7th international conference on Electronic commerce* (ACM, 2005) pp. 85–92.

[34] B. Titterington and F. G. Shellock, *Evaluation of mri issues for an access port with a radiofrequency identification (rfid) tag,* Magnetic resonance imaging **31**, 1439 (2013).

[35] A. Bentonville, *Wal-mart epc pilot begins transition to implementation,* Walmart.com, Retrieved from https://corporate.walmart.com/_news_/news-archive/2005/01/05/wal-mart-epc-pilot-begins-transition-to-implementation, Accessed: 2017-10-30 (2004).

[36] Phys.org, *Gtri is developing protocols for testing effects of rfid systems on medical devices,* Phys.org, Retrieved from https://phys.org/news/2009-10-gtri-protocols-effects-rfid-medical.html, Accessed: 2017-10-30 (2009).

[37] B. P. Rosenbaum, *Radio frequency identification (rfid) in health care: privacy and security concerns limiting adoption,* Journal of medical systems **38**, 19 (2014).

[38] H. J. Yazici, *An exploratory analysis of hospital perspectives on real time information requirements and perceived benefits of rfid technology for future adoption,* International Journal of Information Management **34**, 603 (2014).

[39] J. J. Lou, G. Andrechak, M. Riben, and W. H. Yong, *A review of radio frequency identification technology for the anatomic pathology or biorepository laboratory: much promise, some progress, and more work needed,* Journal of pathology informatics **2** (2011).

[40] X. Fei, S. Li, S. Gao, L. Wei, and L. Wang, *Application safety evaluation of the radio frequency identification tag under magnetic resonance imaging,* Biomedical engineering online **13**, 129 (2014).

[41] T. Steffen, R. Luechinger, S. Wildermuth, C. Kern, C. Fretz, J. Lange, and F. H. Hetzer, *Safety and reliability of radio frequency identification devices in magnetic resonance imaging and computed tomography,* Patient safety in surgery **4**, 2 (2010).

[42] E. Mattei, F. Censi, M. Triventi, P. Bartolini, and G. Calcagnini, *Radiofrequency identification and medical devices: the regulatory framework on electromagnetic compatibility. part ii: active implantable medical devices,* Expert review of medical devices **9**, 289 (2012).

[43] S. J. Seidman, R. Brockman, B. M. Lewis, J. Guag, M. J. Shein, W. J. Clement, J. Kippola, D. Digby, C. Barber, and D. Huntwork, *In vitro tests reveal sample radiofrequency identification readers inducing clinically significant electromagnetic interference to implantable pacemakers and implantable cardioverter-defibrillators,* Heart Rhythm **7**, 99 (2010).

[44] C.-F. Liu, H.-G. Hwang, K.-M. Kuo, and W.-F. Hung, *A call for safer utilization of radio frequency identification in the e-health era,* Telemedicine and e-Health **17**, 615 (2011).

[45] W. Yao, C.-H. Chu, and Z. Li, *The use of rfid in healthcare: Benefits and barriers,* in *RFID-Technology and Applications (RFID-TA), 2010 IEEE International Conference on* (IEEE, 2010) pp. 128–134.

[46] E. Iadanza, F. Dori, R. Miniati, and E. Corrado, *Electromagnetic interferences (emi) from active rfid on critical care equipment,* in *XII Mediterranean Conference on Medical and Biological Engineering and Computing 2010* (Springer, 2010) pp. 991–994.

[47] S. Paaske, A. Bauer, T. Moser, and C. Seckman, *The benefits and barriers to rfid technology in healthcare,* Online Journal of Nursing Informatics **21** (2017).

[48] S. J. Seidman and J. W. Guag, *Adhoc electromagnetic compatibility testing of non-implantable medical devices and radio frequency identification,* Biomedical engineering online **12**, 71 (2013).

[49] B. Houliston, D. Parry, C. Webster, and A. Merry, *Interference with the operation of medical devices resulting from the use of radio frequency identification technology,* (2009).

[50] R. Van Der Togt, E. J. van Lieshout, R. Hensbroek, E. Beinat, J. M. Binnekade, and P. Bakker, *Electromagnetic interference from radio frequency identification inducing potentially hazardous incidents in critical care medical equipment,* Jama **299**, 2884 (2008).

[51] B. Christe, E. Cooney, G. Maggioli, D. Doty, R. Frye, and J. Short, *Testing potential interference with rfid usage in the patient care environment,* Biomedical Instrumentation & Technology **42**, 479 (2008).

[52] M. T. J. Soon, *The new iso technical reference (dtr 20017) on electromagnetic interference (emi) impact of iso/iec 18000 series interrogator emitters on implantable pacemakers and implantable cardioverter defibrillators,* (2011).

[53] Manufacturing Group, *Rfid standard for healthcare industry introduced,* http://www.todaysmedicaldevelopments.com, Retrieved from http://www.todaysmedicaldevelopments.com/article/rfid-medical-manufacturing-standard-101916/, Accessed: 2017-12-10 (2016).

[54] S. Seidman, *Aim standard 7351731, medical electrical equipment and system electromagnetic immunity test for exposure to radio frequency identification readers - an aim standard.* (2016).

[55] Bacheldor, *Aim global to develop protocols for testing effects of rfid emissions in health care,* RFIDJournal.com, Accessed: 2017-12-10 (2008).

[56] European Parliament and Council of the European Union (EU), *Directive 95/46/EG,* (1995).

[57] Raad van State, *Wet op de medische hulpmiddelen,* (1970).